Osmotic Energy-Based Micro Hydroelectric Power System

Samhita Dey

A Thesis

in

The Department

of

Electrical and Computer Engineering

Presented in Partial Fulfillment of the Requirements

for the Degree of Master of Applied Science at

Concordia University

Montreal, Quebec, Canada

September 2016

CONCORDIA UNIVERSITY

SCHOOL OF GRADUATE STUDIES

This is to certify that the thesis prepared

By Samhita Dey

Entitled: "Osmotic Energy-Based Micro Hydroelectric Power System"

and submitted in partial fulfillment of the requirements for the degree of

Master of Applied Science

Complies with the regulations of the University and meets the accepted standards with respect to originality and quality.

Signed by the final Examining Committee:

____ Chair
Dr. Rabin Raut

____ Examiner, External
Dr. Rama B. Bhat (MIE) To the Program

____ Examiner
Dr. A . Rathore

____ Supervisor
Dr. P. Pillay

Approved by____
Dr. W. E. Lynch, Chair
Department of Electrical and Computer Engineering

September 6 , 2016

____
Dr. Amir Asif, Dean
Faculty of Engineering and Computer Science

Abstract

Osmotic Energy-Based Micro Hydroelectric Power System

Samhita Dey

A hydroelectric system has been designed for a distributed generator in the range of 10 to 100 kW. The turbine of this system is run by osmotic power, which is generated from the concentration difference between sea water and fresh water. The concentration difference creates a pressure and a flow rate. This pressure and the flow rate are the power inputs to the turbine. As the system has a high head and a low flow rate, a Pelton turbine is selected, which is the most suitable device or equipment for this power system. Turbine wheel diameter and jet velocity are estimated based on the turbine power and a nominal rotor speed of 1800 rpm, which produces 60 Hz power frequency. Torque and speed are the outputs from the Pelton turbine. By considering ideal conditions the maximum speed and torque outputs are calculated. A permanent magnet synchronous generator (PMSG) is used to generate the electric power.

The whole system is divided into four parts. They are osmotic, hydro, mechanical and electrical. The power in each of these types is calculated and found to be the same. Calculations of higher power levels are also done, (100 kW and 250 kW). In the load side, capacitor, inductor, and resistors are connected. The whole system is first implemented in the Matlab/Simulink and the output values have been achieved. Then, the system is implemented in PSIM software. The PMSG model is used in both Matlab/Simulink and PSIM software packages and the same parameters values of PMSG are considered for both models.

The PMSG outputs are electrical current and voltage. The voltage and current outputs from Matlab and PSIM have been compared and found same. The system is also implemented experimentally. An emulation has been done from this setup. In the experimental setup, all the parameter values are taken same those in Matlab model. The voltage, current, and frequency have been measured from the experimental setup and these results are compared with the Matlab outputs.

Model is validated using experimental results.

Acknowledgment

Foremost, I would like to thank God for making this entire process possible. Appreciation also goes to my supervisor Dr. Pragasen Pillay, for his endless support, great patience and valuable guidance.

I am indebted to my mother and entire family for their all-round support and encouragement.

Special thanks also go to my colleagues in PEER (Power Electronics & Energy Research) group especially, Dr. Maher Al Badri, Dr. Sudarshan Karthik, Dr. Jonathan Maisonneuve, Amir Takbash and Mohammad Masadeh, for their endless support in completing my thesis.

My sincere appreciations go to all of my friends and colleagues for their help during this degree program.

Table of Contents

Chapter 3

CALCULATION OF POWER FLOW IN THE PRO POWER SYSTEM.....34

Chapter 4

Chapter 5

List of figures

List of Tables

List of Main Symbols

J_W	water flux in meter/sec.
A	water permeability through the membrane in meter^2
B	salt permeation coefficient
t	thickness of the porous support layer
FO	forward osmosis
PAO	pressure-assisted osmosis
PRO	pressure-retarded osmosis
ECP	external concentration polarization
ICP	internal concentration polarization
$\Delta\Gamma$	osmotic pressure difference in bar
ΔP	hydraulic pressure difference in bar
P_{gen_in}	input power of the generator
P_{gen_out}	output power of the generator
T	torque
ω	speed
p	no of poles
$P_{turbine\_in}$	input power of the turbine
$P_{turbine\_out}$	output power of the turbine

H	equivalent water height
v_j	jet velocity
C_v	jet velocity co-efficient
V_i	initial jet velocity
u	runner velocity
V_f	final jet velocity
v_t	effective jet velocity
A	nozzle area
d_j	nozzle diameter
D	pipe diameter
Q	flow rate
β	angle between the jet velocity (V) and relative jet velocity (V-U)
M_T	DC motor torque
I	current
R	resistance

Chapter 1

1.1 Introduction

Hydro-power is considered to be one of the most important renewable energy sources. There are many other renewable energy sources like wind, solar, tidal, geothermal etc. 83% of the electricity generated from renewables comes from hydro-power [1]. One of the newly invented hydro-power energy comes from the osmotic energy, where the concentration difference between the sea water and river water is used to produce electricity [2]. As the need for renewable energy is increasing day by day, osmotic energy can also play a vital role in that.

There are many other sources of renewable energy, such as tides, ocean currents and salinity gradients. Salinity gradient power is that which can produce energy by using the chemical potential difference of two liquids. The chemical potential differences are available when fresh water (river water) meet with the saltwater (ocean, sea, gulf, saline lake or brine from desalination plant). This potential difference happens mainly because of the salt concentration. The average salt concentration of sea water (draw water) is 35 gm/ liter, whereas the salt concentration is considered as zero in river water (feed water). Where the salt concentration is more in SWRO brine water and higher in salt-dome solution that the other two solutions. The Great Salt Lake has a very high concentration of salt but the Dead Sea has the highest salt concentration among all, of around 1.24 kg/liter. [3].

The working principle of the PRO (pressure retarded osmosis) process is shown in the Fig.1.1.

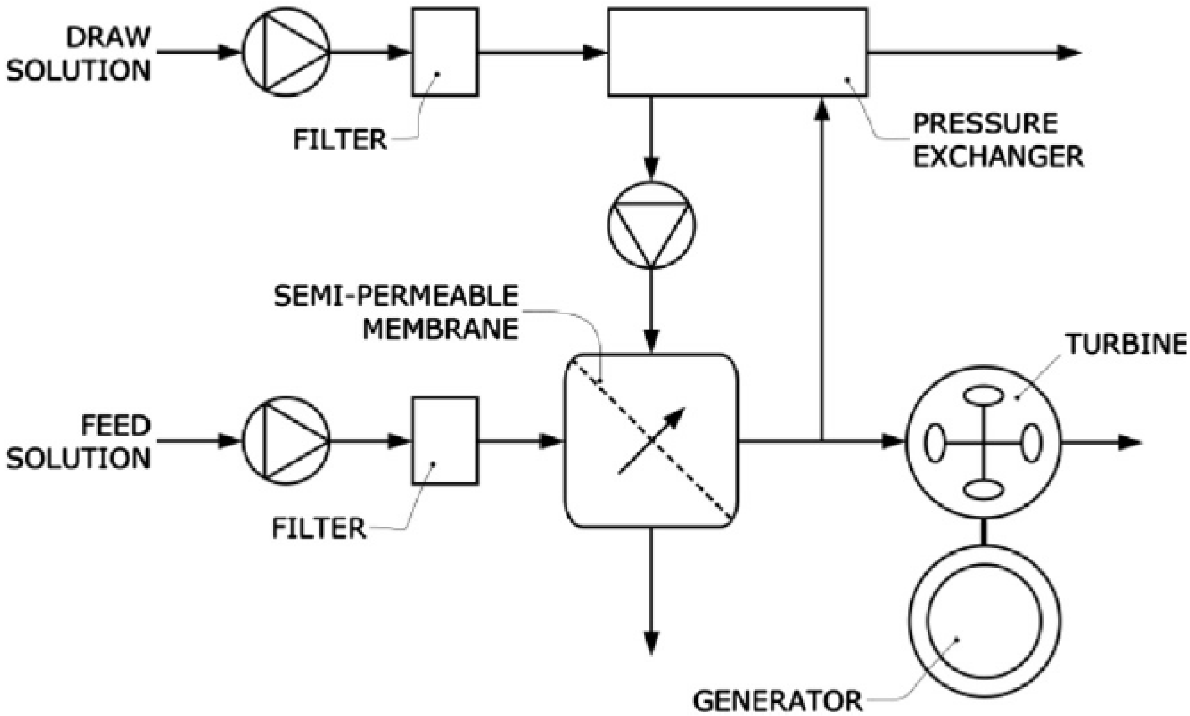

Fig.1.1. Pressure- retarded osmosis power system [5]

There are two chambers in the system, one is for fresh water (feed solution) and other is for salt water (draw solution). After filtration, fresh water is pumped into the chamber. Again saltwater is also pumped into the other chamber after filtration, at a certain hydraulic pressure. There is a membrane between the river water and the salt water chamber. The characteristic of the membrane is such that, it only allows the water to pass but also opposes the salt to pass through it. The tendency of water is to flow from low concentration side to high concentration. Because of this property of water, river water flows through the membrane and goes to salt water chamber. Because of the concentration difference in the chamber, a high pressure is generated in the water, which in turn flows through the turbine to drive the generator. The other portion of this pressurized water goes through the pressure exchanger to recycle the hydraulic pressure on the saltwater side of the system [4].

The schematic diagram of a PRO process is shown in Fig. 1.2.

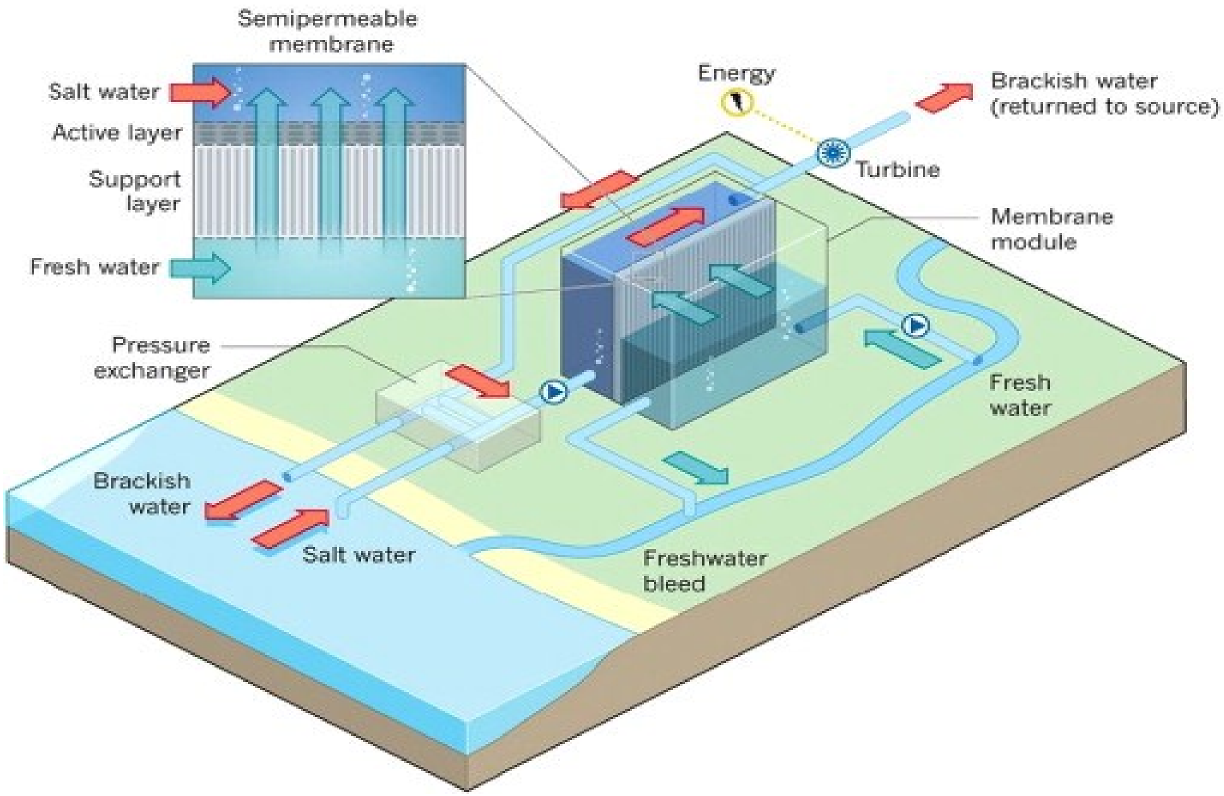

Fig.1.2.Schematic diagram of a PRO plant run on river water and sea water [4]

In the Fig.1.2, the semipermeable membrane is shown separately. It has four layers, which are salt water chamber, active layer, support layer, and fresh water chamber.

PRO system can be classified into two types, depending on its configuration. One is open loop system and another is closed loop system. In the open loop system, it can recovers energy from solar. So it is called a solar-driven process too, where mixing of river water and salt water creates energy.

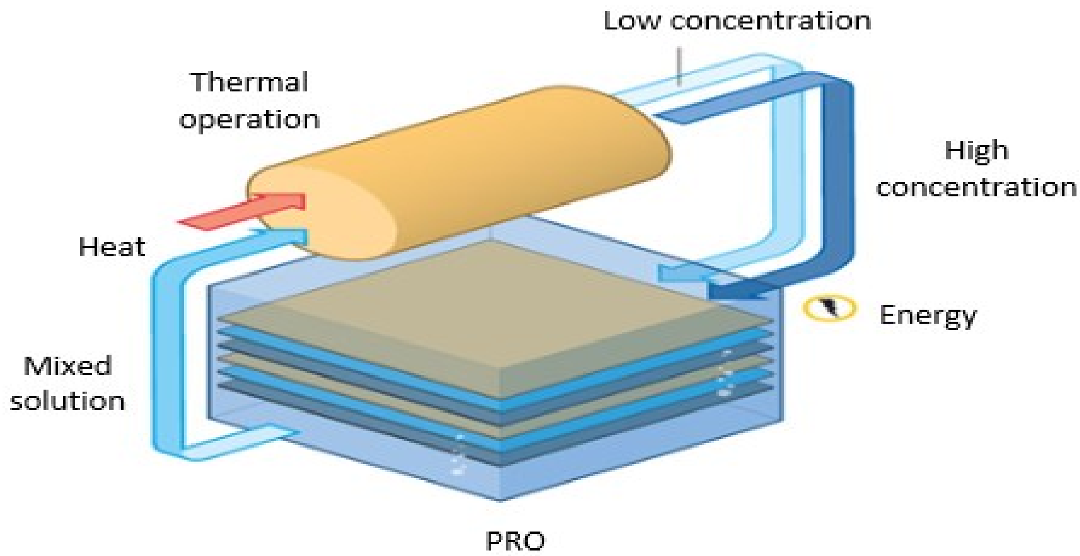

Fig.1.3.Closed loop PRO process [3]

In the closed loop process, both feed solutions and draw solutions flow through two different tubes to the system and meet in PRO block, where energy has been realized. After that, the mixture of feed and draw solution go through another part called distillation. The heat absorption capacity is different in salt water and fresh water. By using this property water can be separated. Low grade heat is applied to separate the feed water from the draw water. So in that process, same water is recycled again and again to produce energy [3].

The PRO model was first reported at 1954. It was concluded by Pattle that osmotic energy can be released by using a permeable membrane. After the oil crisis in 1973, the PRO method received more attention for energy production [16]. The first diagram of an osmotic energy converter was published by Norman in 1974 [16]. Loeb did a lot of work on that by publishing his first experiment in PRO. The experimental investigations of Loeb and Mehta proved that this process can be successful and can produce energy of 1.56 to 3.27 W/ m^2. In 1980 the research interest on this subject grew faster than before. As a result, in 1981 a theoretical and experimental study was published. But the calculated energy production was low, it was 1.6 W/m^2. On the basis of that, Lee (1981) developed a reference PRO performance model, which was used to predict PRO performances. In 1990, Reali highlighted the role of membrane characteristics in water permeability coefficient (A), salt permeation coefficient (B), thickness of the porous support layer (t), and effective salt diffusivity (D). On the other hand, Loeb further concluded that electrical energy can be produced at a cost ranging from $ 0.058 to $ 0.07 /kWh, which was much lower than the average electricity price at that time. ($ 0.067 / kWh). According to Loeb in 2000, it was possible to generate electricity at a price of $ 0.15 / kWh by using the Great Salt Lake water, which was concluded in the year 2002 [16].

1.2 Osmotic process

There are four possible osmotic processes that can occur when pure water mixes with a saline water via a semipermeable membrane. They are

i) Forward osmosis (FO)

ii) Pressure retarded osmosis (PRO)

iii) Stand still process

iv) Reverse osmosis (RO)

The different types of osmotic processes are shown in the Fig. 1.4.

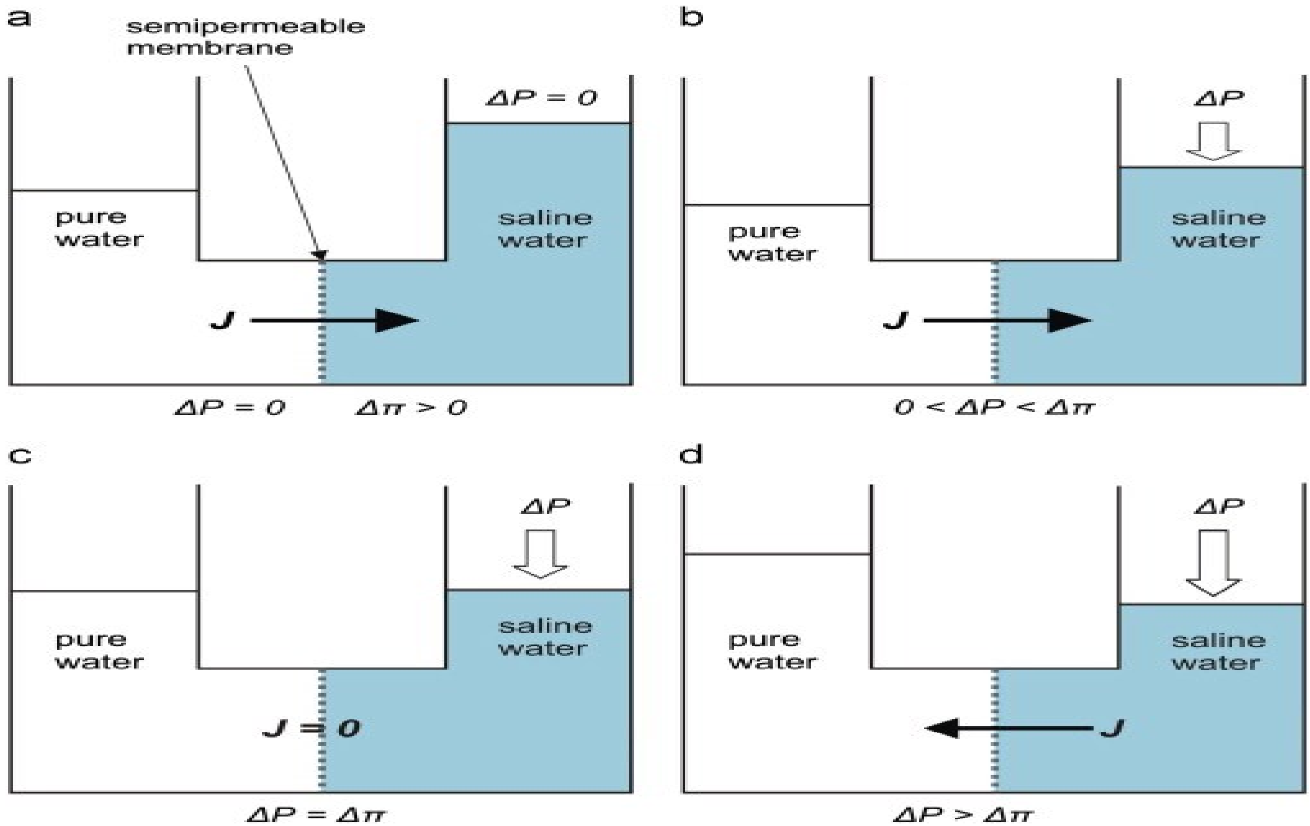

Fig.1.4.Schematic representations of four different types of osmotic processes [4]

From figure 1.4(a), FO (forward osmosis) happens in the presence of osmotic pressure when the hydraulic pressure is zero. The direction of water flux is from river water towards the saline water. In the next stage in figure 1.4(b), when the water starts moving from the less concentrated side to the more concentrated side, the hydraulic pressure starts increasing and opposes the osmotic pressure. However, as the applied force of the hydraulic pressure is less than the osmotic pressure, the net water flux will flow from the river water side to the sea water side.

In the third case, in figure 1.4(c), the hydraulic pressure increases more and becomes equal to osmotic pressure, in this situation they cancel each other. Therefore, there will be no movement of water flux in this system.

In the fourth case, in figure 1.4(d), when hydraulic pressure is more than the osmotic pressure, then the flow direction of the water will change and it will flow from the saline water side to the pure water side [4].

1.3Theoretical background

Characteristics of Osmosis-Driven Processes

There are many factors which can vary the osmosis processes like membrane orientation, the existence of hydraulic pressure and the position of the hydraulic pressure applied. Figure 1.5 below shows the three different types of osmosis processes.

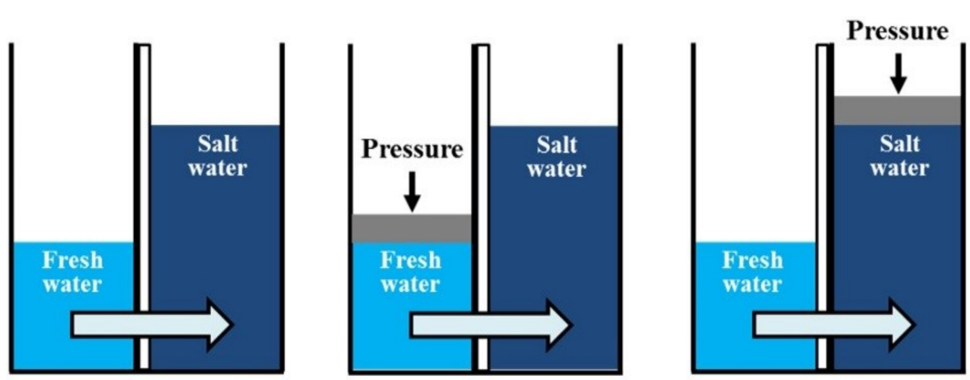

(a)FO (b) PAO (c) PRO

Fig.1.5.Schematic of osmosis-driven processes: (a) forward osmosis (FO); (b) pressure-assisted osmosis (PAO); and (c) pressure-retarded osmosis (PRO) [6].

1.4 Types of PRO process

1) Stand-alone PRO process

In 2008, a company named Stat Kraft worked on salinity gradient power. Their aim was to produce power and the schematic of this technique is shown in Fig.1.6.

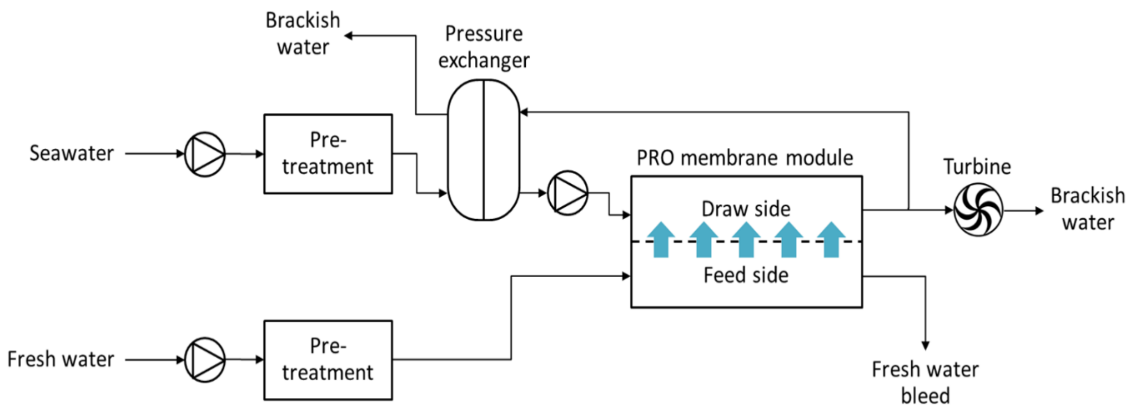

Fig.1.6.Schematic of Stat Kraft's PRO pilot plant [6]

The specifications of this system were

i) 2000 m^2 of membrane area was used in this model.

ii) 10-15 bars of hydraulic pressure was applied.

As a result, an average power density of 3 W/m^2 was produced, which was lower than the economical power density of 5 W/m^2. Because of this low generation, PRO-hybrid process was developed further as in [6].

2) PRO-hybrid process

This type of plants were first discovered in Japan and was achieved the maximum power density of 13 W/m^2 at a hydraulic pressure of 30 bar. Fig.1.7 shows a schematic diagram of this type of processes.

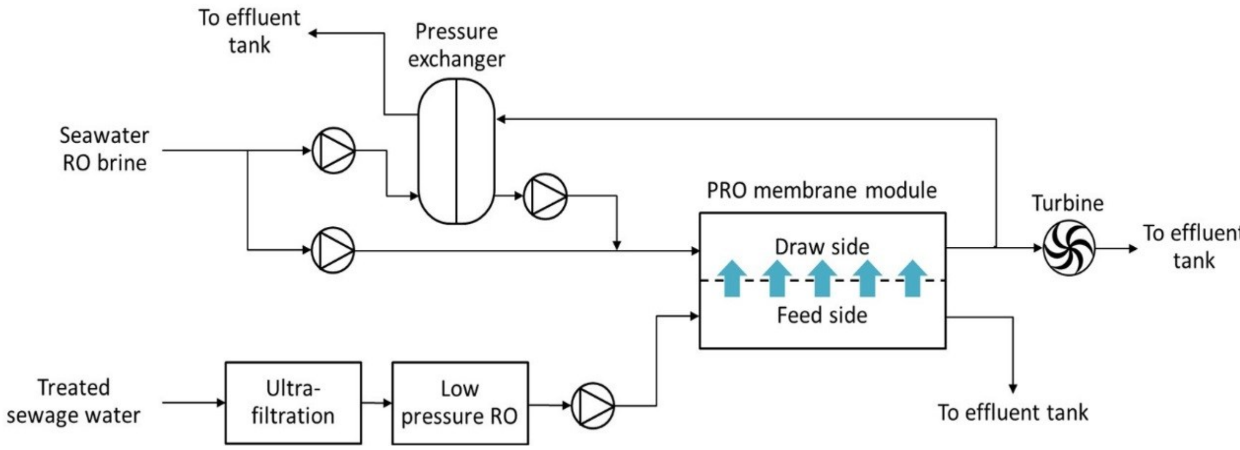

Fig.1.7.Schematic of the RO-PRO hybrid plant [6]

This is also called a RO-PRO process, as it is combined with the RO process. [6] Another process is called RO-MD-PRO hybrid process, where the concentrated RO brine enters in the MD feed side, which is clear in Fig. 1.8.

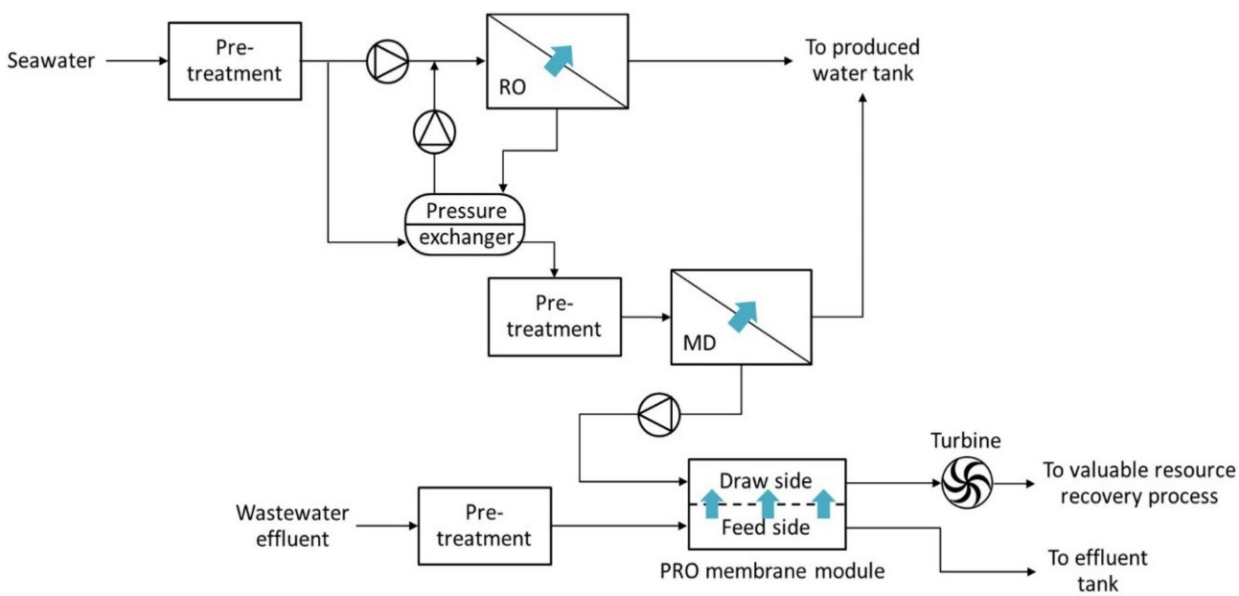

Fig.1.8.Schematic of the RO-MD-PRO hybrid plant [6]

Drawbacks of PRO methodology

PRO has many advantages, but still there are some drawbacks. One main challenge is that, to increase the water permeability the membrane model should be approved ideal. In this case, the membrane should have low salt permeability. Experimentally, when the membrane becomes more permeable to water, it allows more salt to pass through and also reduces energy production. [6] Another challenge creates when the concentration polarization occurs. There are four different types of concentration polarization.

They are

i) External concentration polarization

ii) Internal concentration polarization

And the two sub-categories are

iii) Dilutive ECP and ICP

iv) Concentrative ECP and ICP

Concentration polarization: - As the membrane is not ideal practically and there is some salt permeability (B), in the system. As a result, a thin film of diluted solution is developed on the draw side of the membrane surface. This phenomenon of creating a thin layer of concentrated solution on the feed side of membrane surface is called concentration polarization. As a result, the concentration difference across the active membrane layer reduces significantly, which in turn reduces the power extraction [6].

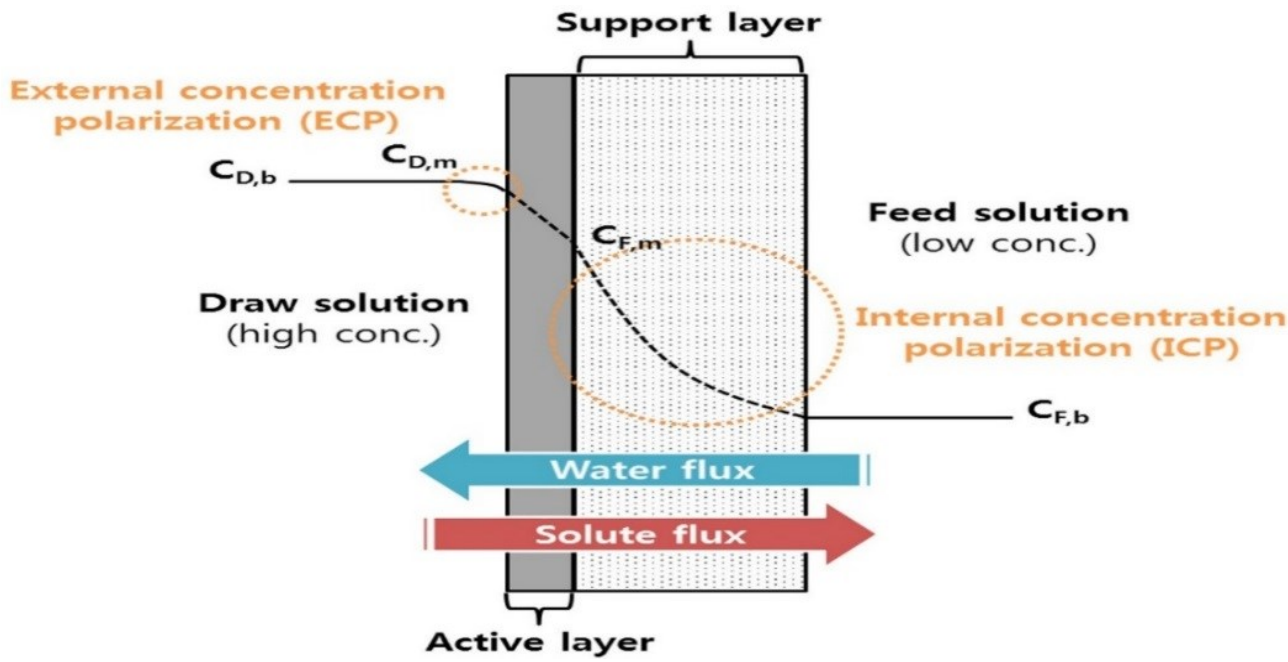

Fig.1.9.Concentration Polarization [6]

The internal concentration polarization takes place in the porous support layer and the external concentration polarization occurs in the inter-phase between the rejection layer and the surrounding solution. When salt permeates through the membrane and makes a concentration layer of solutes on the feed side, it is called concentrative ECP. In the opposite case, when water enters from the feed side to draw side and dilutes the solution, this phenomenon in called dilutive ECP. Dilutive ICP rises when the water permeates through the porous support layer and dilutes the draw solutes inside the support layer. In this case, the dense rejection layer faces the feed solution. In the other case, concentrative ICP happens when the dense rejection layer faces the draw solution and the solutes inside the support are concentrated when water permeates through the membrane.

1.5 Development of membrane in PRO

By making developments in the membranes, the efficiency of PRO can be increased. For RO and PRO process different types of membranes are needed as because the RO membrane which has a thick support layer and causes ICP (internal concentration polarization) further. There are two ways to increase the membrane performance, they are flat-sheet membrane and hollow-fibre membranes.

1) Flat-sheet membranes

The most important thing to increase the membrane performance is to make it high salt rejection and high water permeability. To improve these two factors, research was mainly focused on CA (cellulose acetate) and CTA (commercialized cellulose triacetate). The active and highly-porous support layers mainly need to be developed to improve its performance. There is another membrane called TFC (thin-film composite) which has a relatively higher salt retention rate compared to CTA (commercialized cellulose triacetate) and as a results, it has a lower ICP (internal concentration polarization) and higher water flux. From the research it is found that, by using finger-like and sponge- like structures in the support layer, it will increase the PRO (pressure retarded osmosis) from 6.09 W/m^2 to 10.0 W/m^2 [6].

Further, it is seen that sponge-like membrane consisting of a small structure parameter has a PRO output of 12 W/m^2 at a hydraulic pressure of 15 bar. If the TFC membrane can be applied to the pre-treatment and post-treatment, the power density can reach 18.09 W/m^2. It is seen that the ideal S value for a PRO membrane is around 150 µm. Electrospinning is a process which increases the high porosity, low tortuosity and thin membrane thickness and as a result, it decreases the S value [5].

2) Hollow-fibre membrane

This hollow-fiber membrane has more advantages than flat-sheet membrane because of its high packing density, low footprint, and easy scaling-up. This system is improved further by using a PEI polymer. The hollow-fiber membrane has a high asymmetry, high porosity and small pore size distribution which makes a maximum power density of 24.3 W/m^2 at 20 bar [6].

1.6 Fouling and cleaning in PRO process

1) Membrane fouling in PRO

Because of fouling, overall decrease happens in the performance like a reduction of water flux and an increase in water consumption. Fouling is classified in four areas. They are organic fouling, inorganic fouling, bio-fouling and colloidal fouling. The main drawback in fouling is that, it creates pore narrowing, pore plugging and cake formation. [6].

Figure 1.10 shows the three different processes of the membrane fouling. They are- pore narrowing, pore plugging and gel formation.

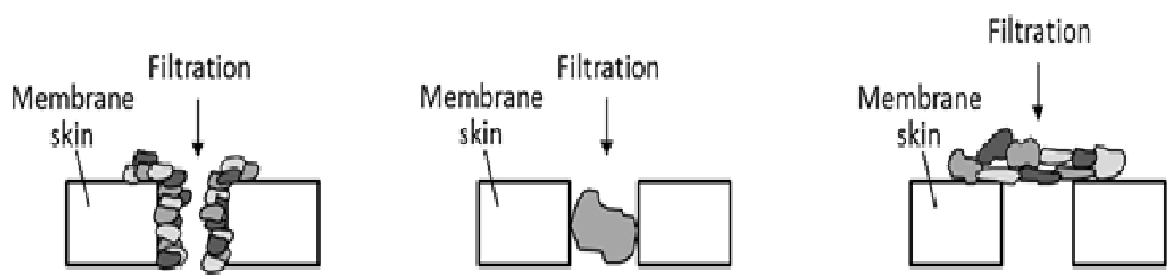

(a) Pore narrowing (b) Pore plugging (c) Gel formation

Fig.1.10. Mechanisms of membrane fouling: (a) pore narrowing; (b) pore plugging; and (c) gel formation [6]

From Fig. 1.10 (a), it is seen that, the internal pole pore narrowing happens only when the pollutants are absorbed. In Fig. 1.10 (b) when pollutants plug pores, then only the pore plugging occurs. From Fig. 1.10(c), cake formation occurs when pollutants pile up onto the membrane surface.

2) Membrane cleaning in PRO

There are many physical and chemical cleaning processes. In physical point of view, they can be reversible or irreversible and chemically, they can be organic or inorganic. These properties mainly affect the cleaning efficiency of the system. For cleaning the strong chemicals, it is not possible by a high cross-flow velocity. Physical cleaning is more suitable in that case. Osmotic backwashing (OBW), is one process for physical flushing which reduces the osmotic backflow caused by the swelling and lifting effects. Because of the organic and inorganic foulants, sometimes hydrodynamic cleaning is not effective. In that case, low shear force can be more applicable rather than an increase of the cross flow. As there are also some drawbacks in osmotic backwashing, as it couldn't completely remove the NOM absorbed into the active support layer [6].

1.7 Possibility to extract energy where river meets the sea

In hydro energy conversion, turbines are placed in the river, where water flows from a certain height. While with PRO (pressure retarded osmosis), an artificial module is installed, where fresh water and sea water has been supplied separately. Therefore, some questions arise on the possibility to produce energy naturally by placing the turbine on the meeting junction of the river and the sea.

However, the main problem arises about the energy density, as it is only 0.256 kWh per cubic meter of initial river water and sea water volume. Therefore, a very large volume of water should be pumped to get a reasonable amount of energy [7].

1.8 Different ranges of energy extraction from different salinity sources

The normal salt water (sea water) has a salt concentration of 35g/L and whereas, the Dead Sea has higher salt concentration of 1.24 kg/L [7].

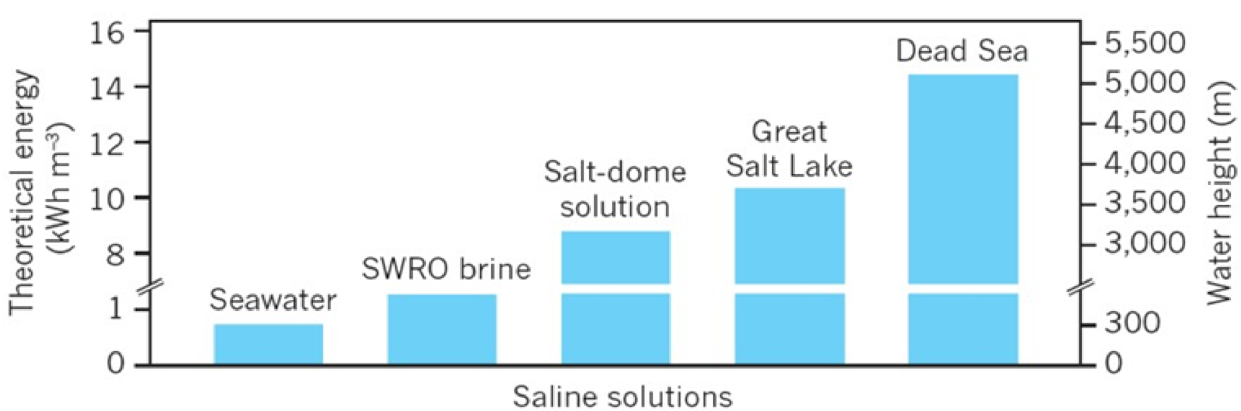

Fig.1.11. The maximum power that can be extracted from different salinity sources [3]

From Fig. 1.11, it is clear that among all these five water sources, seawater has the lowest salt concentration. As the Dead Sea has the highest amount of salt concentration, and it can theoretically provide about 1.6 TWh of energy per year, which is equivalent to 180 MW of continuous power generation [3].

1.9 Increasing the efficiency

By increasing the salt concentration, the output power also increases. But to extract the maximum power, the hydraulic pressure should be half of the osmotic pressure. The latter is about 507 bar, when extremely saline Dead Sea water is used. The problem arises with the membrane structure. For withstanding this much pressure, the membrane thickness should be 700 µm, where the ideal membrane thickness is 150 µm, which allows fresh water to pass easily [7].

In PRO, losses happens mainly because of friction, water impurity and for membrane fouling. Regular cleaning of a membrane can make it performing better and so, increasing the total efficiency. Turbine losses occur because of the friction between the turbine blade and the water.

1.10 PRO-System Energy Losses

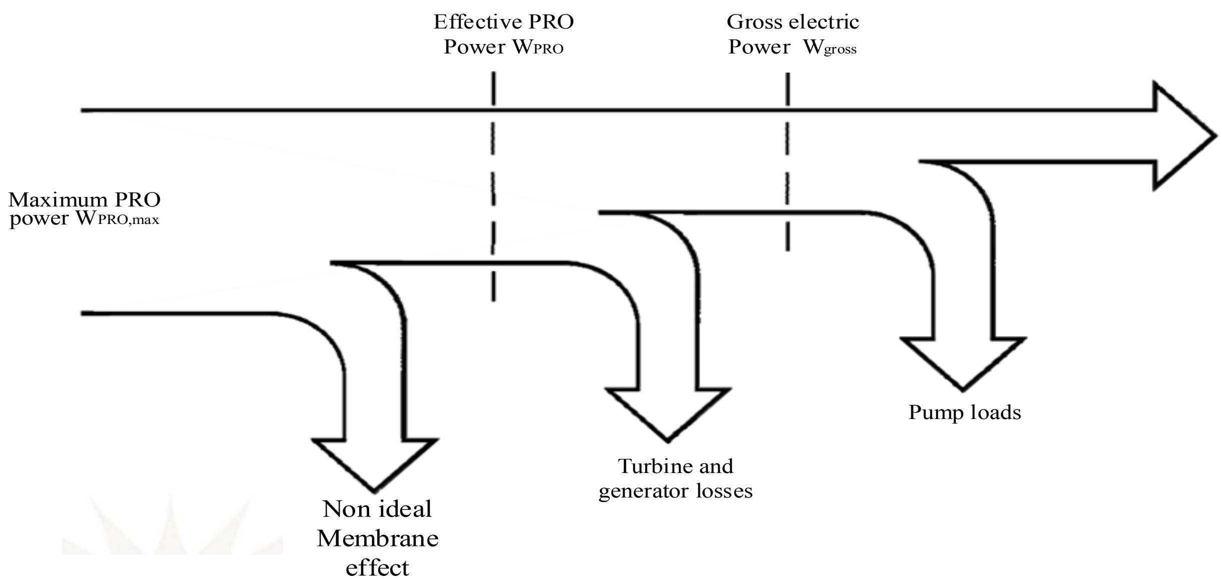

Fig.1.12. Losses in the PRO process [6]

Fig.1.12 shows the different losses in the PRO process. Non-ideal effects and the different types of losses in the turbine and generator sides are the certain conditions, which happens in this type of models. Non ideal effect mainly happens in the membrane portion, which in turn, reduces the output power. Losses are mainly related to turbine and generator losses, which make the gross electric power less than the effective PRO power.

Chapter 2

SYSTEM MODELING

2.1 Model of the PRO system

In this system, a semipermeable membrane is used, where in one side is supplied with feed water (fresh water especially river water) and the other side with draw water (sea water with a high concentration of salt). It is considered that river water has almost zero concentration. The tendency of water is to move from the low concentration side to the high concentration side. Because of that movement of fresh water (low concentration) to sea water (high concentration) creates a pressure difference, which in turn passes through the turbine to rotate and generate electricity. The semipermeable membrane also allows the flow of water but prevents the salt to pass through it. Fig.2.1 shows the basic operating principle of semipermeable membranes and how the pressure develops across it.

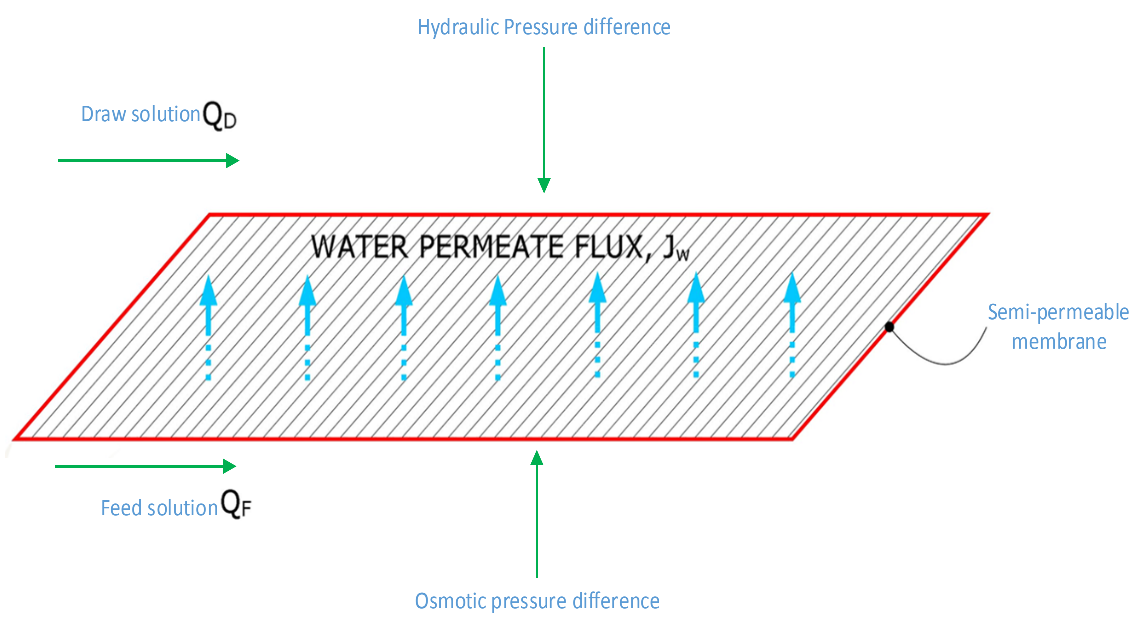

Fig.2.1. Flow of feed solution through the semipermeable membrane [28]

Water permeate flux (flow rate per unit of membrane surface area) can be expressed as (2.1), and power per unit membrane surface area can then be expressed as shown in (2.2)

$$J_w = A * (\Delta\Gamma - \Delta P) \tag{2.1}$$

A = water permeability ($\frac{m^3}{Pa.s.m^2}$)

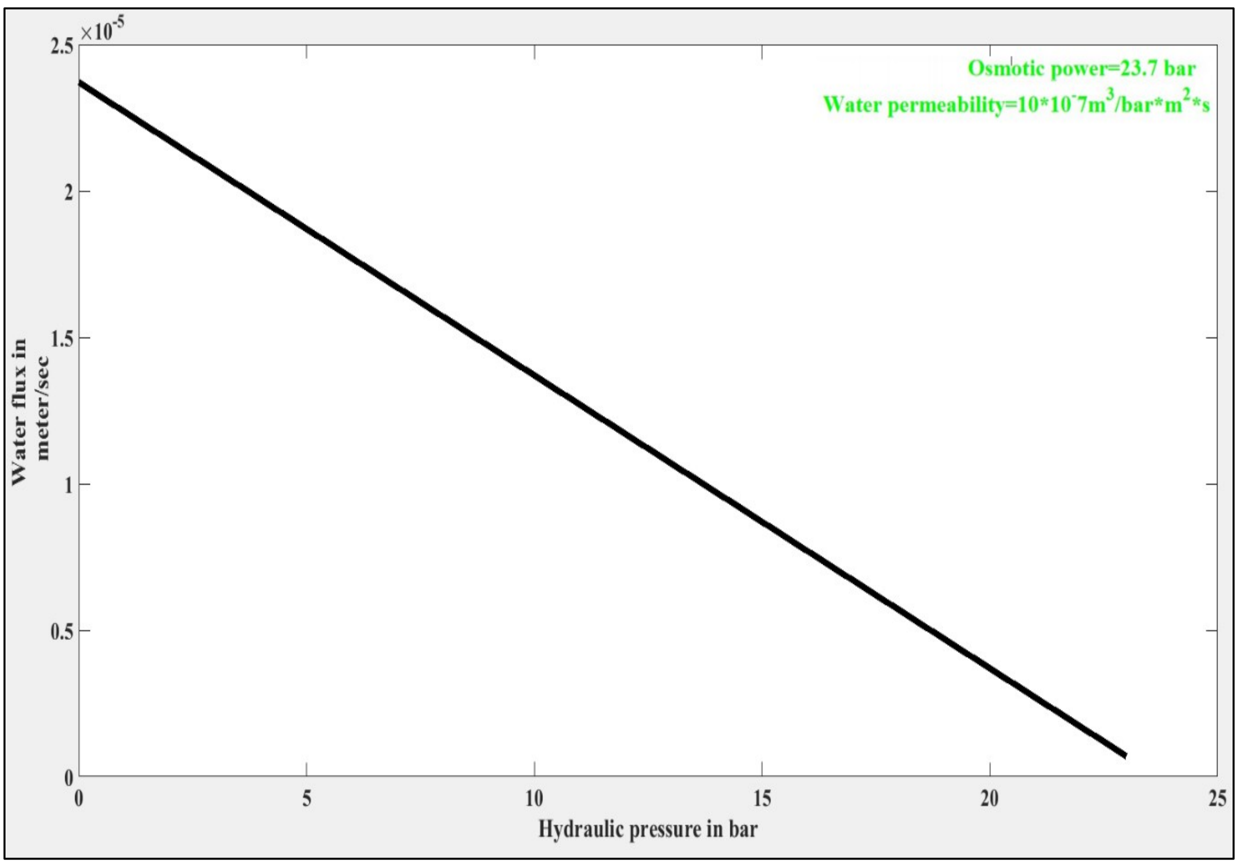

Fig.2.2.Hydraulic pressure versus water flux in an osmotic system

Here, J_w is the water flux in m/s.

A is the water permeability through the membrane in $meter^2$

$\Delta\Gamma$ is the osmotic pressure difference in bar or Pascal.

ΔP is the hydraulic pressure difference in bar or Pascal

$$W = J_w * \Delta P \tag{2.2}$$

where, W = output power in $\frac{watt}{m^2}$.

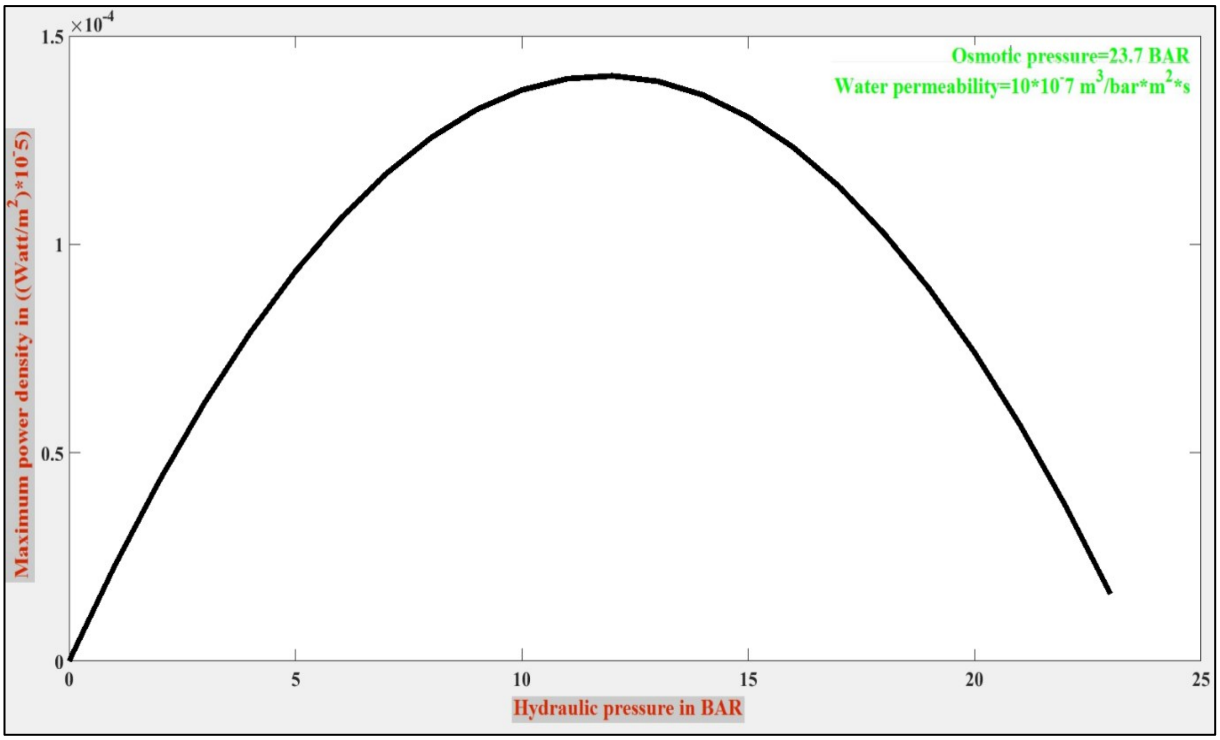

Fig.2.3.Hydraulic pressure versus the Maximum power density

By equating both two equations (2.1) and (2.2), we get:

$$A * (\Delta P)^2 - (A * \Delta\Gamma) * \Delta P + W = 0 \tag{2.3}$$

By taking the derivative with respect to ΔP,

$\Delta P = \Delta\Gamma/2$.

It can be observed from equation (2.3) that the power will attain its maximum value when the applied hydraulic pressure is half of the osmotic pressure. This is also proved from the above Fig. 2.3. To convert these mathematical equations into an electrical circuit, a Matlab simulation study is carried out in the following section.

Case study

Let us consider a case, where the value of osmotic pressure ($\Delta\Gamma$) is equals to 23 bar. To extract the maximum energy, the hydraulic pressure should be half of the osmotic pressure value. Therefore, the hydraulic pressure (ΔP) will be 11.5 bar or 1150000 Pascal. Let us assume the water permeability (A) through the membrane is 10×10^{-9} $m^3/bar\times m^2\times s$.

By substitution of all the values in the equation (2-3), we can get, W = 13225 W or 13.225 kW.

2.2 Circuit model of the PRO system

To represent the osmotic system in the electrical domain, an equivalent circuit is developed based on the resistive load and source voltages, as shown in Fig.2.4. This system is a representation of a PRO model, where one side is fed by sea water and other side is fed by the river water. A membrane with a certain water permeability is inserted in between. The Table. 2.1. shows the proper values of the PRO system.

Table.2.1.Equivalent circuit parameters

Parameters	Presents
Feed side (Fresh water)	Hydraulic pressure
Draw side (Salt water)	Osmotic pressure
Membrane resistance	Inverse of water permeability

Water flux (J)	Flow of current because of the concentration difference

J represents the water flux i.e. practically, the flow of current because of the concentration difference between salt water and fresh water. The source of osmotic pressure has been considered constant, but the hydraulic pressure can be varied by a pump. As the hydraulic pressure should be half the osmotic pressure to extract the maximum power.

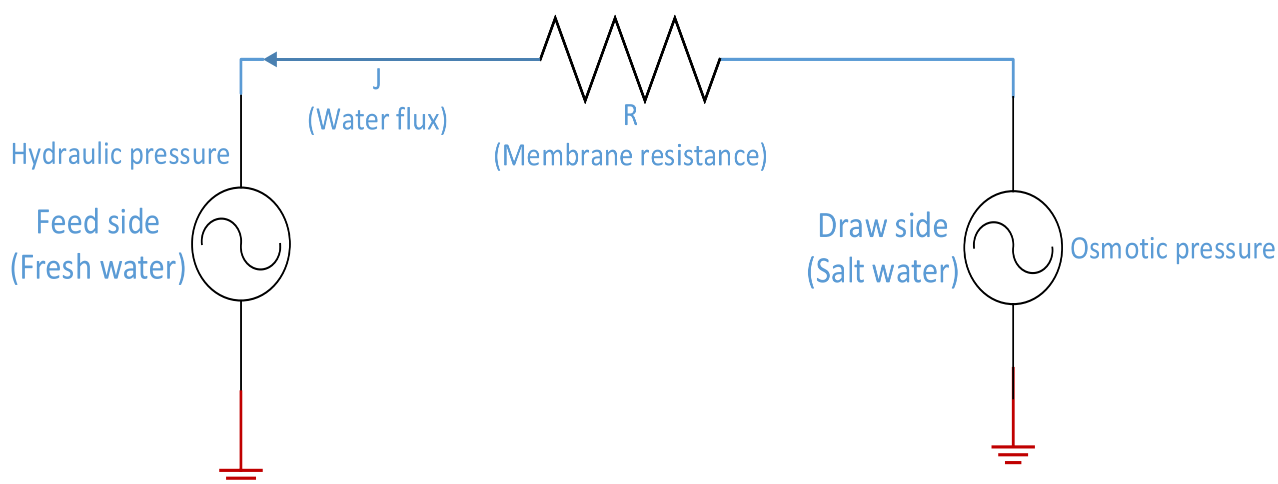

Fig.2.4.Equivalent circuit of Osmotic and Hydraulic pressure

Numerical example

The table below shows all the values for a practical PRO system.

Table. 2.2. Values of equivalent circuit parameters

Parameters	Value
Feed side (Hydraulic pressure)	11.85 bar
Draw side (Osmotic pressure)	23.7 bar
Membrane resistance (Inverse of water permeability)	10×10^{7} pa ×s/m

By using Table 2.2, the water flux J and the power extract W can be calculated as the following:

We know that, $\mathrm{J} = \mathrm{A} * (\Delta\Gamma - \Delta\mathrm{P})$

By putting all the values in this equation, we can find the value of J, which is 0.01185 $m^3/s\times m^2$.

$\mathrm{W} = \mathrm{J} \times \Delta\mathrm{P}$.

By substituting the given values, we can find the value of extract energy, which is 14042 W or 14 kW.

2.3 PSIM of the PRO system

Further the PSIM model is built to derive the system. The practical circuit to derive the system is shown in Fig. 2.5.

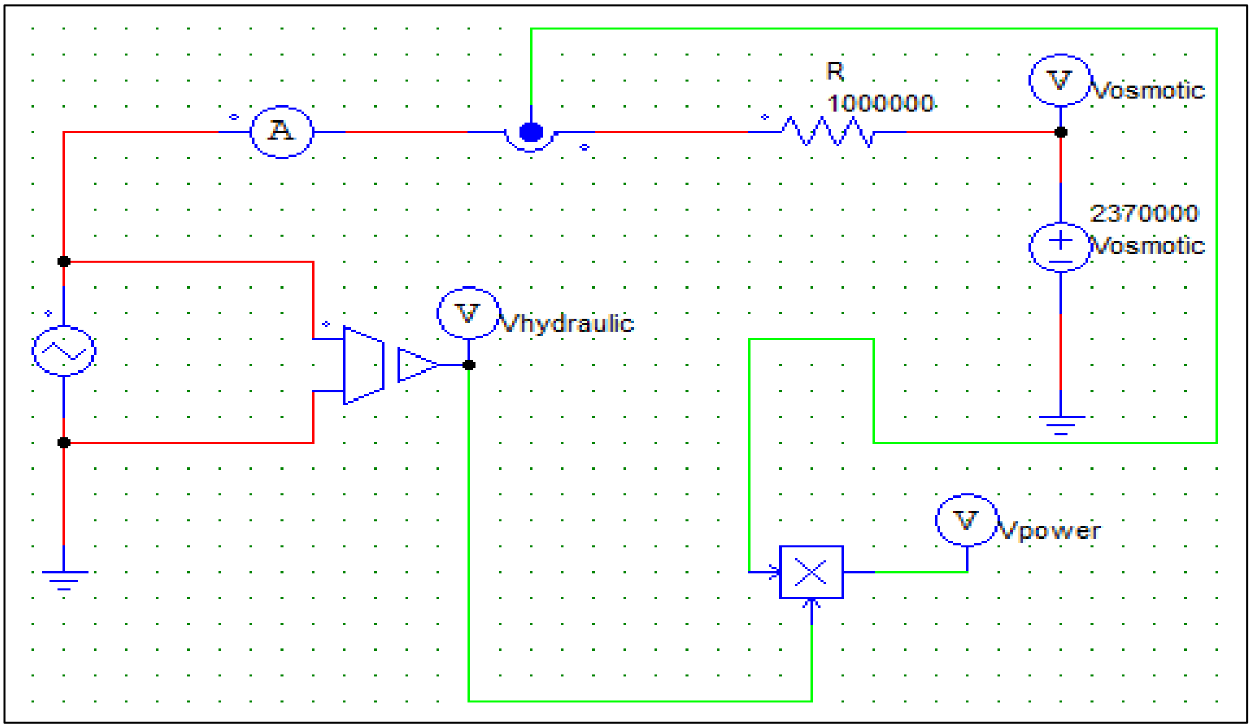

Fig.2.5. The equivalent circuit of the system model in PSIM

In the practical equivalent circuit model, the values of osmotic and hydraulic pressures are taken as 23.7 bar and 11.85 bar, respectively. Where the osmotic pressure has a fixed value, but the hydraulic pressure is changing. The range of hydraulic pressure starts from zero to 2370000 pascal, which is the fixed value of the osmotic pressure. Membrane resistance is taken as 1000 kΩ, which is inverse to the water permeability.

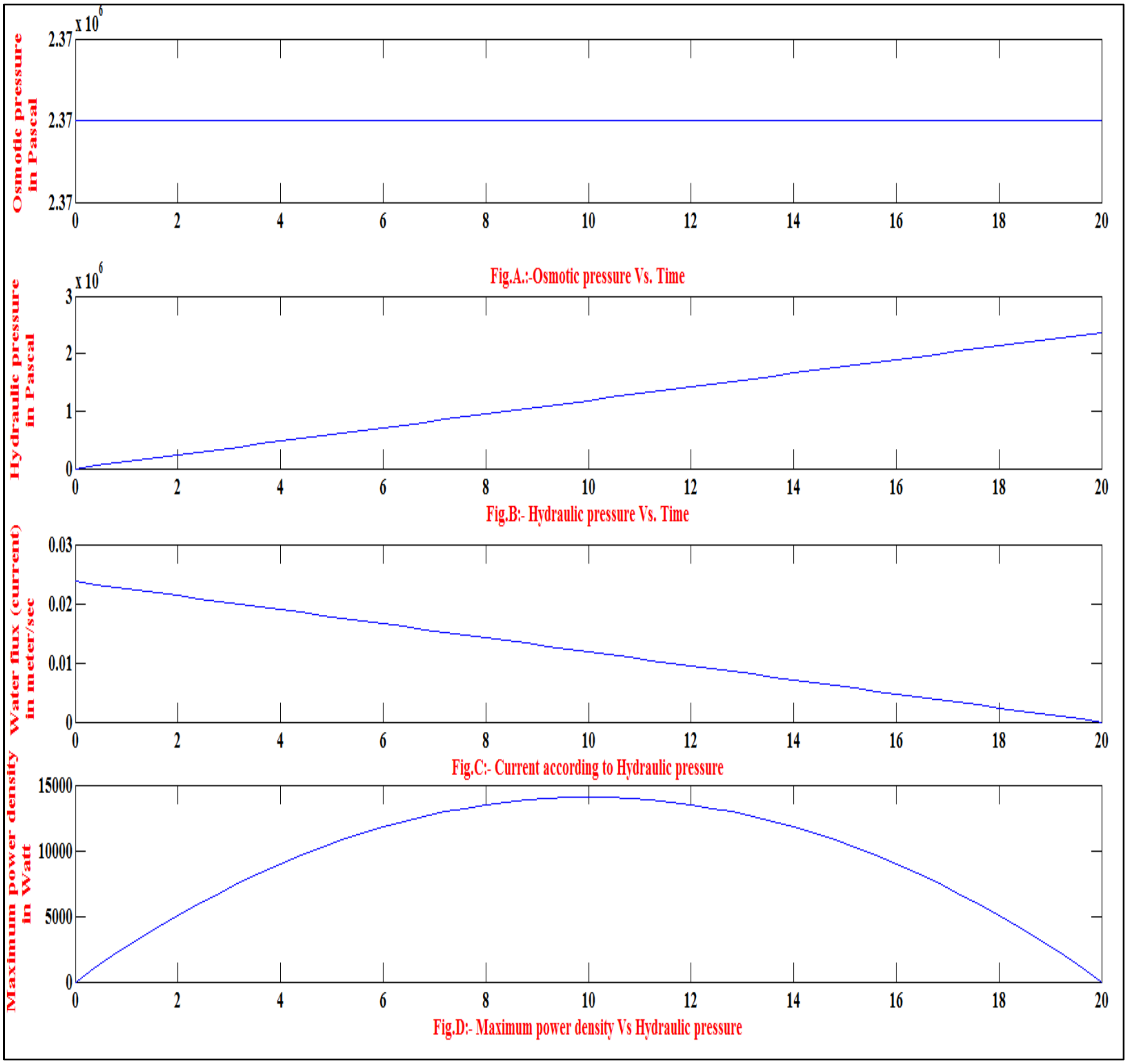

Fig.2.6.Simulation results for change in water flux with hydraulic pressure

Fig. 2.6 shows the simulation results for the change in water flux (Fig. 2.6 C) due to the change in hydraulic pressure (Fig. 2.6 B), when the osmotic pressure kept constant at 23.7 bar (Fig.2.6 A). From the figures it is clear that at starting when hydraulic pressure is zero, it produces the maximum flux and after that, it reduces gradually. For this simulation analysis water permeability is considered as $10x10^{-7}$ $m^3/bar.m^2.s$. When the hydraulic pressure becomes equal to osmotic pressure, the water flux will be zero. (Fig.2.6 D) shows the change in power density of the system, due to the change in hydraulic pressure. It attains its peak when hydraulic pressure is half of the osmotic pressure, as derived in (2.3).

A permanent magnet synchronous generator (PMSG) is used in the load side of the model to generate the voltage and the current outputs. Some model descriptions of the PMSG are given below:

2.4 Some description of permanent magnet synchronous generator (PMSG)

A permanent magnet synchronous generator, where a permanent magnet is used as an excitation field, rather than a coil. As it is called a synchronous generator because the rotor and the magnetic field rotates at the same speed. It runs at the synchronous speed since the magnetic field is generated through a shaft mounted permanent magnet mechanism and the stationary armature is where the current is induced.

A) Mathematical equations of PMSG

The equations for three-phase sinusoidal model electrical system is given below [38].

$$\frac{d}{dt}i_d = \frac{1}{L_d}V_d - \frac{R}{L_d}i_d + \frac{L_q}{L_d}p\omega_m i_q \tag{2.4}$$

$$\frac{d}{dt}i_q = \frac{1}{L_q}V_q - \frac{R}{L_q}i_q - \frac{L_d}{L_q}p\omega_m i_d - \frac{\lambda p\omega_m}{L_q} \tag{2.5}$$

$$T_e = 1.5p[\lambda i_q + (L_d - L_q)i_d i_q] \tag{2.6}$$

The description of parameters and variables used in equations (2.4) to (2.6) are given in Table. 2.3.

Table 2.3.Name of the parameters of PMSG

Symbol	Name of the symbol
$L_{q,}L_d$	q and d axes inductances
R	Resistance of the stator windings
$i_{q,}i_d$	q and d axes currents
$V_{q,}V_d$	q and d axes voltages
ω_m	Angular speed of the rotor
λ	Amplitude of the flux induced by the permanent magnets of the rotor in the stator phases
p	Number of pole pairs
T_e	Electromagnetic torque

B) Phasor diagram of PMSG

In PMSG, the voltage is determined by the load supplied by the generator. The load can be inductive or capacitive. In inductive load, the angle between the rotor and the stator fields will be greater than 90^0 with respect to increased generator voltage. Then it is called overexcited generator. On the other hand, if the load is capacitive, then it is called under excited generator.

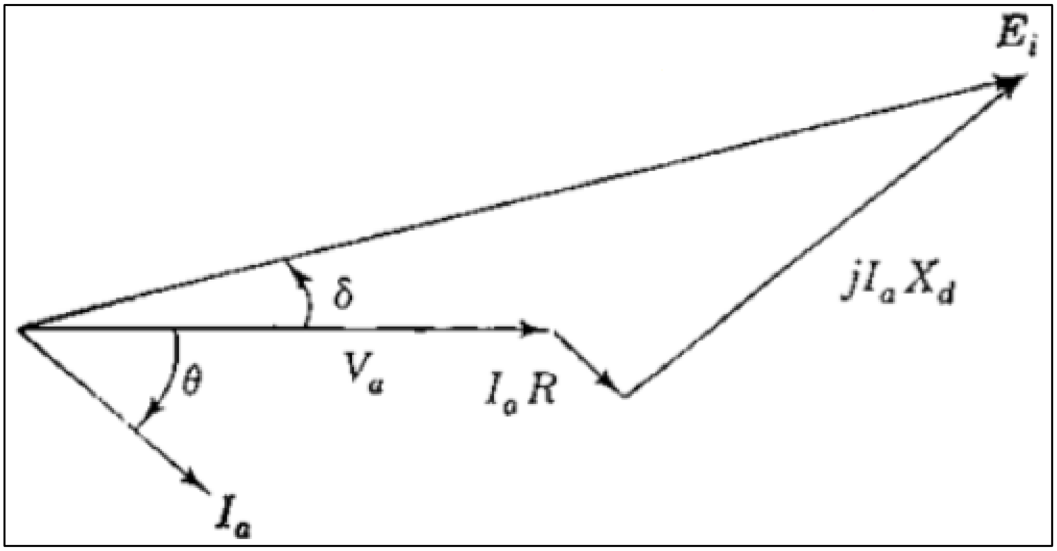

Fig2.7.Phasor diagram of PMSG [38]

In the Fig.2.7, the phasor diagram is shown for an inductive load type where, E_i is the voltage of the generator. V_a and I_a are the voltage and current per phase, respectively. θ is the angle between them. From the resistance R and the reactanceX_d, the angle δ can be determined [38].

2.5 Permanent magnet synchronous generator (PMSG) model in PSIM

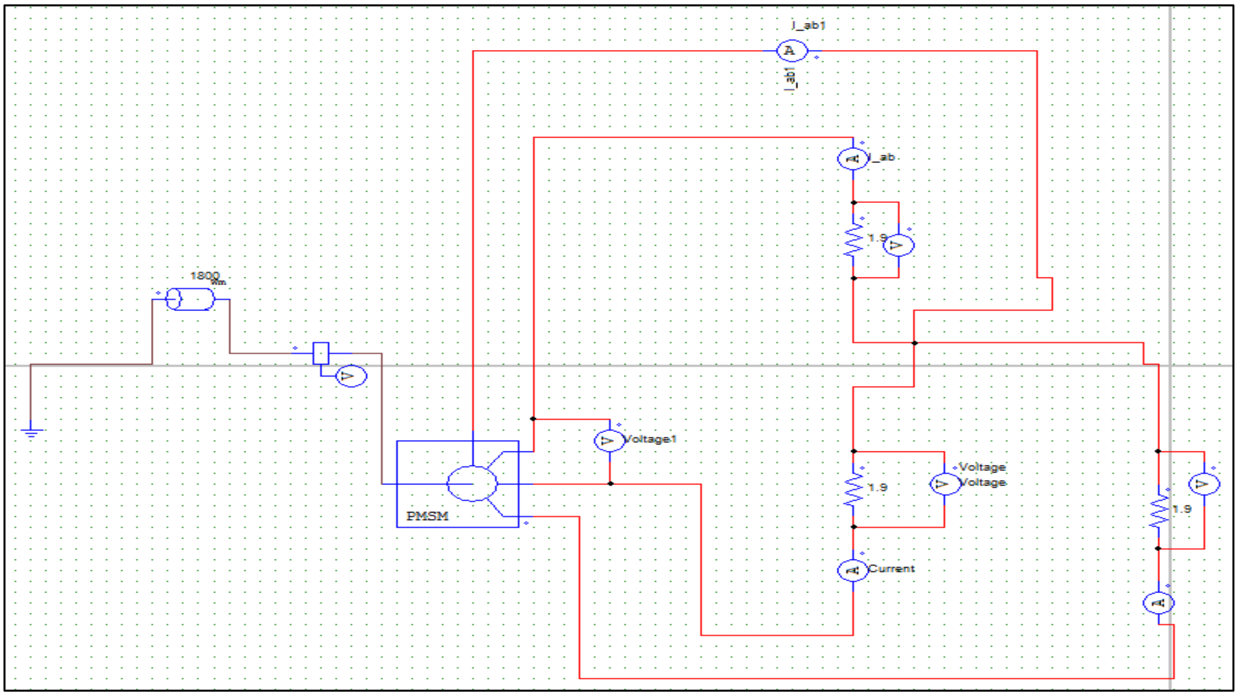

Fig.2.8.Star connection of PMSG in load side

The Table. 2.4. shows the parameters values taken for PSIM.

Table.2.4. Parameters value of PMSG in PSIM model

Parameters	Value
Speed (given as an input)	1800 rpm
Rs (stator resistance)	0.1 Ω
Ld (d-axis inductance)	0.0027 H
Lq (q-axis inductance)	0.0027 H
Vpk/krpm	160 V/rpm
No. of poles	4
Moment of Inertia	0.00179 Kg/m^2

Shaft time constant	10 sec
Torque flag	0
Master/Slave flag	1
Load resistance	1.9 Ω

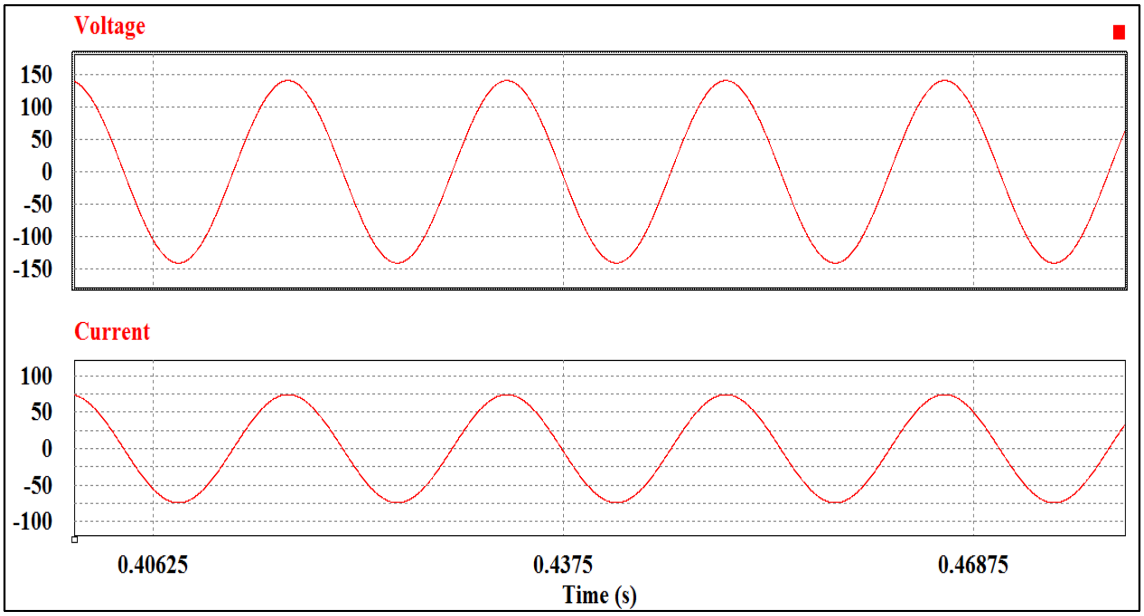

Fig.2.9.Voltage and current outputs from PSIM

Figure 2.9 shows the voltage and current outputs from the PSIM model. A PMSG is used in this model. This model is built to check the system accuracy. As the whole system is built in Matlab/Simulink also and both the output values are compared. The speed input is given same for both Matlab and PSIM model.

2.6 Matlab model of PMSG

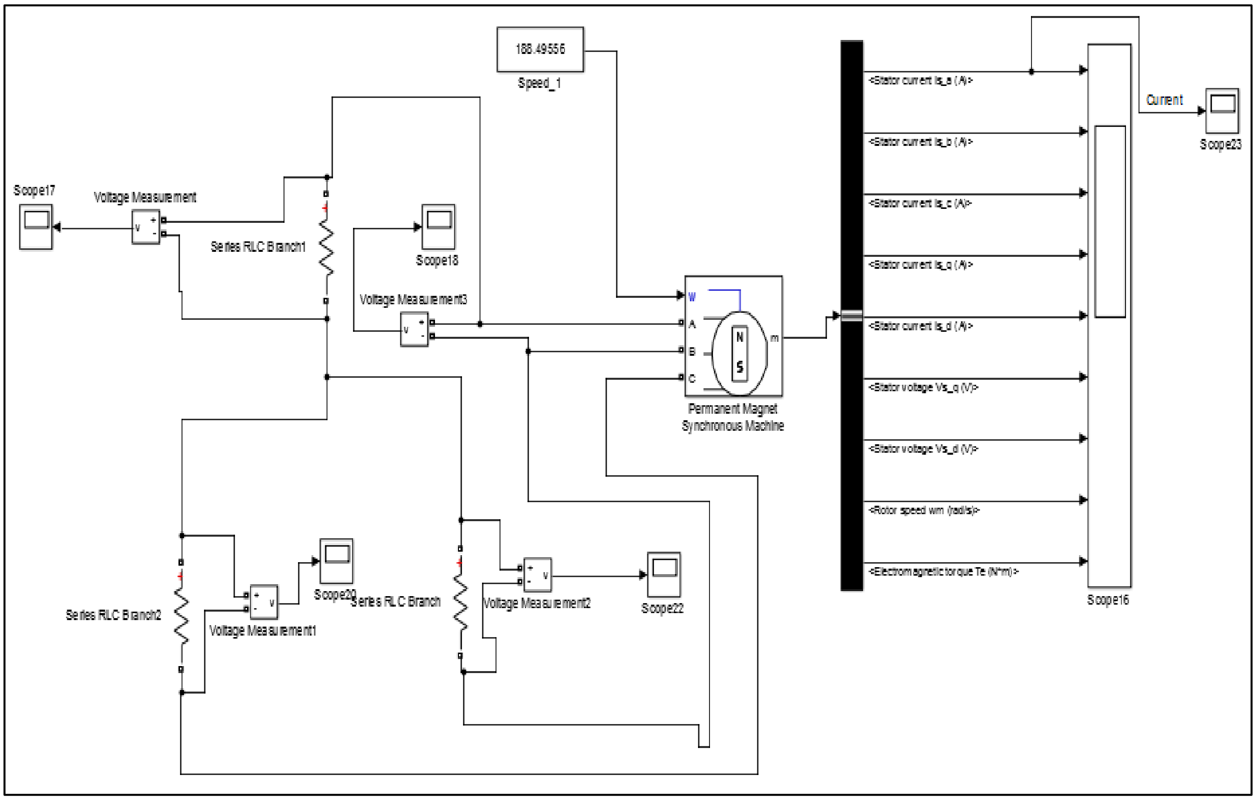

Fig.2.10.The load side of a star-connected PMSG.

Both torque and speed input values are given separately to the PMSG to see the voltage and current. Fig. 2.10 shows the star connection of the load side of the model. The parameter values are given in the table 2.5.

Table.2.5. Parameter values of PMSG in Matlab model

Parameters	Value
Mechanical input (speed)	1800 rpm
No. of phases	3
Back EMF waveform	sinusoidal
Rotor type	round
Stator phase resistance (Rs) in ohm	0.1 Ω
Armature inductance (H)	0.0027 H
Voltage constant (V_peak L-L/krpm)	160 V/rpm
Pole pairs	4
Load resistance	1.9 Ω

Voltage and current output signals from the Matlab model.

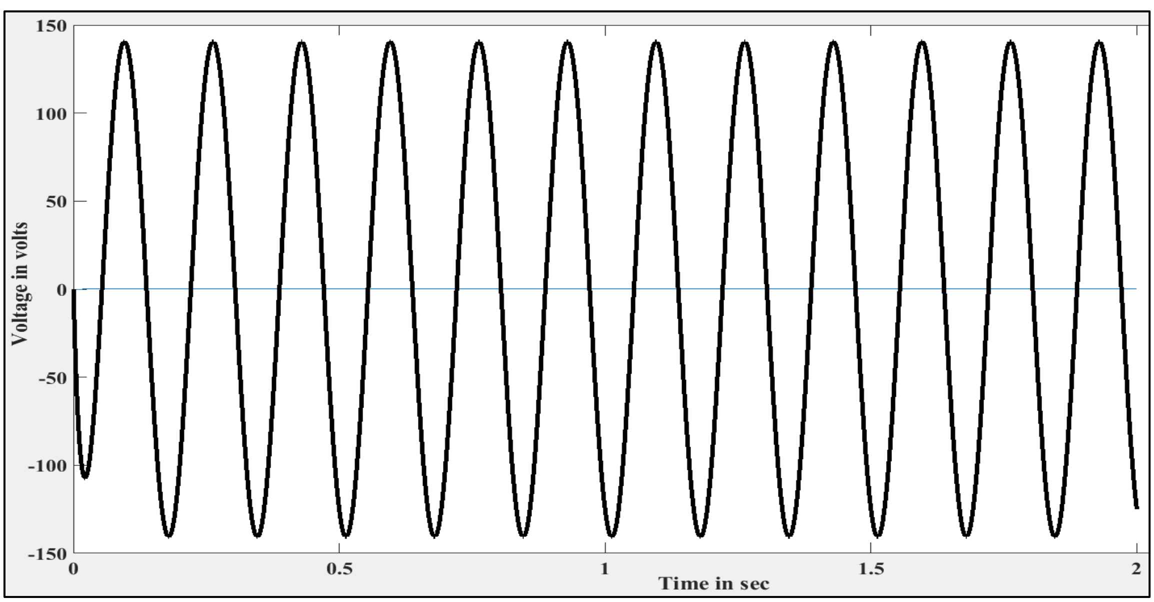

Fig.2.11 (a).Voltage output of Matlab

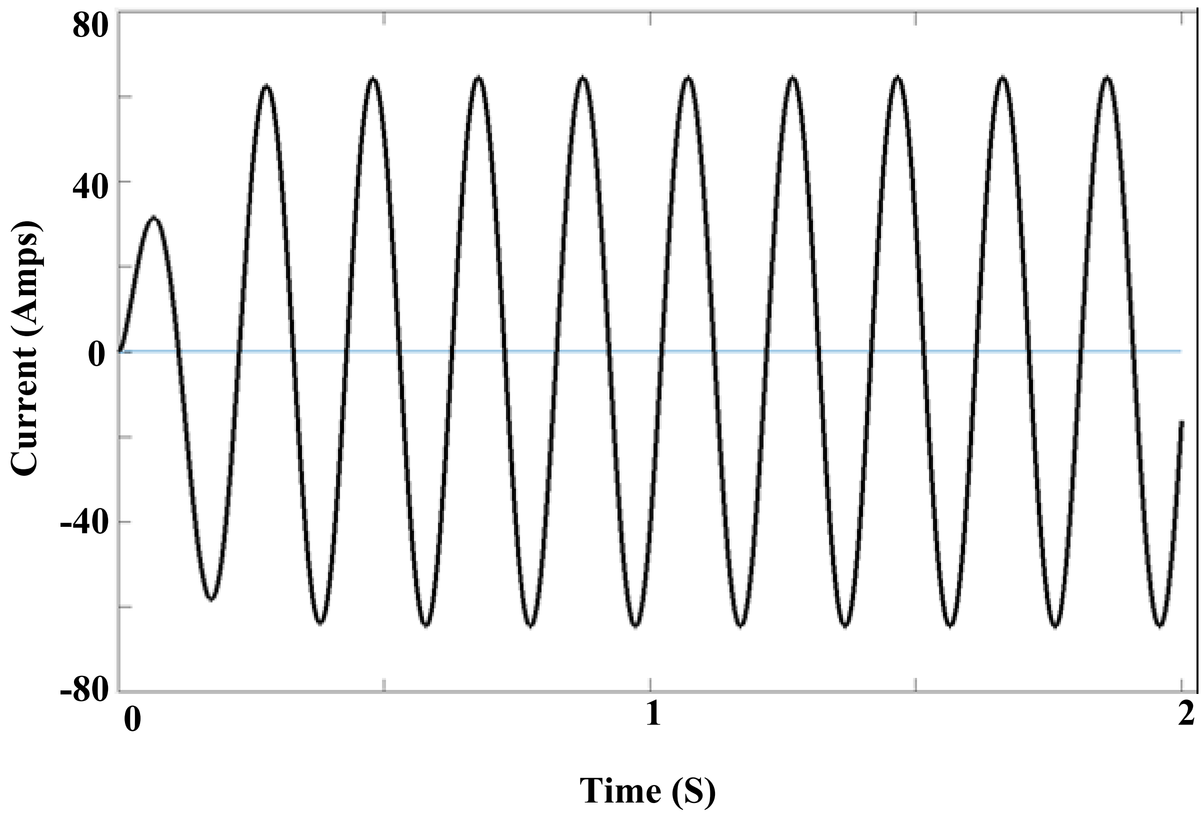

Fig.2.11 (b).Current output of Matlab

It is seen from the Fig.2.11 (a) and (b) that the voltage and current output waveforms are similar to those shown in Fig .2.9, where the voltage and current output waveforms are measured, from the PSIM model. From the both models it is clear that the output values of voltage and current are equal and similar in both Matlab and PSIM.

Chapter 3

CALCULATION OF POWER FLOW IN THE PRO POWER SYSTEM

Figure 3.1 shows the schematic representation of the entire system starting from osmotic power to utility. All the assumptions regarding generator and turbines are provided in table I.

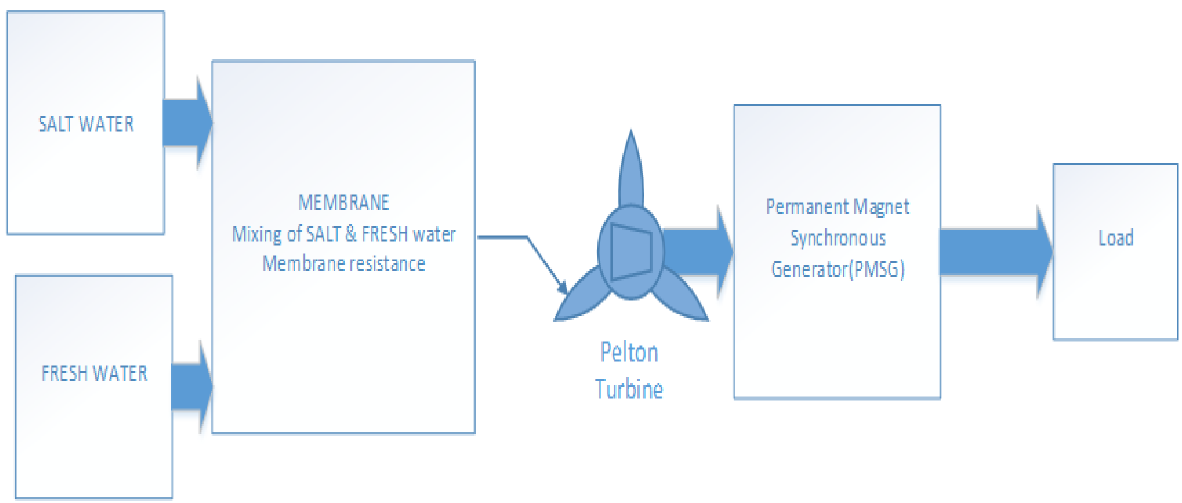

Fig.3.1. The block diagram representation of a hydroelectric system by using a Pelton turbine

A hydro-electric system that uses a Pelton turbine is represented by the block diagram shown in Fig. 3.1 in which, the system starts with two reservoir sources. One represents salt water reservoir and the other represents the fresh water reservoir. Both the sea water and fresh water blocks are then connected to another block, where both the two sources of water are mixed up. There is a membrane in this block, one side of the membrane keeps the sea water and the other side keeps the fresh water, where the membrane prevents the salt to cross it to mix with the fresh water but allows fresh water to come into the salty portion. The water flux which is created because of the pressure across the membrane passes through turbine blade to rotate and run it. A nozzle is also required to control the water flow rate. The turbine is then connected with a permanent magnet synchronous generator (PMSG) to supply the utility. The turbine always needs to run at fixed speed by controlling the nozzle diameter to keep the supply frequency constant.

Another way, in which the nozzle diameter is controlled to allow the maximum flow to pass through it and to control the generator to run at a fixed speed. This can be done by using a gearbox in between the turbine and the generator. Hence, the frequency is maintained constant.

Detailed calculation of turbine parameters for a fixed load is provided in the following section.

3.1 Turbine selection

Selection of an appropriate turbine totally depends on two factors: the available flow rate and water head. The impulse turbines are used for high head sides and reaction turbines are used for low head sides. Another concept is that for reaction turbine, flow rate should be high, while in Pelton turbine the head should be between 50 to 1300 m.

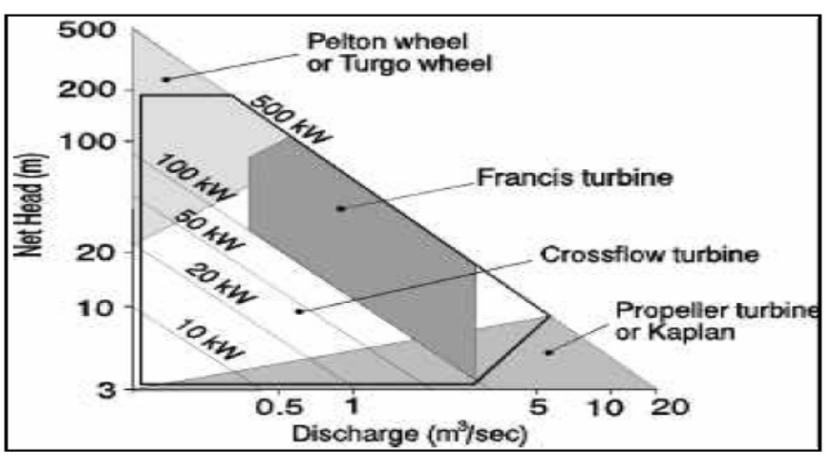

Fig.3.2.Turbine selection based on head and discharge rate

3.2 Turbine parameters calculations

This system is designed for a fixed load with a direct drive, where turbine is directly connected with PMSG by flexible shaft coupling. Hence, turbine and generator will run at the same speed. When the load power increases, the generator speed reduces and the supply frequency drops. To maintain the supply frequency at its desired level, turbine needs to provide the additional torque. This is done by varying the jet diameter (d) to increase the flow rate of water that strikes the buckets attached to the turbine.

$$P_{gen\_in} = \frac{P_{gen\_out}}{efficiency} \tag{3.1}$$

where, P_{gen_in} represents the input power of the generator and P_{gen_out} represents the output power of the generator.

As we need to get a fixed output power, whereas our load frequency and generator efficiency is also constant. Therefore, we can calculate the generator input power.

Once we know the generator input power, we can calculate the torque (T) from the equation.

where,

$$\text{torque(T)} = P_{gen\_in} / \omega(\text{speed}) \tag{3.2}$$

and ω (speed) can be calculated from the following equation,

$$\omega = 2 \times \pi \times N \tag{3.3}$$

$$N = \frac{(120 \times f)}{P} \tag{3.4}$$

where f and P represents frequency and no. of poles respectively.

Therefore,

$$\omega = (2 \times \pi \times \left(\frac{(120 \times f)}{P}\right))/60 \ \text{rad/sec} \tag{3.5}$$

as there is no gearbox between the turbine and the generator. So turbine and generator will run at the same speed. And the turbine output is equal to the generator input.

Again, $$P_{turbine\_in} = P_{turbine\_out} / \text{ efficiency} \quad (3.6)$$

Once we calculate the turbine input, we can calculate the height of the water fall.

Practically, for a PRO (pressure retarded osmosis), the sea and the river water are at same level. So net height is zero. But for Pelton turbine, the osmotic pressure difference is considered as a height.

As 20 bar of osmotic pressure different can produce an energy equivalent from a waterfall of 210 m height [4].

Then water height will be, $$H = P/(\rho * 9.81) \quad (3.7)$$

where δ, P, and H represents the water density, turbine input power and equivalent water height respectively. Once calculating the equivalent height, jet velocity can be calculated further. We consider an ideal (frictionless) case for a Pelton turbine, where all the potential energy is converted to kinetic energy. The potential energy, Eg is mgH and the kinetic energy E_k is $mv^2/2$. By equating both of them, Potential energy is equal to Kinetic energy.

$$mgH = mv^2/2.$$

Therefore, $v = \sqrt{2 \times H \times g}$

Jet velocity, $$v_j = C_v \times \sqrt{2 \times H \times 9.8} \quad (3.8)$$

where c_v represents the jet velocity co-efficient.

3.3 Calculation of jet velocity

An assumption can be held, the applied jet velocity is higher than the runner velocity, as there will be some losses in the runner. According to the conservation of mass, the mass entering the runner must be equal to the mass leaving the runner.

As how much jet velocity we apply, it will not be fully converted into the turbine speed (Because of losses and other issues). We need to calculate exactly how much converter to the turbine speed will be. And we consider a constant jet speed relative to the runner. Therefore, the jet velocity relative to the runner is, $\{-(V_i - u)\}$

where V_i = initial jet velocity and u is the runner velocity.

The final velocity will be, $V_f = [\{-(V_i - u)\} + u] = -V_i + 2u$

For ideal runner speed, the water speed leaving the runner should be zero.

Therefore, $[-V_i + 2u] = 0$

So the optimal runner speed will be $u = V_i/2$ (3.9)

Therefore, the effective jet velocity will be,

Effective jet velocity, $v_t = 0.46 v_j$ (3.10)

$$P_{turbine\_inp} = (Q \times \rho)\{(v_j - v_t)(1 - \cos\beta)\}v_t \quad (3.11)$$

From equation no (3.11), we can calculate the water flow rate (Q).

$Q = v_j . A = v_j .(\pi.d_j^2/4)$ (3.12)

where, A= nozzle area,

Once we find the nozzle diameter (d_j), we can calculate the pipe diameter.

where pipe diameter, $D = (60.\ v_t)/(\pi.\omega_{rpm})$

3.4 Numerical calculations

Table.3.1. List of assumed parameter values

Variables	Corresponding values
Turbine & generator speed	1800 rpm
No of poles in the generator	4 pole
Generator efficiency	95%
Pelton turbine efficiency	90%
Penstock diameter between the reservoir to the turbine in mm (from the manufacturer)	100 mm
Membrane resistance	100000000 pa.s/m^3
Salt concentration of sea water in g/L	35 g/L
Pressure available from the salt water in bar	23.7 bar
Pressure available from the fresh water in bar	11.85bar

For numerical calculations, we consider we need an output of around 12 kW.

For our application, load frequency is fixed at 60 Hz and generator efficiency is (η) 95.0%. Hence, input power of generator and torque would be

$$P_{gen_{in}} = \frac{12000}{\eta} = 12631.57 \text{ W} \quad (3.13)$$

$$T_{gen\_in} = P_{gen\_in} / \omega \quad (3.14)$$

Here, to generate 60Hz supply frequency with 4 pole generator, speed (ω) needs to be at

$$\omega = (2 \times \pi \times \left(\frac{(120 \times f)}{P}\right))/60 = 188.49 \text{ rad/sec} \quad (3.15)$$

Hence, from (3.14) generator torque would be

$$T_{gen\_in} = 67.01 \text{Nm} \quad (3.16)$$

As, the turbine is connected directly to the generator, turbine also needs to supply the same load torque and power.

P turbine_out $= 12631.57$ W

If we consider turbine efficiency of 90%, the input power will be

$P_{turbine\_inp} = 14035.077$ W

Now, based on the simulation studies the volume flow rate (Q), pressure difference (P) and water density (δ) are calculated as 0.0125 m^3/sec, 11850000 Pac and 1029 kg/m^3 respectively.

Hence, from Bernoulli's equation, the reserve height (H) and fluid velocity (v) can be calculated as

$$H = \frac{P}{(\delta.9.81)} = 117.39 \text{ m} \quad (3.17)$$

$$v_j = C_v \times \sqrt{2 \times H \times 9.8} = 45.08 \text{ m/sec} \quad (3.18)$$

Here, c_v is the jet velocity coefficient. So, to extract the maximum power from turbine, the maximum speed of rotation will be

$$v_t = 0.46 \times v_j = 0.46 \times 45.08 = 20.74 \text{ m/sec} \tag{3.19}$$

Now, the power developed by turbine can be represented as:

$$P_{turbine\_inp} = (Q \times \delta)\{(v_j - v_t)(1 - \cos\beta)\}v_t \tag{3.20}$$

$\therefore Q = 0.01373 \text{m}^3\text{/sec}$

Here, β is considered as 180° and all other values are taken from the other derived equations.

Again, flow rate can be represented as

$$Q = v_j \times A = v_j \times \left(\pi \times \frac{d_j{}^2}{4}\right) \tag{3.21}$$

$d_j = 0.01$ m

Here, A is the nozzle cross sectional area and d_j is the effective diameter of the nozzle.

From turbine speed, turbine diameter can also be calculated as:

$$D = \frac{(60 \times v_t)}{(\pi \times \omega_{rpm})} = 0.22 \text{ m} \tag{3.22}$$

Hence, the ratio between turbine and jet diameter can be represented as

$d_j / D = 11.17$

C) Case study 1

(For 100 kW power generation)

For numerical calculations, we consider we need a output of around 100 kW.

For our application load frequency is fixed at 60 Hz and generator efficiency is (η) 95.0%. Hence, input power of generator and torque would be

$$P_{gen_{in}} = \frac{100000}{\eta} = 105{,}263.1579 \text{ W} \tag{3.23}$$

$$T_{gen\_in} = P_{gen\_in} / \omega \tag{3.24}$$

Here, to generate 60Hz supply frequency with 4 pole generator, speed (ω) needs to be

$$\omega = \frac{2\times\pi\times\left(\frac{(120\times f)}{P}\right)}{60} = 188.49 \text{ rad/sec} \tag{3.25}$$

Hence, from (13) generator torque would be

$$T_{gen\_in} = 558.45\text{Nm} \tag{3.26}$$

As, the turbine is connected directly to the generator, turbine also needs to supply the same load torque and power.

$$P\ turbine\_out = 105{,}263.15 \text{ W}$$

If we consider turbine efficiency of 90%, the input power would be

$P_{turbine\_inp}$ = 116,959.06 W

Now, based on the simulation studies the volume flow rate (Q), pressure difference (P) and water density (δ) are calculated as 0.0125 m^3/sec, 11,850,000 Pascal and 1029 kg/m^3 , respectively.

Hence, from Bernoulli's equation the reserve height (H) and fluid velocity (v) can be calculated as

$$H = \frac{P}{(\delta.9.81)} = 117.39 \text{ m} \tag{3.27}$$

$$v_j = C_v \times \sqrt{2 \times H \times 9.8} = 45.08 \text{ m/sec} \tag{3.28}$$

Here, c_v is the jet velocity coefficient. So, to extract the maximum power from turbine, the maximum speed of rotation would be

$$v_t = 0.46 \times v_j = 0.46 \times 45.089 = 20.74 \text{ m/sec} \tag{3.29}$$

Now, the power developed by turbine can be represented as

$$P_{turbine\_inp} = (Q \times \rho)\{(v_j - v_t)(1 - \cos\beta)\}v_t \tag{3.30}$$

$\therefore Q = 0.11358\ m^3/sec$

Here, β is considered as 169° and all other values are taken from the other derived equations.

Again, flow rate can be represented as

$$Q = v_j \times A = v_j \times \left(\pi \times \frac{{d_j}^2}{4}\right) \tag{3.31}$$

$d_j = 0.05$ m

Here, A is the nozzle cross sectional area and d_j is the effective diameter of the nozzle.

From turbine speed, turbine diameter can also be calculated as

$$D = \frac{(60 \times v_t)}{(\pi \times \omega_{rpm})} = 0.22 \text{ m} \tag{3.32}$$

Hence, the ratio between turbine and jet diameter can be represented as

$d_j / D = 11.17$.

D) Case study 2

(For 250 kW power generation)

For numerical calculations, we consider we need an output of around 250 kW.

For our application load frequency is fixed at 60 Hz and generator efficiency is (η) 95.0%. Hence, input power of generator and torque would be

$$P_{gen_{in}} = \frac{250000}{\eta} = 263{,}157.89 \text{ W} \tag{3.33}$$

$$T_{gen\_in} = P_{gen\_in} / \omega \tag{3.34}$$

Here, to generate 60Hz supply frequency with 4 pole generator, speed (ω) needs to be at

$$\omega = (2 \times \pi \times \left(\frac{(120 \times f)}{P}\right))/60 = 188.49 \text{ rad/sec} \tag{3.35}$$

Hence, from (3.34) generator torque would be

$$T_{gen\_in} = 1396.13 \text{ Nm} \tag{3.36}$$

As, the turbine is connected directly to the generator, turbine also needs to supply the similar load torque and speed.

$$\text{P turbine}_{out} = 263{,}157.89 \text{ W}$$

If we consider turbine efficiency of 90% (assume), the input power would be

$$P_{turbine\_inp} = 292{,}397.66 \text{ W}$$

Now, based on the simulation studies the volume flow rate (Q), pressure difference (P) and water density (δ) are calculated as 0.0125 m^3/sec, 11850000 Pac and 1029 kg/m^3 respectively.

Hence, from Bernoulli's equation the reserve height (H) and fluid velocity (v) can be calculated as

$$H = \frac{P}{(\delta.9.81)} = 117.39 \text{ m} \tag{3.37}$$

$$v_j = C_v \times \sqrt{2 \times H \times 9.8} = 45.08 \text{ m/sec} \tag{3.38}$$

Here, c_v is the jet velocity coefficient. So, to extract the maximum power from turbine, the maximum speed of rotation will be

$$v_t = 0.46 \times v_j = 0.46 \times 45.08 = 20.74 \text{ m/sec} \tag{3.39}$$

Now, the power developed by turbine can be represented as

$$P_{turbine\_inp} = (Q \times \delta)\{(v_j - v_t)(1 - \cos\beta)\}v_t \tag{3.40}$$

$\therefore Q = 0.283 \, m^3/\text{sec}$

Here, β is considered as 169° and all other values are taken from the other derived equations.

Again, flow rate can be represented as

$$Q = v_j \times A = v_j \times \left(\pi \times \frac{d_j^2}{4}\right) \tag{3.41}$$

$d_j = 0.056633$ m

Here, A is the nozzle cross sectional area and d_j is the effective diameter of the nozzle.

From turbine speed, turbine diameter can also be calculated as

$$D = \frac{(60 \times v_t)}{(\pi \times \omega_{rpm})} = 0.22 \text{ m} \tag{3.42}$$

Hence, the ratio between turbine and jet diameter can be represented as

$d_j /D = 11.173$.

3.5 The range of osmotic pressure in seawater

Salinity and temperature affect the density of seawater. At a salinity of 35%, and a temperature of 0^0 C, seawater has an osmotic pressure of 23.37 bar (23.07 atm).Whereas at the same salinity but at 20^0 C, it has an osmotic pressure of 25.01 bar (24.96 atm).

At 0^0 C, seawater having a salinity of 30-37%, has a corresponding density range of 1.024 to 1.030 g cm^{-3}. There are some other causes that affect the sea water density [27].

They are

i) Dilution of seawater by less-saline water.

ii) Dilution by rain or snow.

iii) Concentration through the surface evaporation.

iv) Freezing, which excludes salts from ice and thus leaves any residual, unfrozen water more saline.

v) Thawing the ice, which dilutes the already existent saline.

3.6 The effect of temperature on the water permeate flux

There is an effect of temperature on the water permeate flux. For this test, we increase the feed water temperature, where the coolant temperature was constant. After calculating different values of ΔT (temperature difference), where ΔT is the difference between the feed temperature and the coolant temperature. It can be seen that when we increase the temperature, the water flux also increases. For an example, water flux will go from 0.9 kg/(h m^2) to 5.3 kg/(h m^2), if we increase the temperature from 20^0 C to 65^0 C. This phenomenon happens because of the increased vapor pressure and heat transfer at higher temperature difference. From Fig. 3.4, it is clear that the permeate flux is highly sensitive to the temperature difference across the membrane [27].

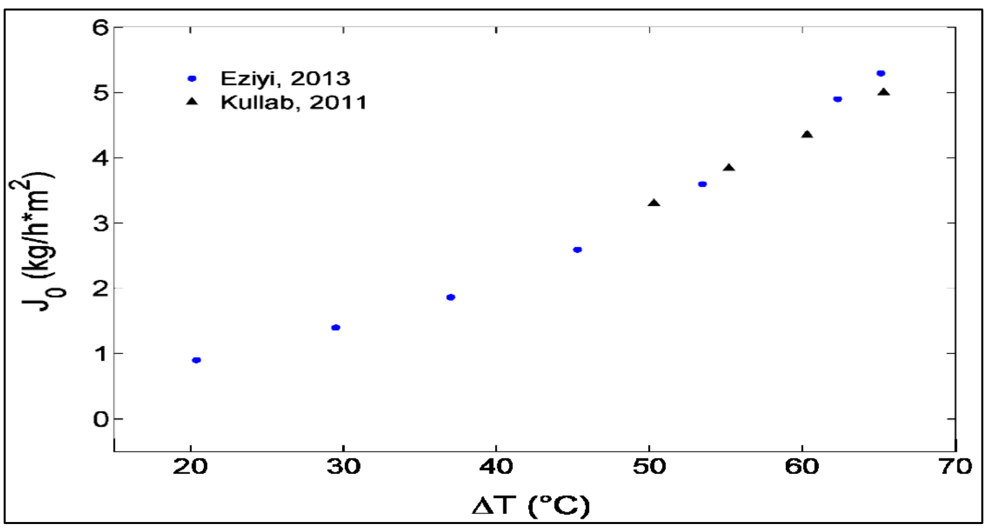

Fig.3.3. Effect of temperature difference (feed temperature – coolant temperature) on the water permeate flux [27]

Temperature has another effect such as the specific energy consumption (kWh/m^3), which decreases when the feed temperature increases. The reason behind is that by increasing the feed water temperature, the vapor pressure also increases. This increased pressure is nothing but the driving force for the water vapor to pass through the membrane. As a result, the consumption of energy has become lower, when the vapor pressure increases. Another effect is that, when salt concentration increases in feed water, the energy consumption also increases [27]. These two phenomena are clear in Fig. 3.4.

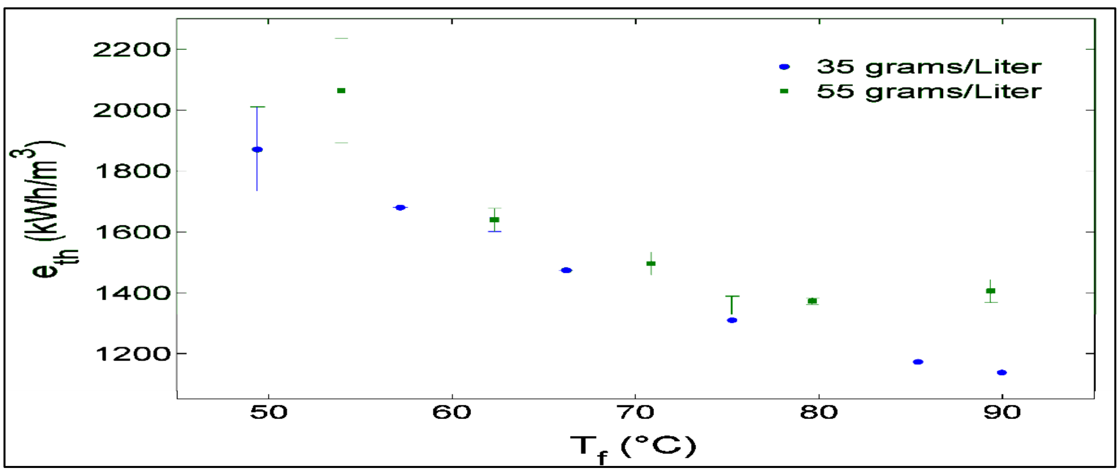

Fig.3.4. Variation of energy consumption with different feed solution temperature and for different salt concentration [27]

CASE STUDY

From the above explanations, it is clear that the salt concentration can be affected by temperature and other issues.

i) We consider a salt concentration of 35 g/L.

The osmotic pressure, $\Delta\Gamma$ can be calculated from the following equation.

$$\Delta\Gamma = (i_v \times \Delta C_m \times R_g \times T) / M \qquad (3.43)$$

where, $\Delta\Gamma$, i_v, $\Delta C_{m,}$ R_g ,T, and M represents the osmotic pressure, vants Haff co-efficient, salt concentration, universal gas constant, temperature and molar mass of the salt, respectively[4].

The value of R_g is 0.083145 L.bar/moles.K and temperature is 293.15 kelvin (20^0 C).

Where i_v has a constant value of 2. And the value of M is 58.44 g/ mol.

By putting all the values in equation (3.43), we can get,

$\Delta\Gamma$= 29 bar.

ii) We consider the salt concentration drops because of some environmental effect.

Therefore, new salt concentration will be 30 g/L (ΔC_m)

Again by putting all the values in equation (3.42), we can find $\Delta\Gamma$ (osmotic pressure), which is 25 bar.

where the water permeate flux (J_w) is given by the following equation.

$$J_W = A \times (\Delta\Gamma - \Delta P) \tag{3.44}$$

Where ΔP is the hydraulic pressure difference and A is the water permeability. We consider the hydraulic pressure as half of the osmotic, because the maximum power can be extracted when the hydraulic pressure is half of the osmotic.

Therefore, ΔP (hydraulic pressure) will be 12.5 bar.

The water permeability (A) is 10^{-12} $m^3/m^2 \times s \times pa$ [5].

By substituting all the values in equation (3-44), we can get the water permeate flux of 1.25×10^{-6} m/s.

We calculated the osmotic pressure as 25 bar, which is equal to 2,500,000 Pascal. To extract the maximum power, the hydraulic pressure should be half of the osmotic and it will be 12.5 bar. The pressure difference (p) will be (osmotic pressure – hydraulic pressure), which is 12.5 bar or 1,250,000 Pascal. Where the water density (ρ) is 1029 kg/m^3.

We know that, equivalent height (H)= $\frac{\text{pressure(p)}}{(\rho \times 9.81)}$.

From this equation, we can get the equivalent height, which is 123.8299 m.

From this, we can calculate the jet velocity (v_j), where the jet velocity comes from the following equation,

$$v_j = C_v \times \sqrt{2 \times \mathrm{H} \times 9.8} \tag{3.45}$$

where C_v is the jet velocity co-efficient. The calculated v_j will be 46.309 m/sec.

If we consider the nozzle diameter as constant, which is 0.0196 meter, the flow rate (Q) can be calculated from the following equation [33].

$$\mathrm{Q} = v_j \times \mathrm{A} = v_j \times \left(\pi \times \frac{{d_j}^2}{4}\right) \tag{3.46}$$

Therefore Q (flow rate) will be 0.013 m^3/sec.

Here we know that the flow rate (Q), water density (ρ), jet velocity (v_j) will be 0.013972 m^3/sec, 1029 kg/m^3 and 46.309 m/sec, respectively.

For calculating the effective jet velocity (v_t), it will be 21.302 m/sec.

By putting all these values in equation (3.46) we find,

$$P_{\text{turbine\_inp}} = (Q \times \delta)\{(v_j - v_t)(1 - \cos\beta)\}v_t \tag{3.47}$$

Turbine input will be 15317.43 W, where β is considered as 169^0 [33].

As we know that the turbine and generator outputs are 90% and 95% respectively. Therefore turbine output is 13785.777 W and the generator output is 13,096.488 W. So at the load we can get a power of 13,096.488 W.

3.7 Calculating the desired torque and speed of the Pelton turbine

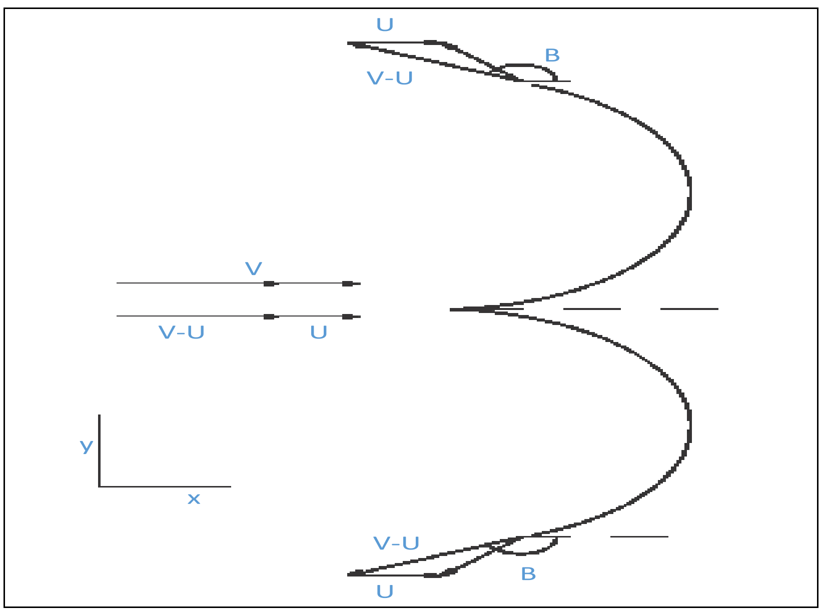

Fig.3.5.Water flow over the Pelton turbine bucket

The above figure shows the flow of water through the Pelton turbine, where V is the jet velocity and U is the blade velocity. Therefore the change in velocity along the X axis is

$$dv = (V - U) - (V - U)\cos\beta \tag{3.48}$$

For the change in velocity, the expression for the force on the bucket becomes

$$f = \rho \times Q \times (V - U) \times (1 - \cos\beta) \tag{3.49}$$

where the torque is measured by the force multiply by the displacement.

Therefore, the DC motor torque equation becomes:

$$M_T = \left[\left(\rho \times Q \times V \times \frac{D}{2}\right) - \left(\rho \times Q \times U \times \frac{D}{2}\right)\right] \times (1 - \cos\beta) \tag{3.50}$$

where, ρ = water density = 1029 kg/ m.

Q is the flow rate.

V is the jet velocity.

U is the turbine blade speed.

D is the turbine blade diameter.

From the above equation, by substituting all the values, we can get the motor torque which is 69.4 Nm. This value is applied to the DC motor side as the input torque [40].

3.8 MPPT for finding the speed for getting the maximum Power

By putting U= D/2×ω, the relationship between speed and torque can be found as the following:

where,

$$M_T = (\rho \times Q \times V \times D) - (\rho \times Q \times \frac{D^2}{2} \times \omega) \tag{3.51}$$

Therefore the Power equation will be,

$$P = (\rho \times Q \times V \times D \times \omega) - (\rho \times Q \times \frac{D^2}{2} \times \omega^2) \tag{3.52}$$

Values can be found from the Table 3.2

Table.3.2. Parameters values for calculating MPPT

Parameters	Value
Water density (ρ)	1029 kg/m^3
Flow rate (Q)	0.013 m^3/sec
Jet velocity (V)	45.08 m/sec
Turbine blade diameter (D)	0.22 m

Putting this equation in Matlab code, we can find the value of the particular speed, where power will be maximum [40]. The Power-speed curve is shown in Fig. 3.6.

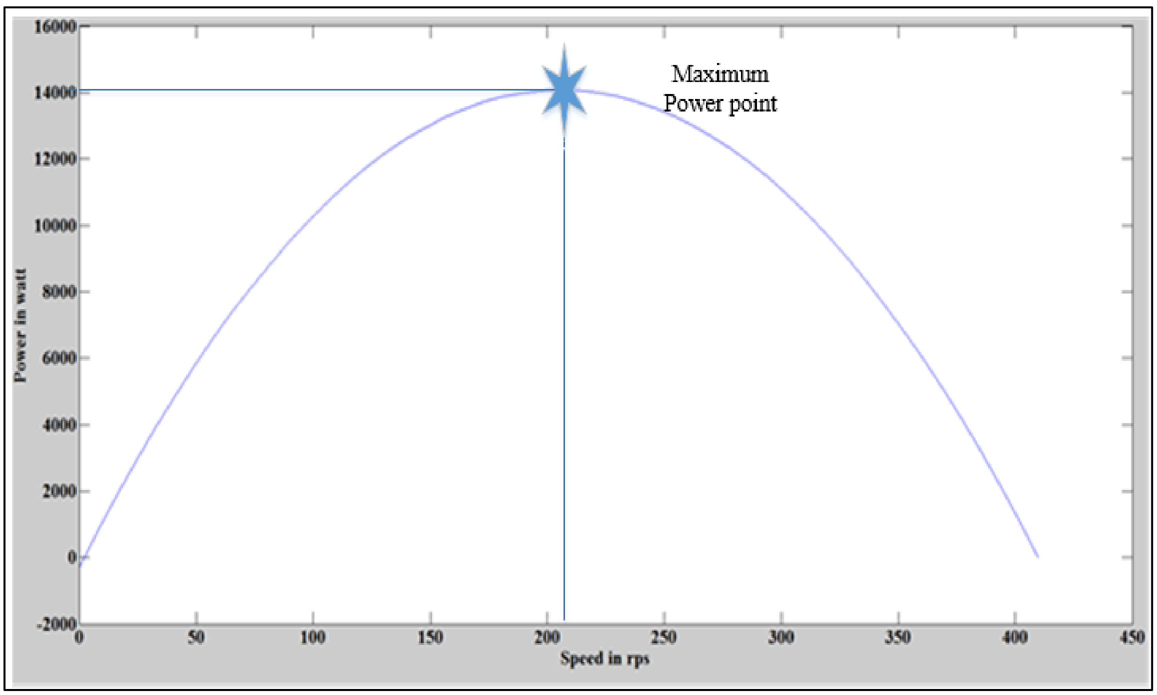

Fig.3.6.Power-speed characteristics

From Fig. 3.6, speed starts from zero, when power achieved also zero at the starting condition. At that time, rotation of the turbine is zero. After that when turbine rotation increases the extracted power also increases. At a certain speed, which is around 205 rps, maximum power can be extracted. This point is called maximum power point, where power is around 14000 W or 14 kW. After that point, if we increase the speed, the power will reduce and eventually comes to zero.

3.9 Calculation for the Hydro-electric model

Fig.3.7. shows the basic hydro-electric model and then we calculate all the parameters in each step. Once we get the parameters then we match the results both from the PSIM and Matlab/ Simulink model.

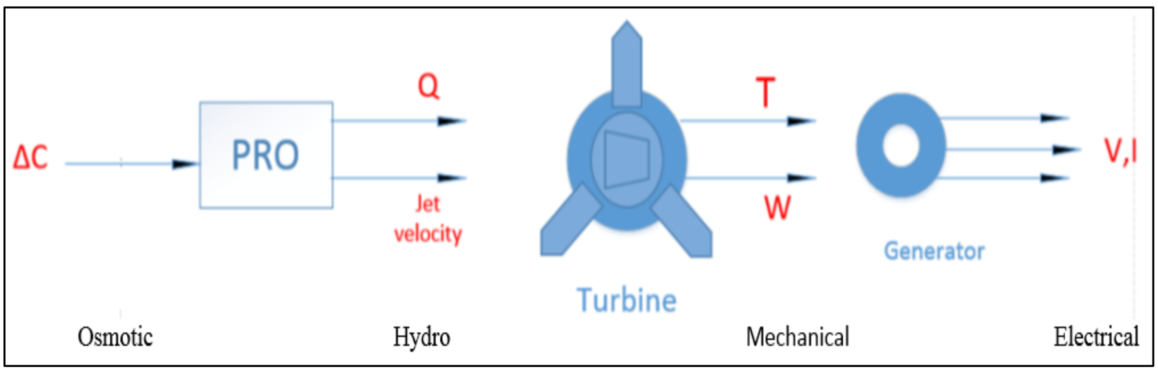

Fig.3.7. Overall schematic model of the hydro-electric system

Fig.3.7. shows the overall schematic model of the hydro-electric system. The PSIM model is summarized as the following:

i) Calculation of the osmotic pressure

Osmotic pressure, $\Delta\Gamma = (i_v \times \Delta C_m \times R_g \times T)/M$

where, i_v=vant's Haff co-efficient=2

- ΔC_m=salt concentration=30 g/L
- R_g=universal gas constant=0.083145 L.bar/moles.K

- T= 293.15 kelvin (20^0 C)
- M= molar mass of the salt = 58.44 g/ mol
- By putting all the values in the equation, we can find,
- $\Delta\Gamma$ is 25 bar.

  Because of the water impurity, friction and other disturbances, the practical osmotic pressure is around 23.7 bar [4].

ii) Calculation of the flow rate

For flow rate calculation, we consider the value of osmotic pressure is 23.7 bar, which is the practical value of the system.

The equation of flow rate (Q) is given by

- Flow rate:

Q = [(Water permeability) × (Osmotic pressure – Hydraulic pressure)×Membrane area]

=10^{-12} × (2370000-1185000) ×11120

= 0.013.

The PSIM model gives the exact value of flow rate as the calculated value. Once we find the flow rate, our next step to calculate the Osmotic power here, which is calculated from the following equation

- $P_{osmotic}$=Q × ($\Delta\Gamma$-ΔP)

  =0.0131772 × (2370000-1185000)

  =15614.982 watt

Then, we need to calculate the height and compare the output value from the PSIM. As the sea and the river are at the same level, therefore there is no practical height.

The height is given by the following equation

- Height= Hydraulic pressure/(Water density×9.81)

  =1185000 / (1029×9.81) = 117.39 m

Once we calculate the height, we can find out the velocity, as this height is converted into velocity. As this potential energy is equal to the converted kinetic energy.

$$\left(\frac{1}{2}\right) \times \mathrm{m} \times \mathrm{V_{jet}}^2 = \mathrm{m} \times \mathrm{g} \times \mathrm{H}$$

$$V_{jet} = \sqrt{2 \times \mathrm{g} \times \mathrm{H}} = \sqrt{2 \times 9.8 \times 117.39}$$

$$= 47.96 \text{ m/sec}$$

Once we find the jet-velocity and flow rate (Q), we can calculate the hydro power, which is come from the following equation.

$P_{hydro}=(1/2)\rho Q V_{jet}^2$,where ρ is water density.

$=(1/2)\times 1029 \times 0.01317 \times 47.96^2$

=15594.3 W

Blade diameter calculation

- $V_{jet} = \sqrt{2 \times \mathrm{H} \times 9.8} = 47.96 \text{ m/sec}$
- Effective jet velocity, V_t =0.50×V_{jet}=23.98 m/sec
- $\frac{\mathrm{V_{jet}}}{2} = \mathrm{w} \times \left(\frac{\mathrm{D}}{2}\right)$
- Tubine blade diameter , $\mathrm{D} = \frac{\mathrm{V_{jet}}}{\mathrm{W}} = \frac{47.96}{188.49} = 0.25$ m

- **Mechanical (Torque & Speed)**
  - $T_{mech} = [(\frac{1}{2})\{\rho QD(V_{jet}\text{-}\omega\times\frac{D}{2})\}(1\text{-}\cos\beta)]$

    where, ρ is the water density = 1029 kg/m^3, U is the turbine blade speed = $(\frac{1}{2})\times V_{jet}$, D is the turbine blade diameter = 0.254 m.
  - T_{mech}=82.733 Nm
  - W_{mech}=188.49 rad/s
  - P_{mech}= 188.49 * 82.733 = 15594.33 W
- **Electrical**
  - $P_{\ elec} = 3 \times I^2 \times R$
  - $=3\times 23.63^2\times 9.31$ =15595.46 W

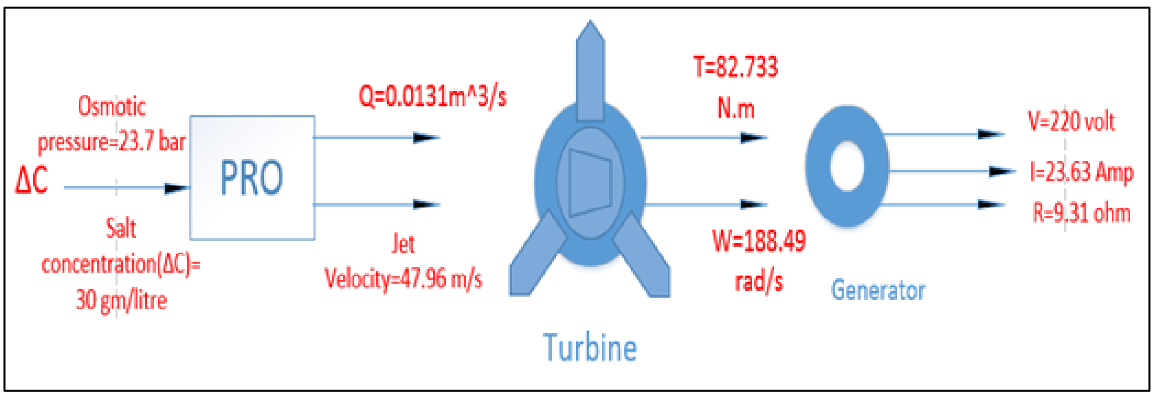

Fig.3.8. Flow chart of the micro hydro-power system [37]

The values of all parameters of the flow chart (Osmotic, Hydro, Mechanical and Electrical) are given in the Table 3.3.

Table.3.3. Flow chart model parameters values.

Parameters	Value
Osmotic pressure	23.7 bar
Salt concentration	30 g/L
Flow rate (Q)	0.0131 m^3/sec
Jet velocity	47.96 m/sec
Torque	82.733 Nm
Speed	188.49 rad/sec or 1800 rpm
Voltage	220 V
Current	23.63 A
Resistance	9.31 Ω

Chapter 4

SIMULATION AND EMULATION OF THE PRO SYSTEM

4.1 Simulation results

The proposed system has been simulated using Matlab-Simulink and the results are shown below.

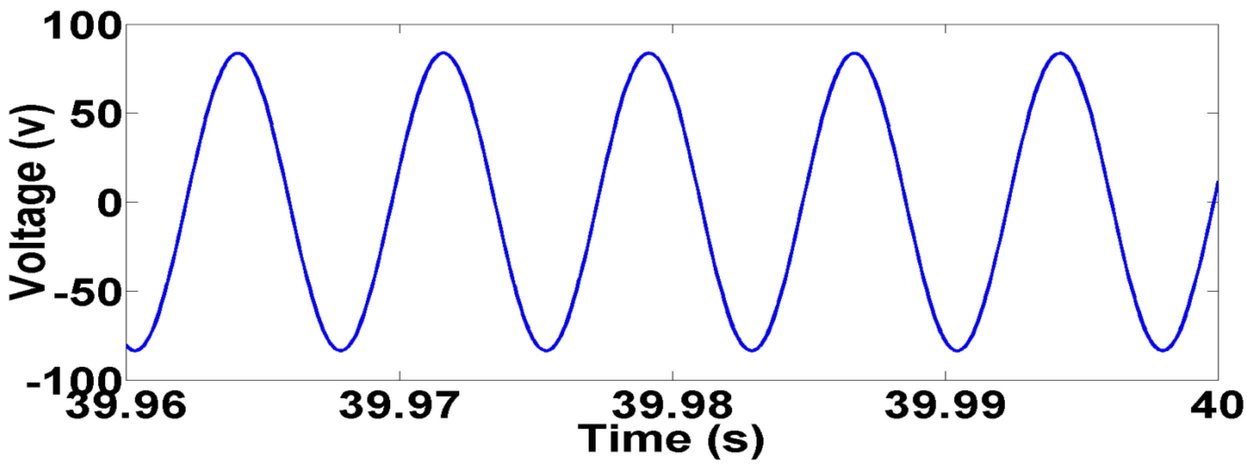

(a)

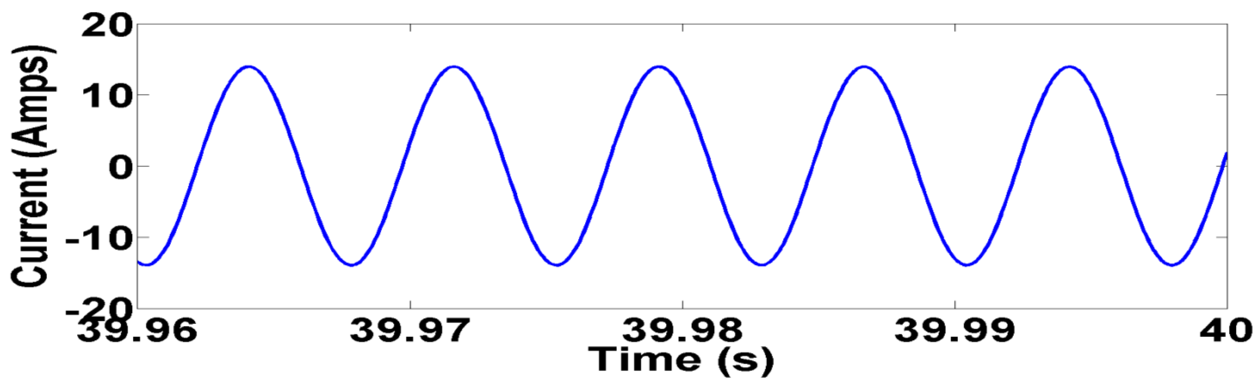

(b)

Fig. 4.1. (a) Terminal voltage and (b) current of the PMSG when the PRO plant is operating at its MPP

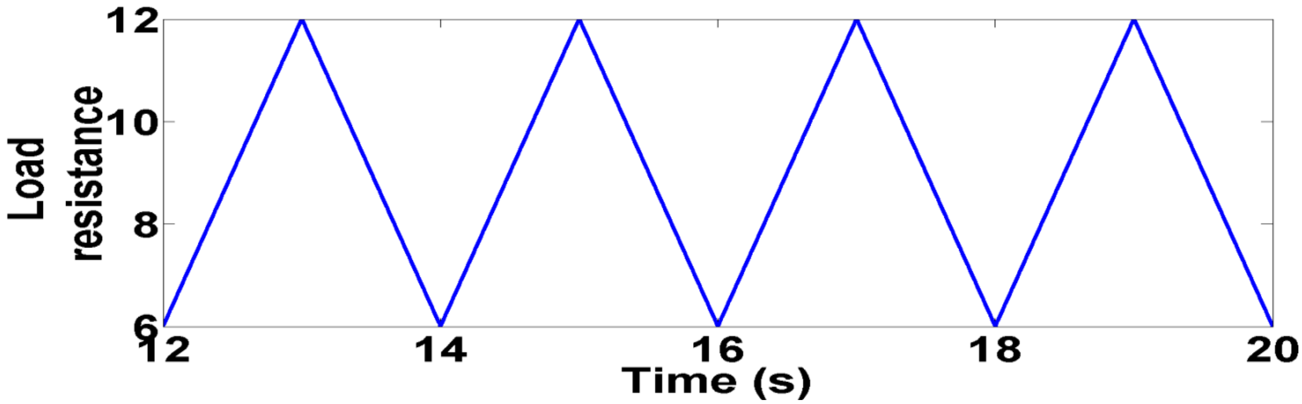

(a)

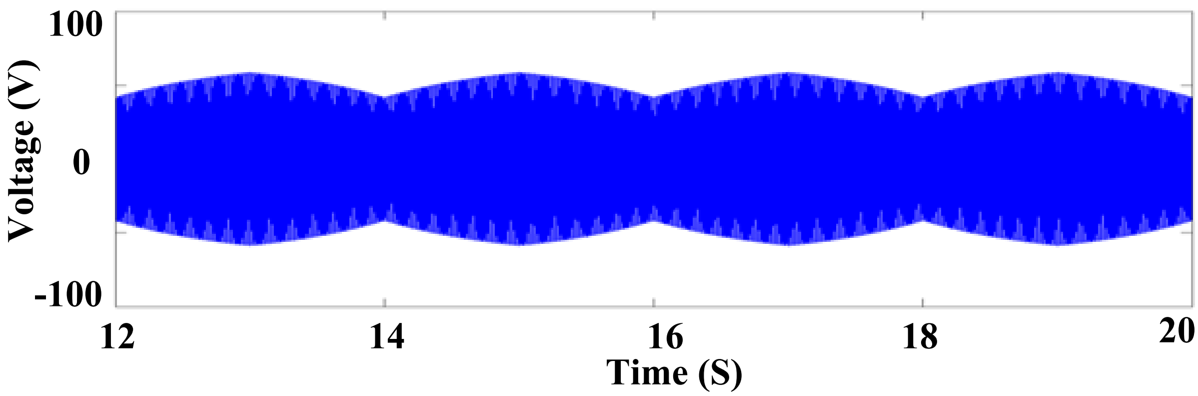

(b)

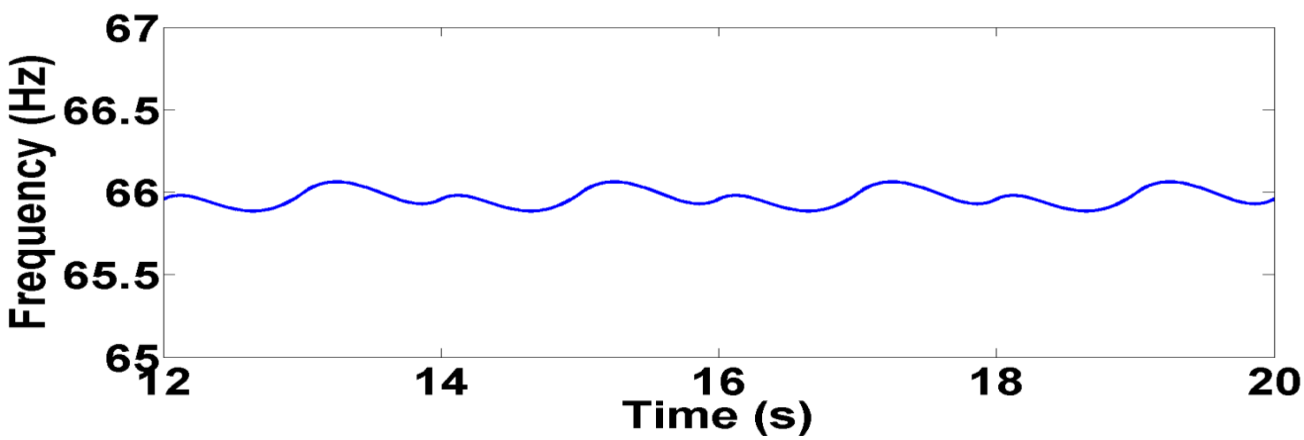

(c)

Fig. 4.2. (b) Output voltage and (c) frequency variation when the load is changing

Fig. 4.1 (a) shows the load voltage and (b) show the current at the maximum power point operation. Fig. 4.2 (b) shows the variation of load voltage and (c) shows the output voltage frequency when the electrical load is varying.

From the above chapters it shows that MPP happens only when hydraulic pressure is half of the osmotic. For getting the desired voltage and current, the values of hydraulic and osmotic pressure are given in Table 4.1.

Table.4.1.Values of hydraulic and osmotic pressure taken in the model

Parameters	**Value**
Hydraulic pressure	11.85 bar
Osmotic pressure	23.7 bar

Fig.4.1 (a) shows the maximum voltage and (b) shows the maximum current achieved. As this is the ideal condition.

From the figure 4.2 (b) and (c) , it is clear that according to the load changes, the voltage and frequency will change. As when the load is at the peak position, the voltage will be maximum.

When the load is increasing, the voltage will increase as well. To understand this phenomenon clearly, the load is given as a triangular shape. So according to that, the voltage will change.

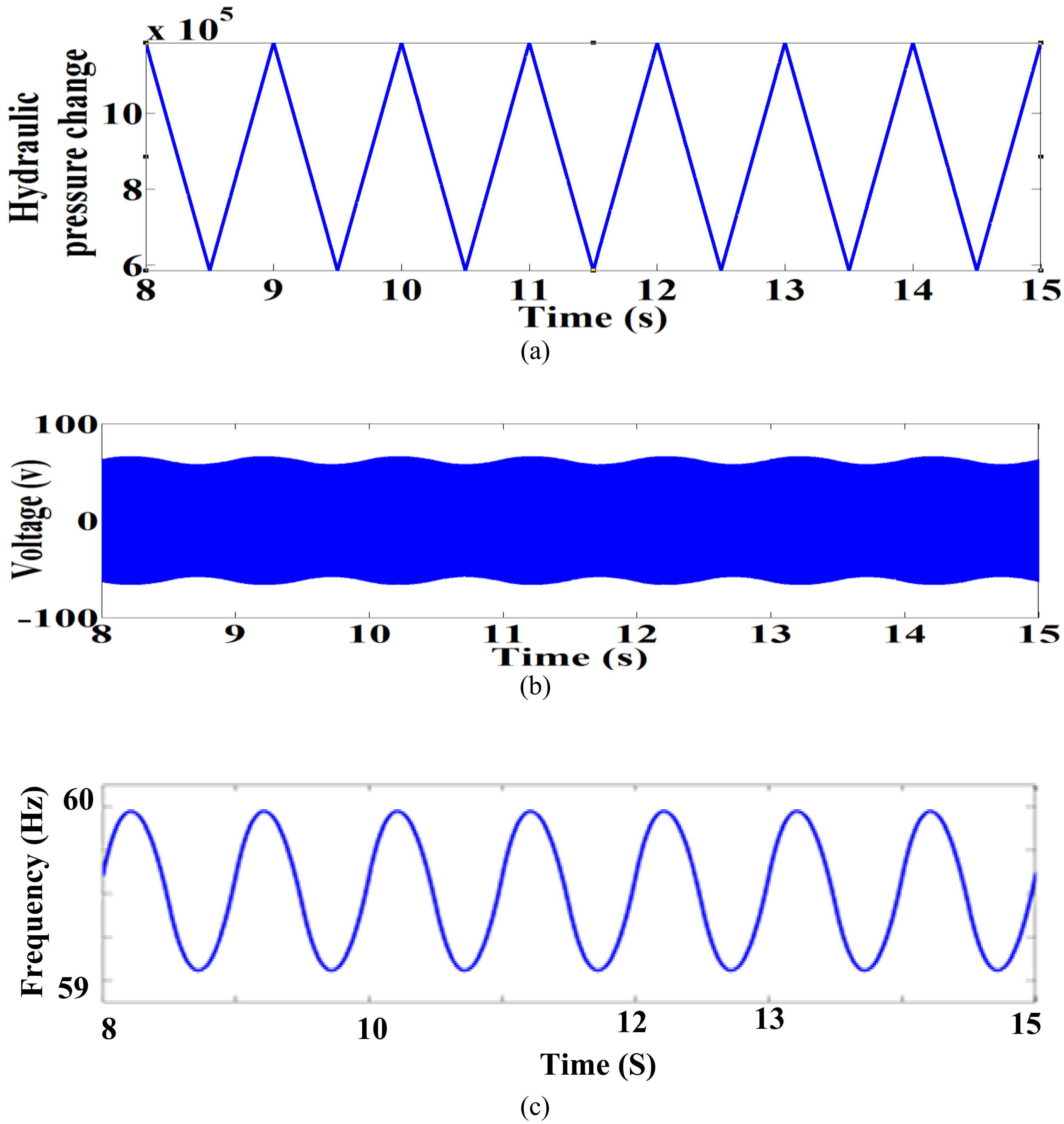

Fig. 4.3. (b) Output voltage and (c) frequency variation of the PMSG when the hydraulic pressure of the PRO plant is varying

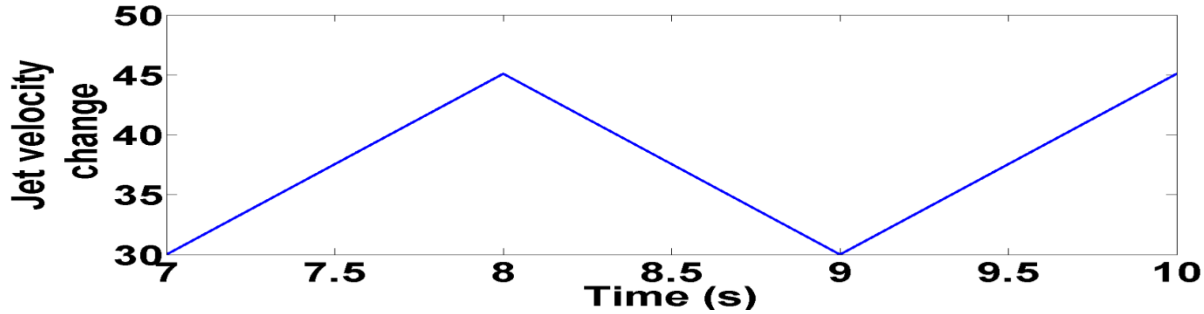

(a)

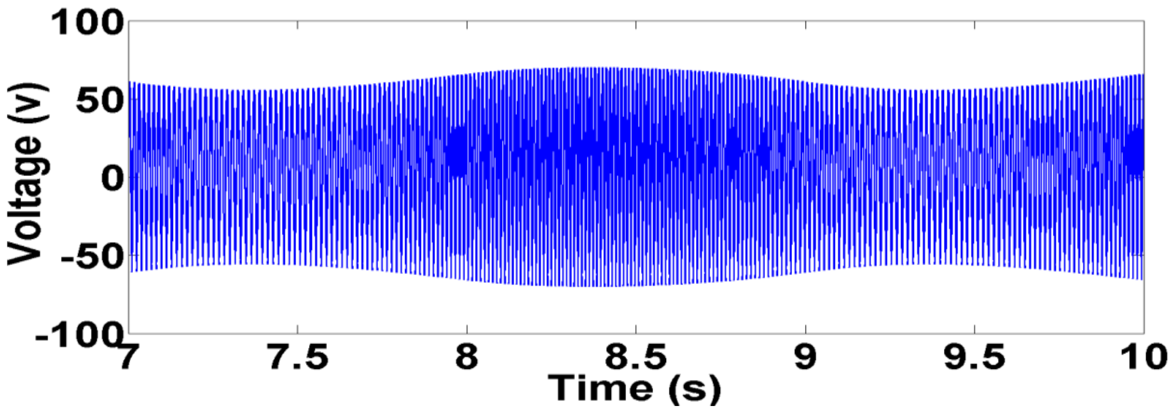

(b)

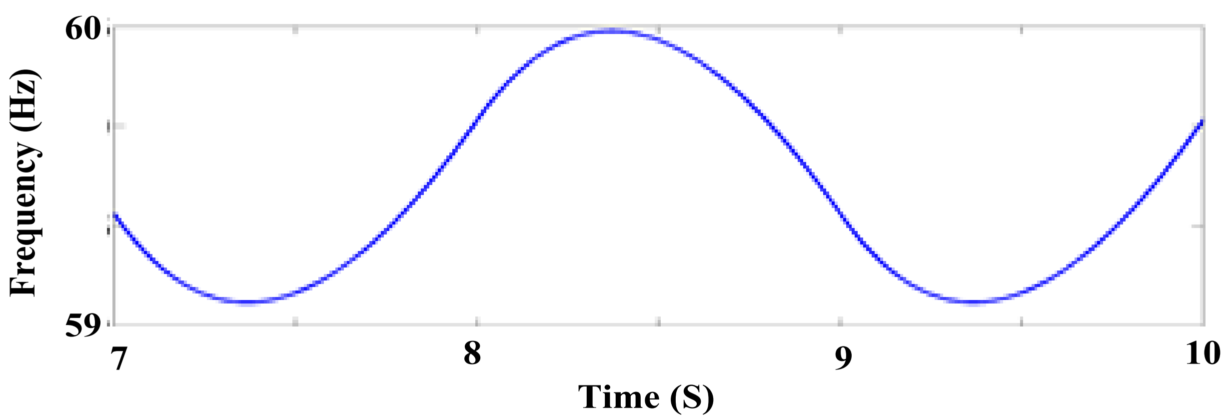

(c)

Fig. 4.4 (b) Output voltage and (c) frequency variation when the jet velocity is varying

.

Fig. 4.3. and Fig. 4.4. shows the variation in the load voltage and frequency when the hydraulic pressure and jet velocity are varying respectively. The variation of the hydraulic pressure and the jet velocity is shown in the first plot in the figures.

As the hydraulic pressure and the flow rate are very important parts in this PRO model. The hydraulic pressure can be changed by using a pump. From the equations (2-1) and (2-2), we know that, hydraulic pressure is used as an opposing force to achieve power, since it is always opposing the osmotic pressure.

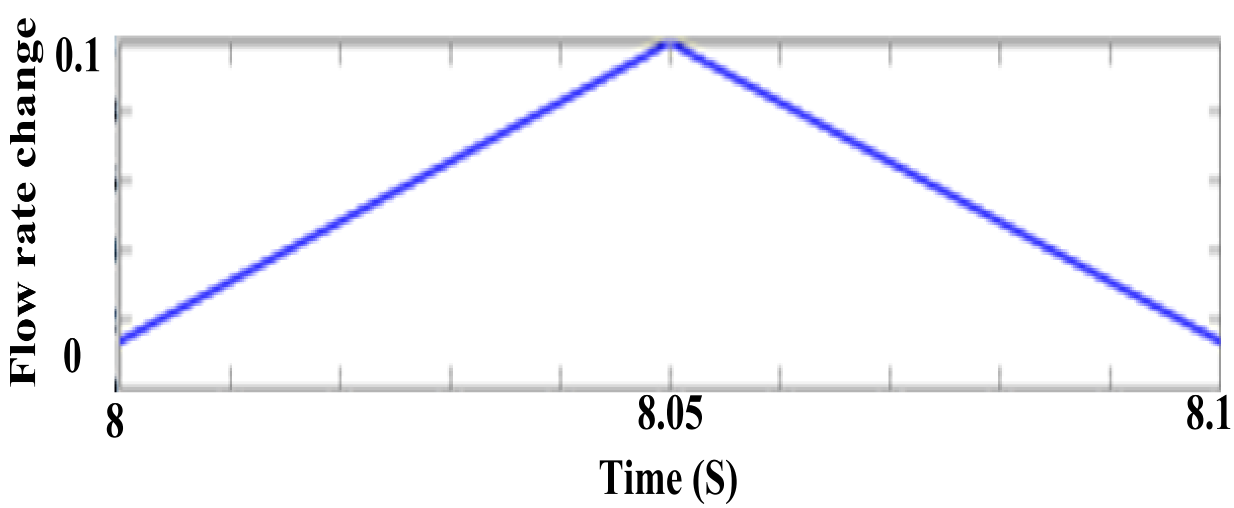

(a)

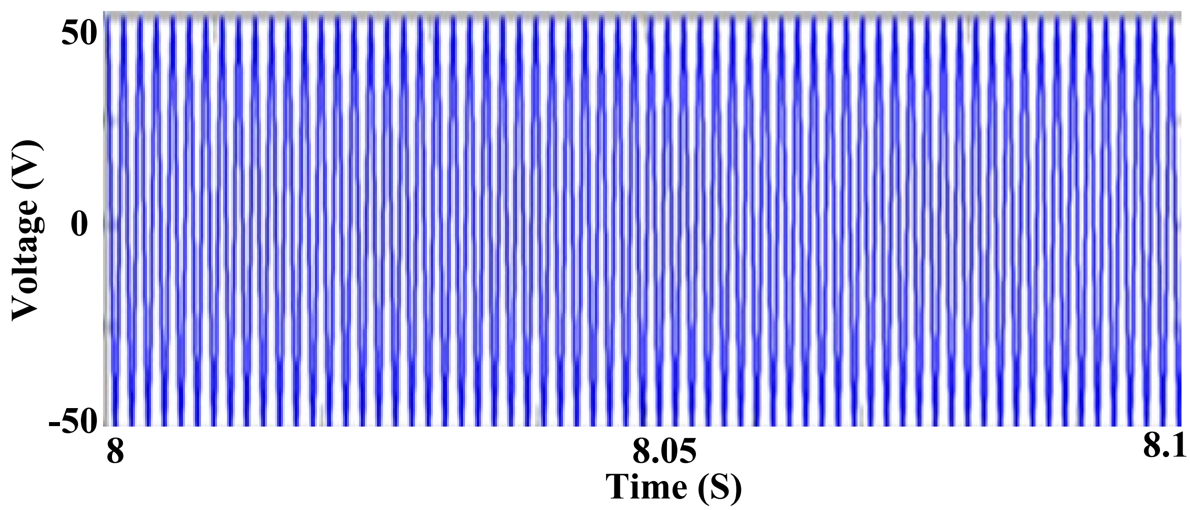

(b)

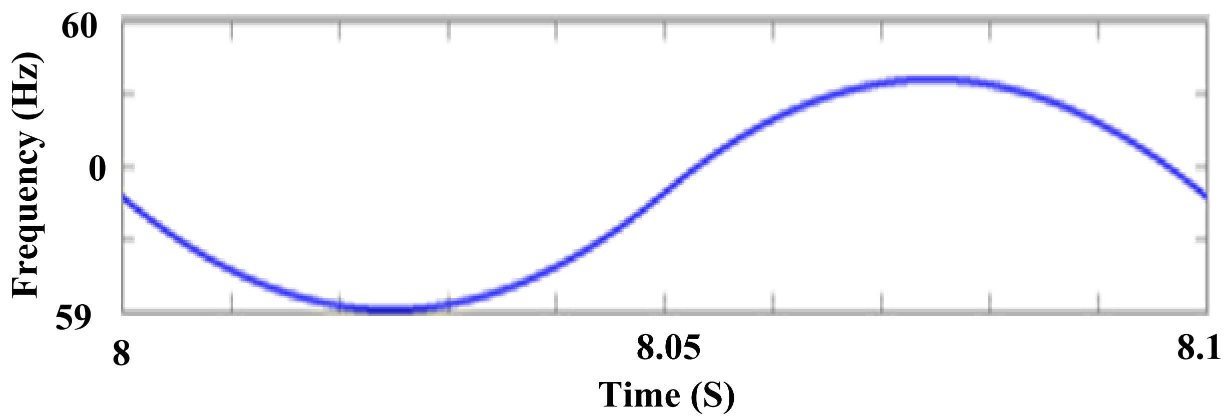

(c)

Fig.4.5.(b) Voltage and (c) frequency output by changing the flow rate

Fig.4.5.(b) shows the variation in the voltage and (c) shows the frequency variation when the flow rate is changing

4.2 Simulation results by using same value as experimental

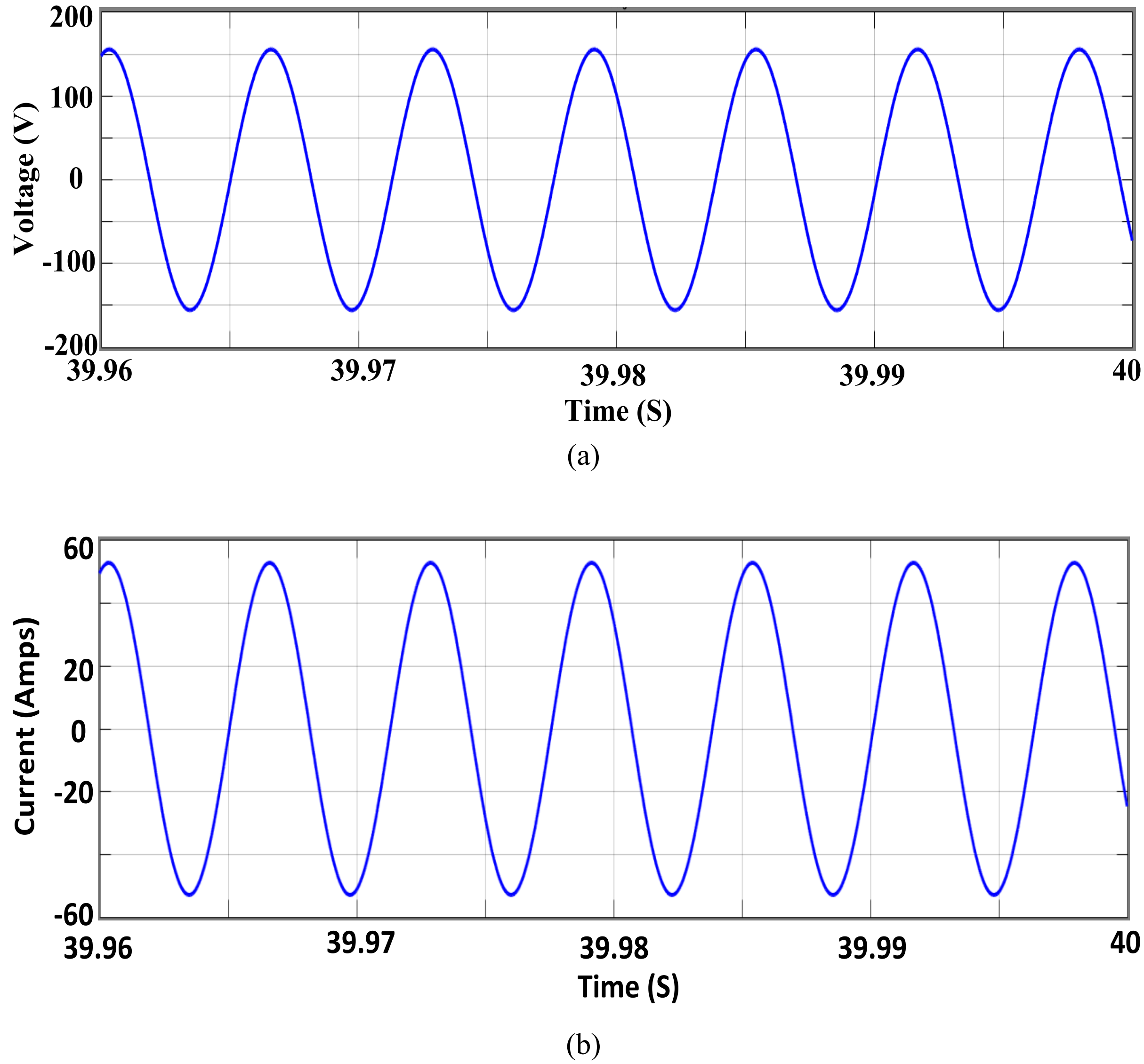

Fig.4.6.(a) Terminal voltage and (b) terminal current of the PMSG when the PRO plant is operating at its MPP

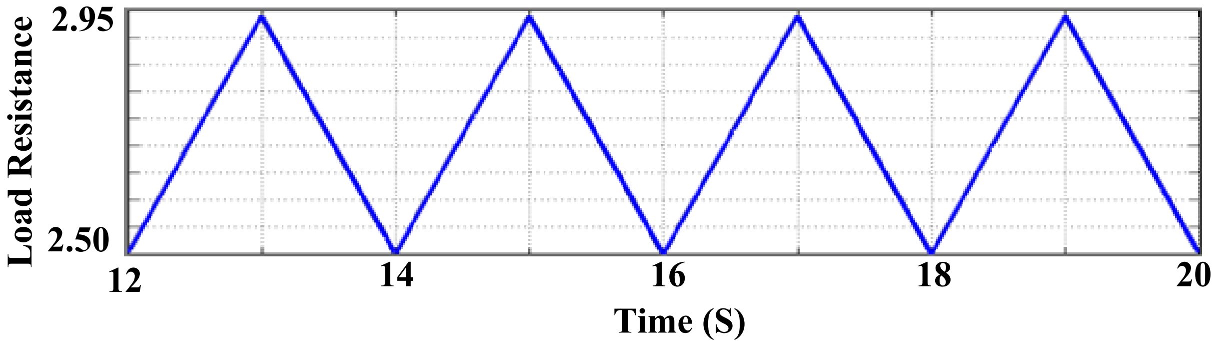
Load Resistance
2.95
2.50
12
14
16
18
20
Time (S)

(a)

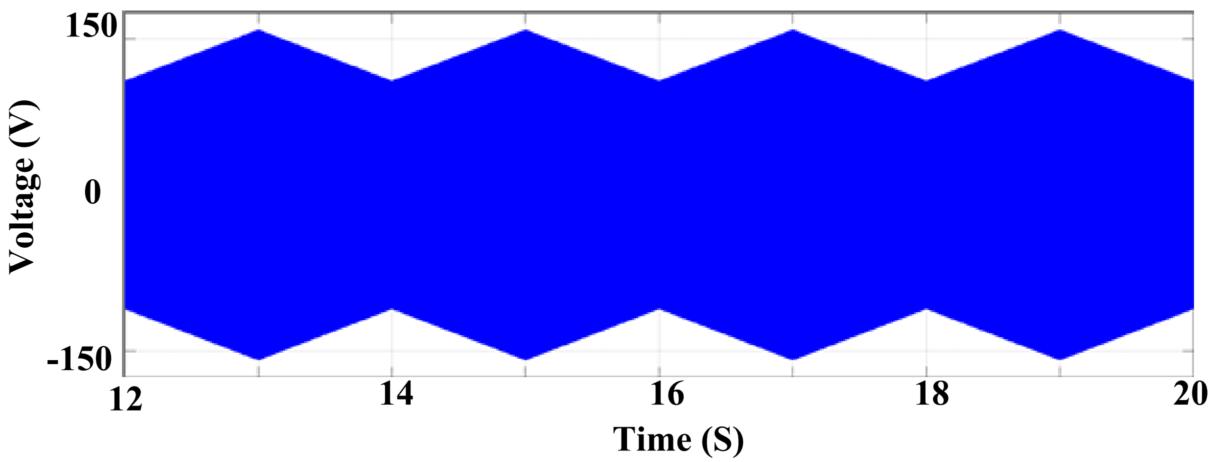
Voltage (V)
150
0
-150
12
14
16
18
20
Time (S)

(b)

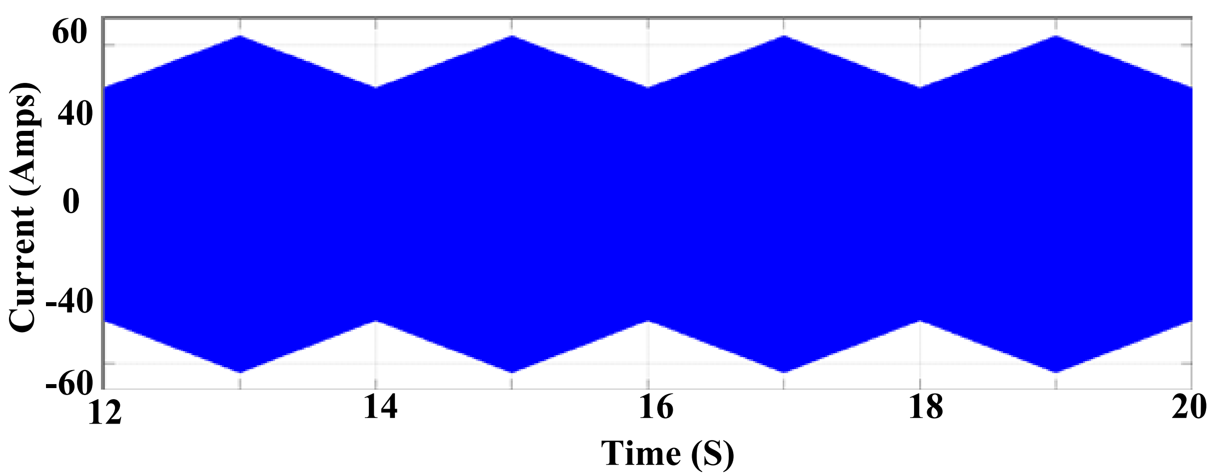
Current (Amps)
60
40
0
-40
-60
12
14
16
18
20
Time (S)

(c)

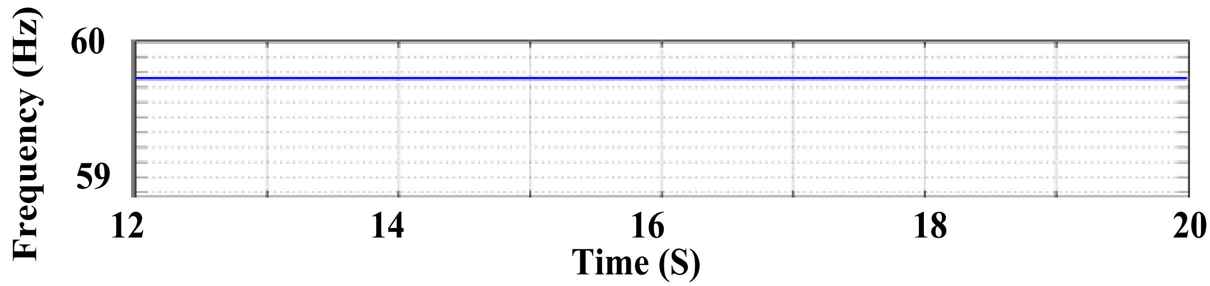

(d)

Fig.4.7.(a) Load resistance change, (b) Output voltage, (c) output current and (d) frequency variation when the load is changing

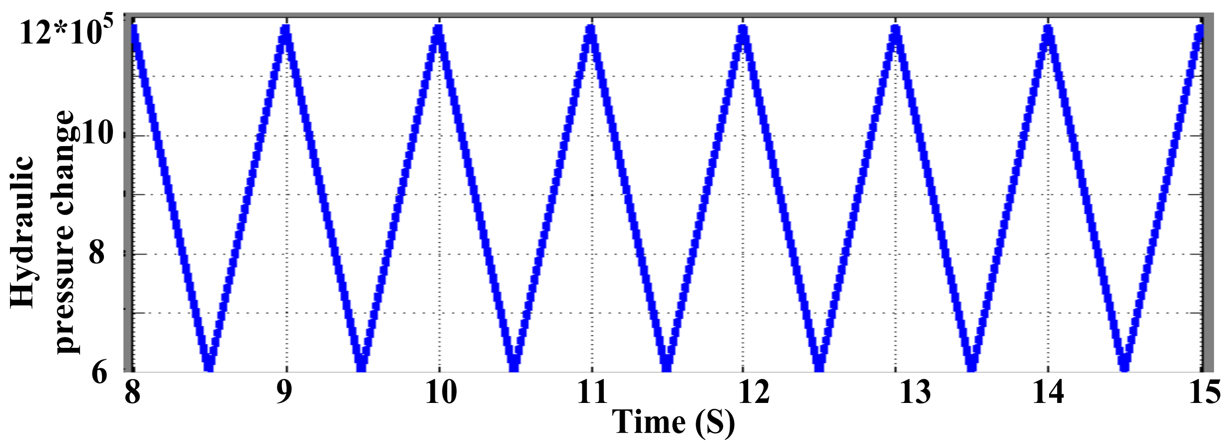

(a)

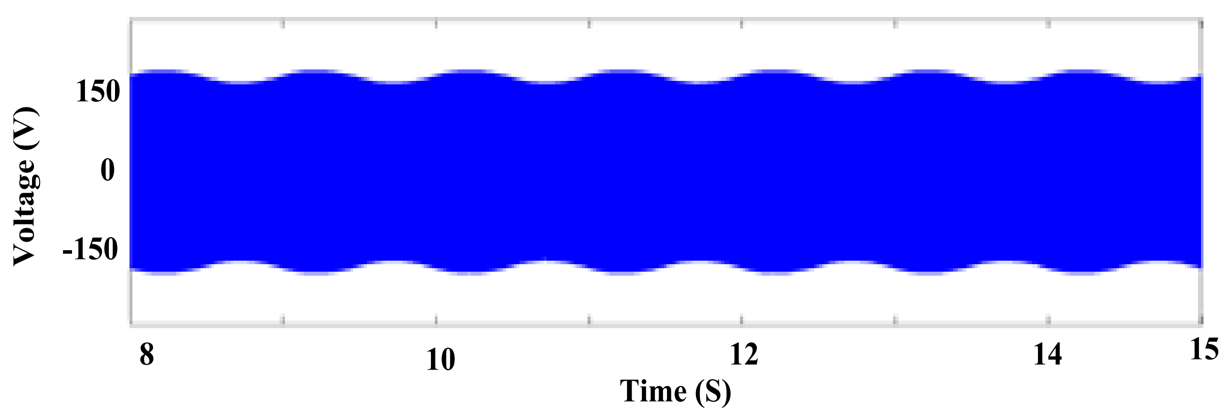

(b)

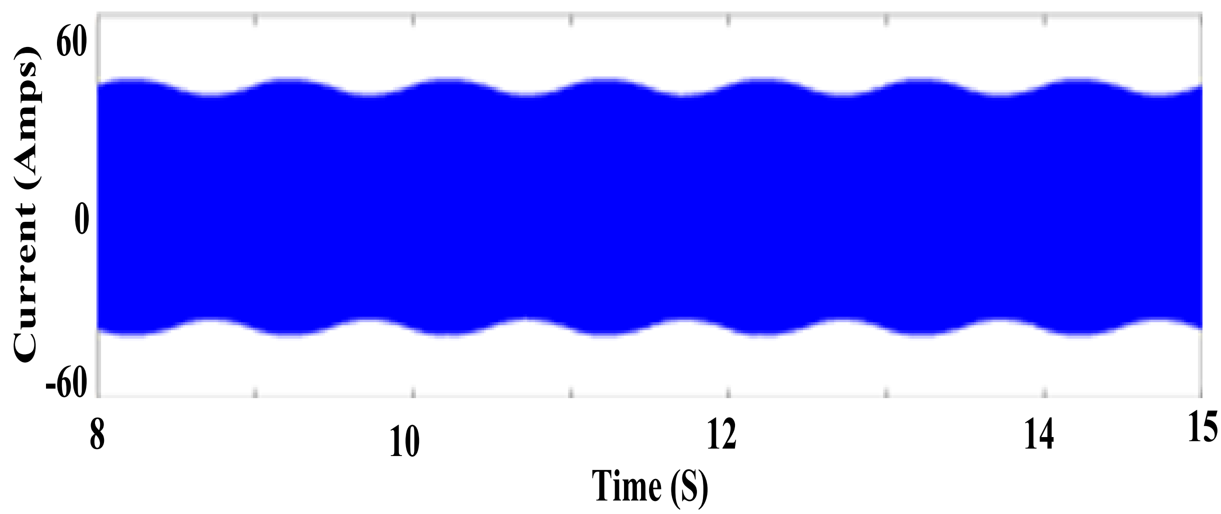

(c)

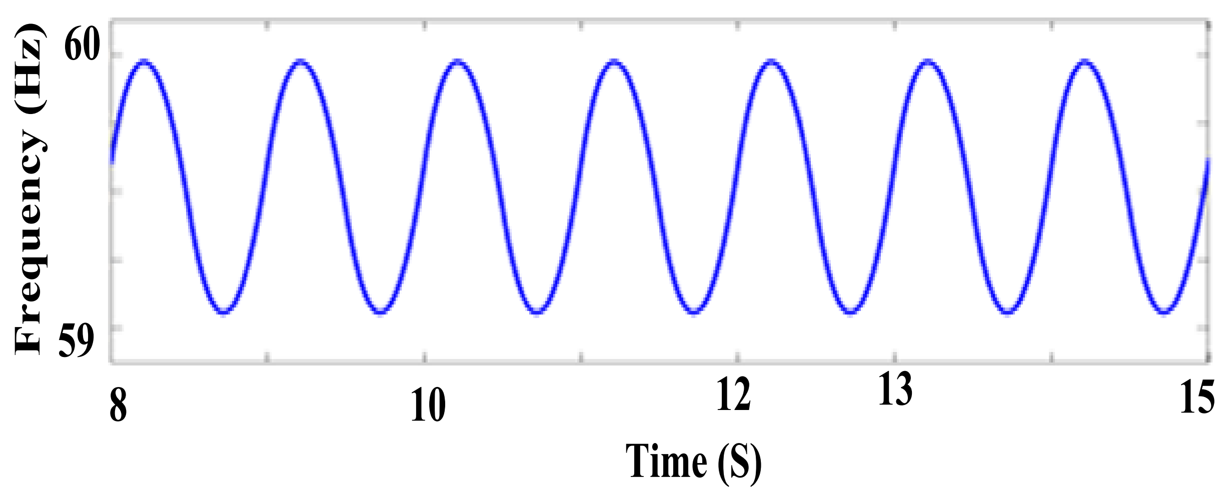

(d)

Fig.4.8.(b) Output voltage , (c) output current and (d)

Frequency variation of the PMSG when the hydraulic pressure of the PRO plant is varying

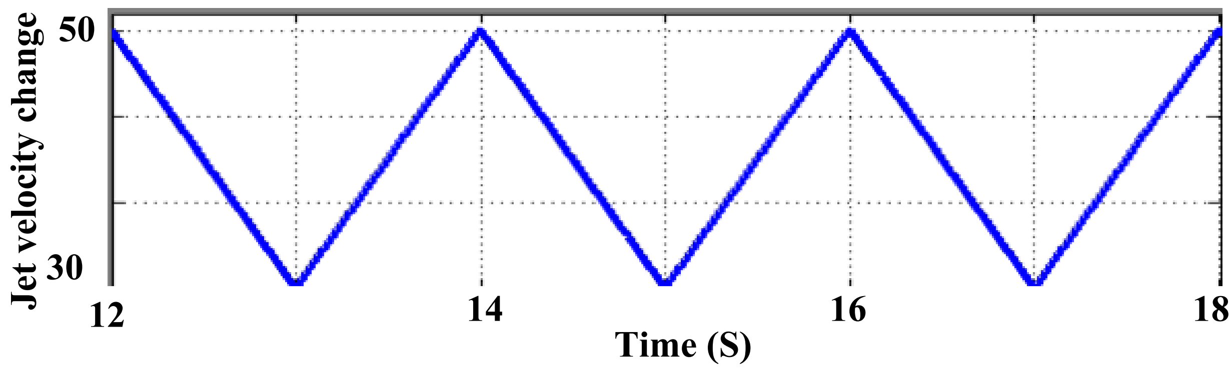

(a)

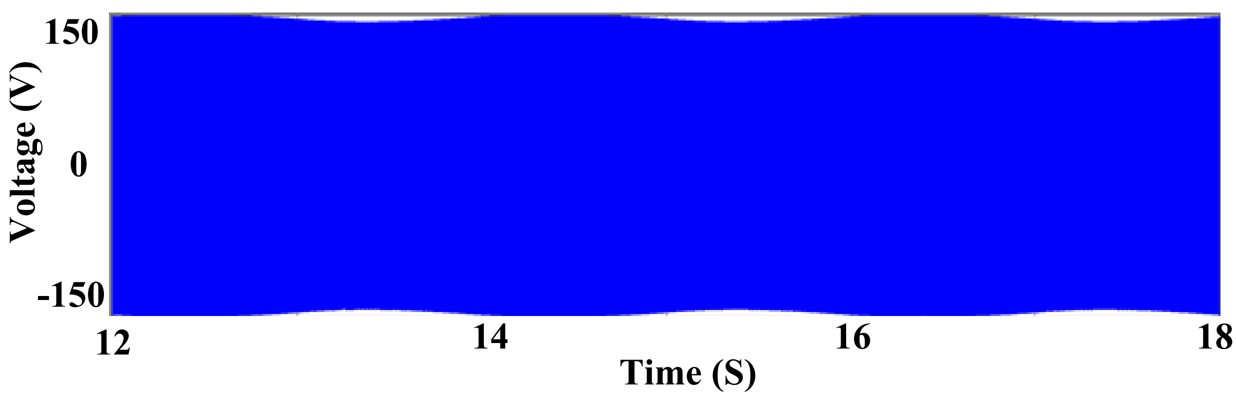

(b)

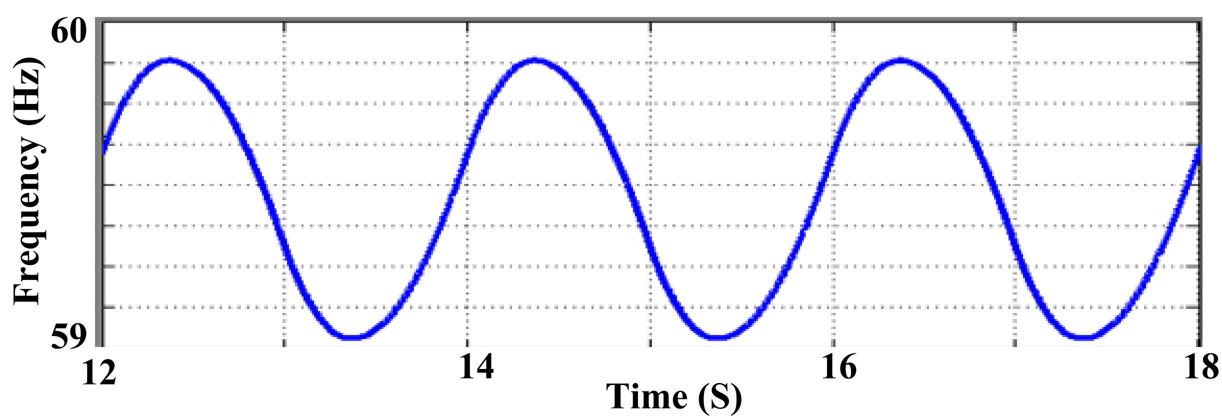

(c)

Fig.4.9.(b) Output voltage and (c) frequency variation when the jet velocity is varying

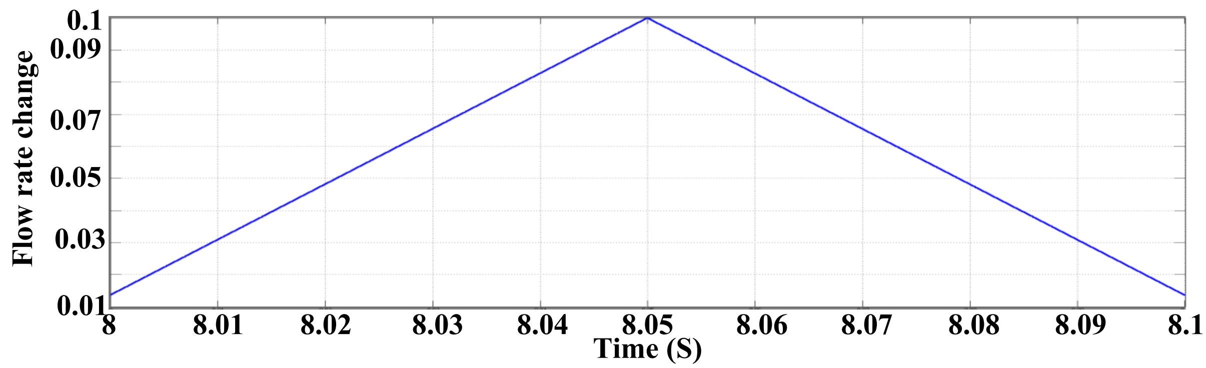

(a)

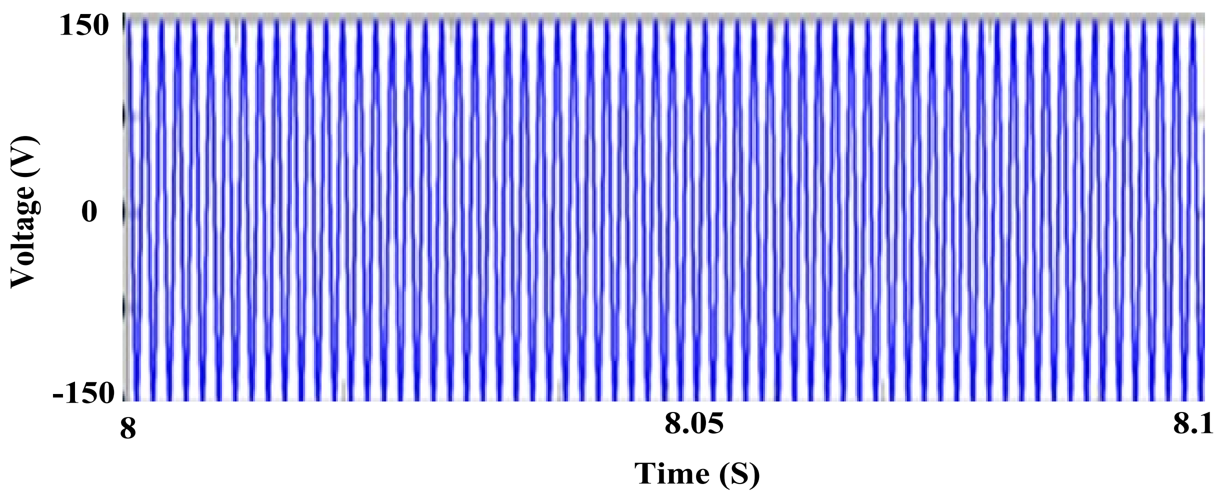

(b)

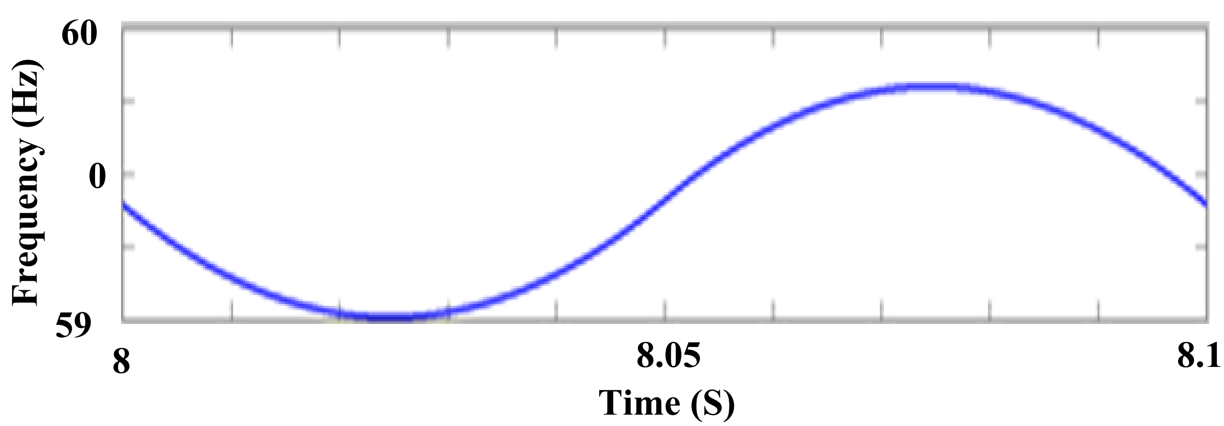

(c)

Fig.4.10.(b) Voltage and (c) frequency output by changing the flow rate

4.3 Emulator block diagram

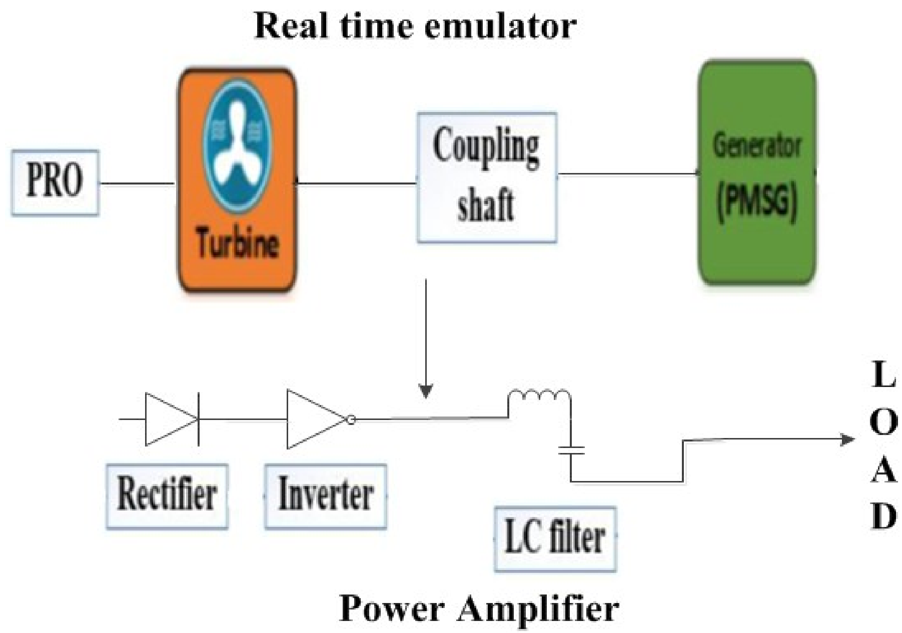

Fig.4.11. Block diagram of the Emulator

Fig.4.11. shows the basic block diagram of the emulator, in which, the PRO is the source of energy. As discussed earlier, the concentration difference between the hydraulic and the osmotic pressures will generate the electric power. This outputs from PRO are flow rate and jet velocity, which are the inputs to the Pelton turbine. Where from the Pelton turbine, speed and torque can be developed. The torque and speed signals are given as input signals to the PMSG model in order to generate the voltage and current (electric power). Once we build this model, then it is given as supply to the hardware. We need DC source as an input to the IGBT inverter, therefore, a rectifier is necessary. An auto-transformer is used to make the voltage level to 280 volt, which is the desired voltage input to the IGBT. The output of IGBT is connected to the inductor. Capacitors are connected after that. Voltage and current sensors are connected in between the inductor and the capacitor. The voltage and current sensors are used to measure the voltage and current to

generate the required signal. Digital multimeter is used here to calculate the value of voltage and current. As well as an oscilloscope is measuring the sinusoidal waveforms of voltage and current. Three phase resistors are connected before the load.

4.4 Experimental setup and Experimental Results

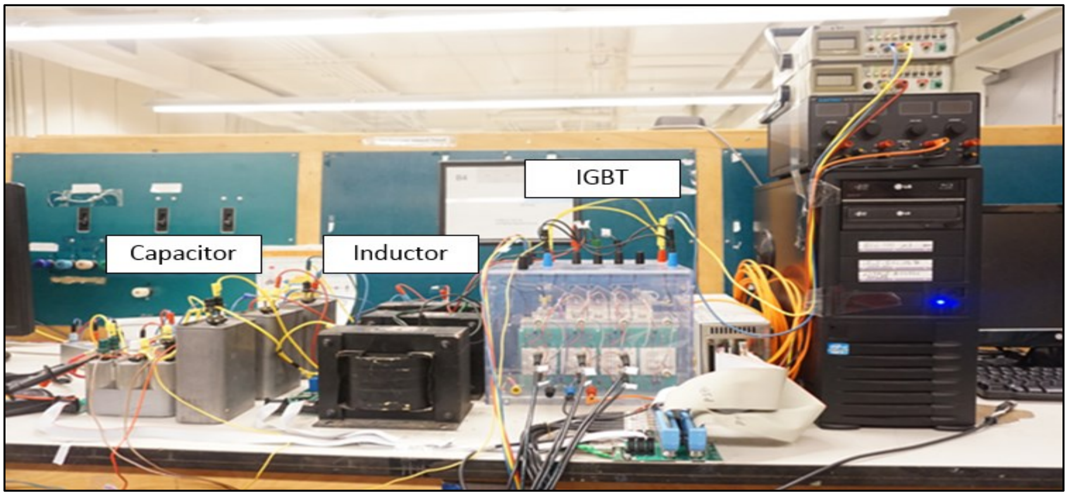

Fig.4.12.Experimental setup

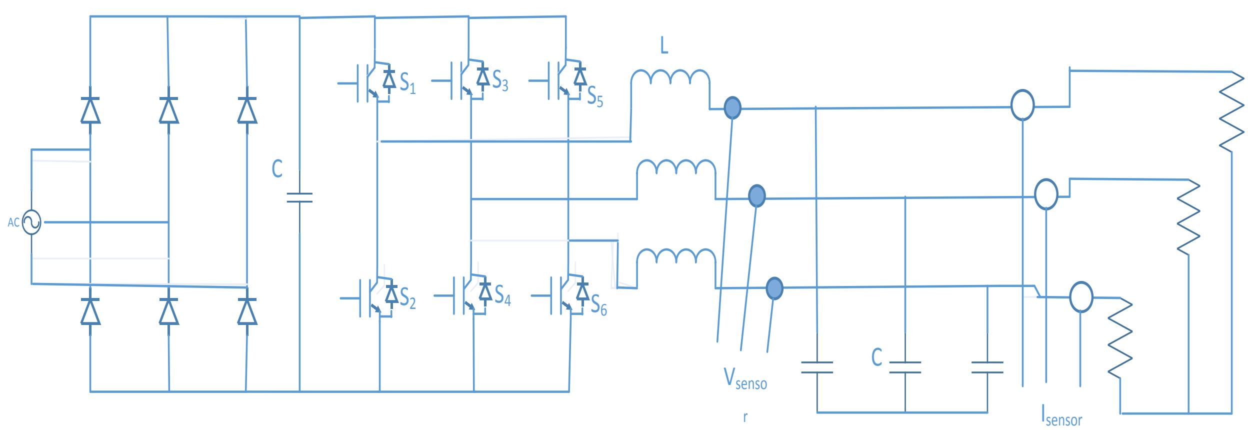

Fig.4.13. Circuit diagram

A) Hardware Description

For experimental validation using the power hardware-in-the-loop (PHIL), a test bench including a 3-phase IGBT switch pack, filters and controller is built to emulate the PRO power system (Fig. 4.12). The designed VSI is rated at 15 kVA, 110 V, 60 Hz for continuous operation. The control algorithm is first simulated in Simulink and then implemented in a real-time controller. The system shown in Fig. 4.12 is modeled and implemented within the real-time controller DS-1103 for capturing and controlling digital and analog signals. Since the measured signals have noise, an active filter is designed for noise reduction and phase shift compensation of the output filter and the measurement devices.

i) Source

We use a Matlab model to build the basic structure. We build both PSIM and Matlab model. Matlab model is in this practical model.

ii) IGBT

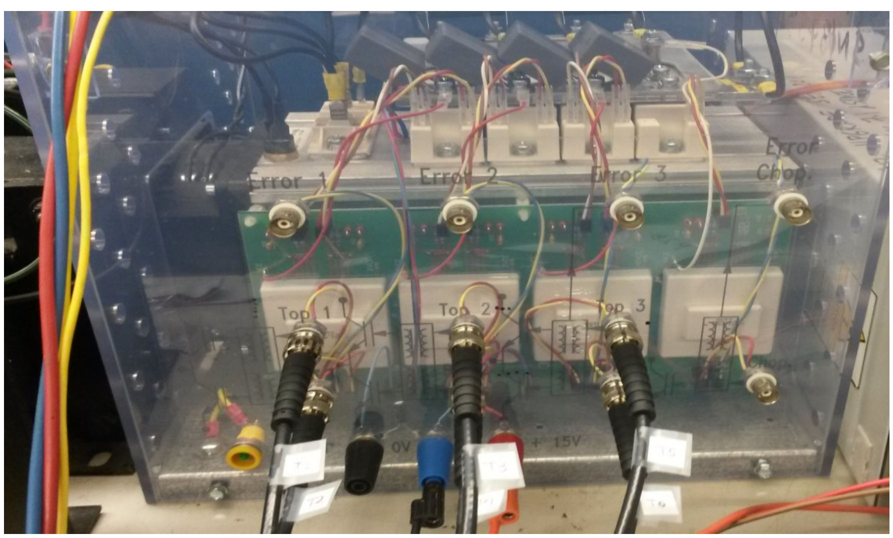

Fig.4.14.IGBT

IGBT (insulated gate bipolar transistor) is a three-terminal power semiconductor device, which is used as a switch here. There are 6 switches are shown in Fig. 4.14. At a time, one upper switch from one leg and another lower switch from another leg become ON while the remaining switches will be OFF.

iii) Gate driver

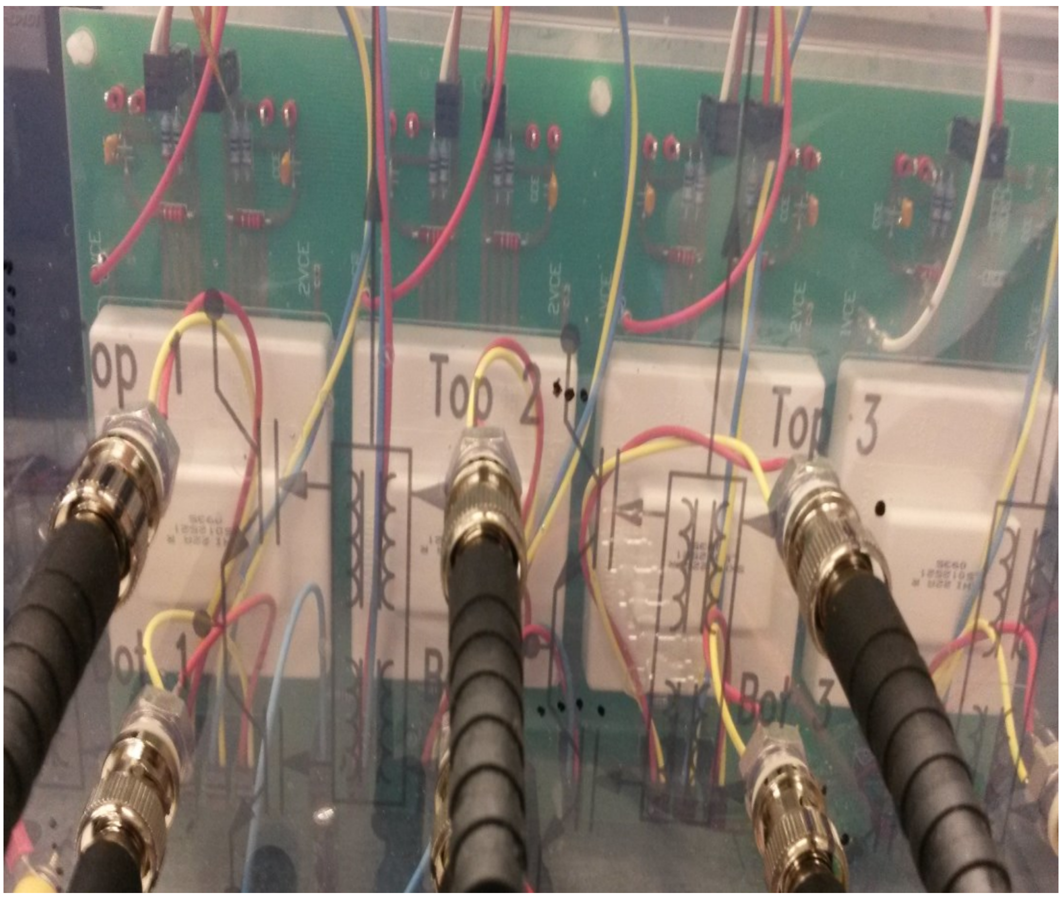

Fig.4.15.Gate driver

The gate drivers are used as a power amplifier here, which accepts low power input and produces a high current input for the gate of the IGBT.

iv) Auto-transformer variac

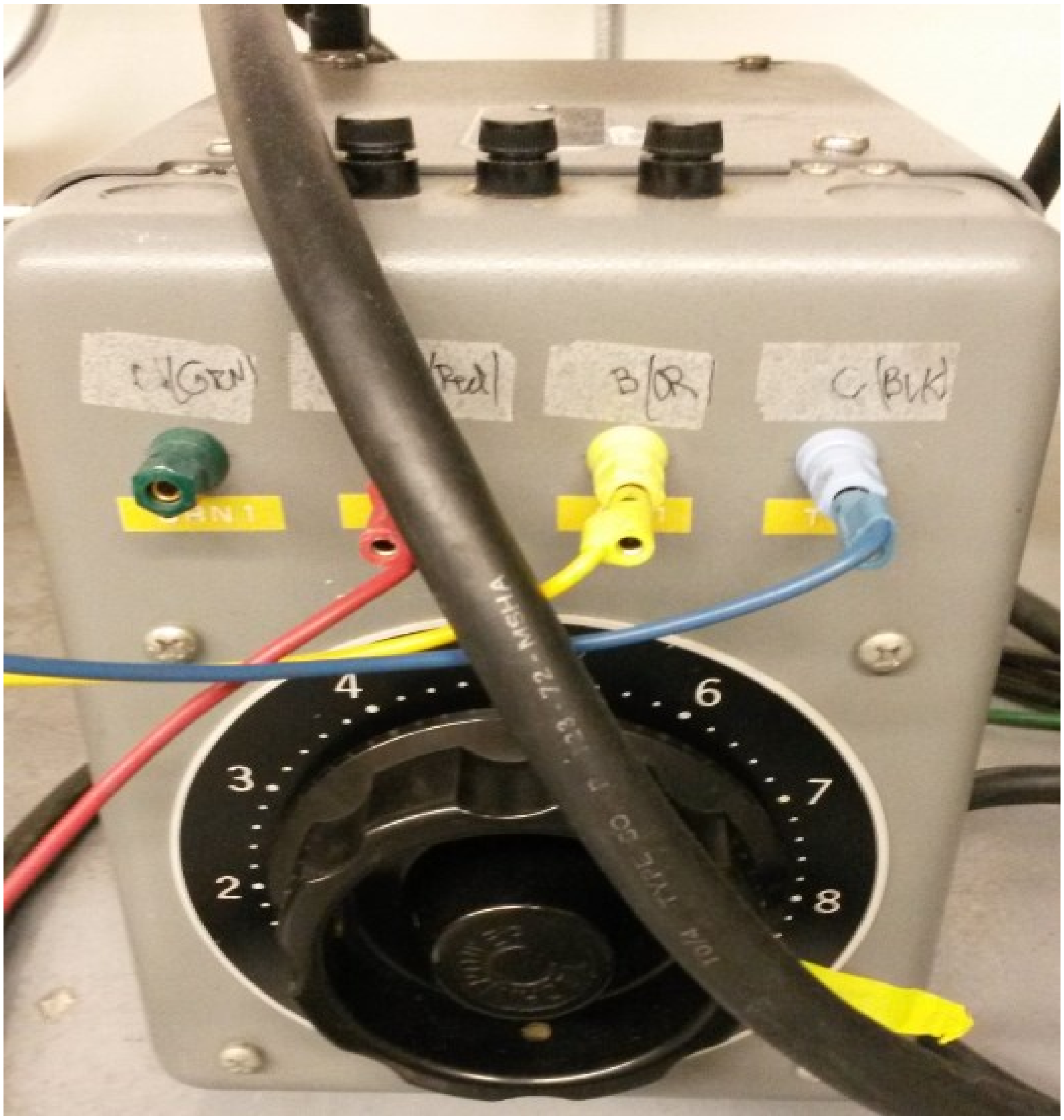

Fig.4.16.Auto-transformer

An auto-transformer is used here, which ensures the voltage constant at a certain level. From the DC voltage source, the supply is coming to the auto-transformer, where this transformer is making the voltage constant and send this to the IGBT.

v) Inductor

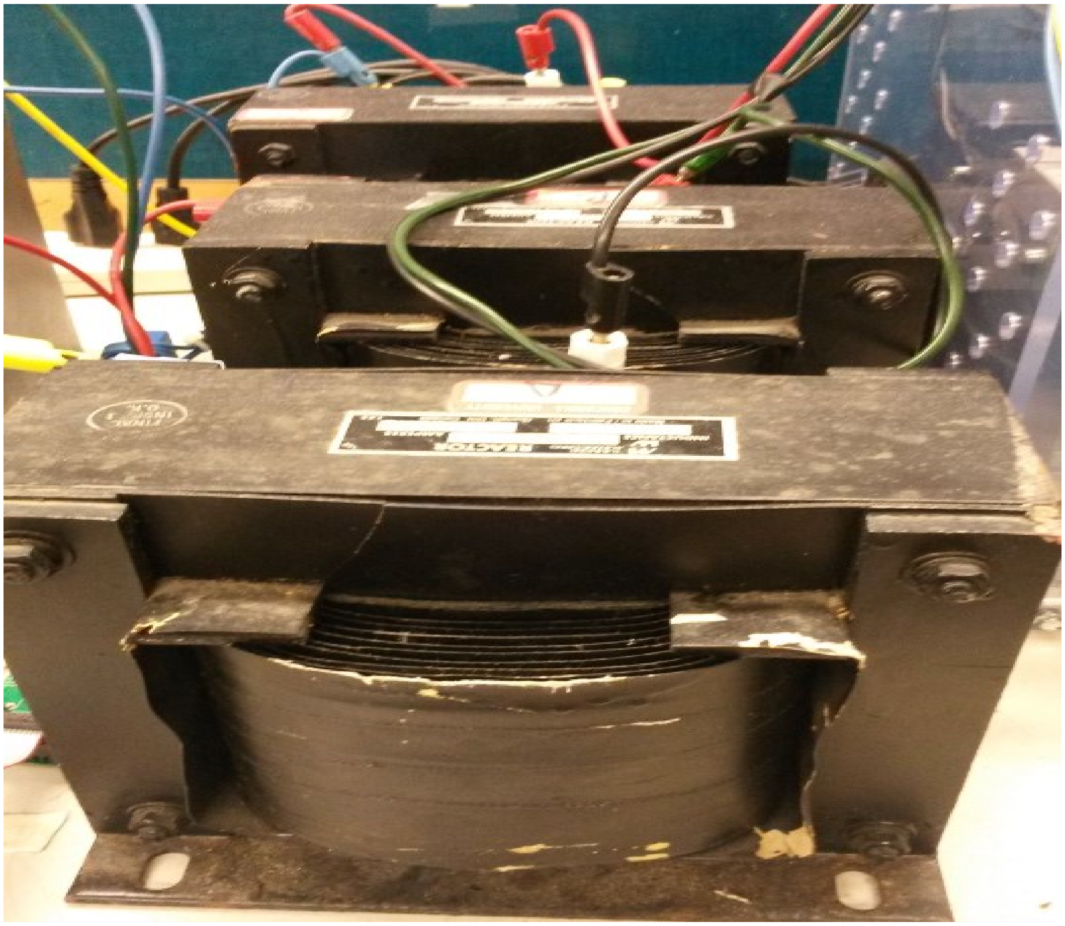

Fig.4.17.Inductor

Fig. 4.17 shows the three inductors, which are connected in parallel with the three phase lines. Each one has a value of 15 mH

vi) Voltage and current sensors

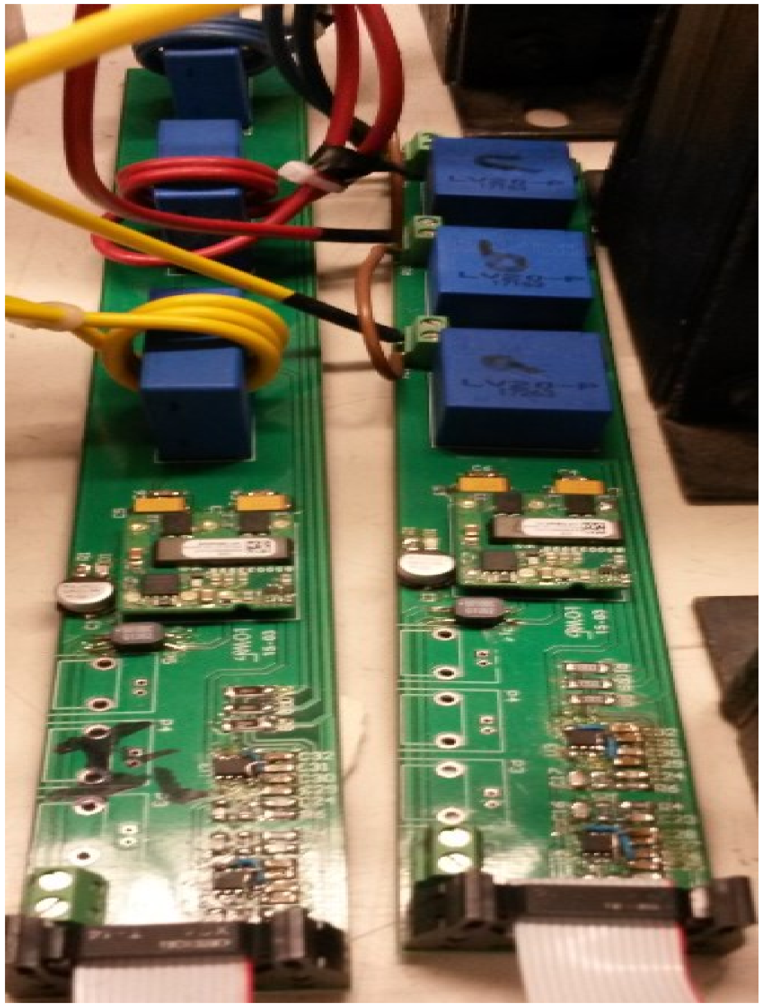

Fig.4.18.Voltage and current sensors

The voltage and current sensors are then connected between the inductor and the capacitor. This voltage sensor determines, monitor, and measure the supplied voltage. It is then able to take those measurements and turn them into a signal. The current sensor also detects the electrical current and generates a signal, which is proportional to it.

vii) **Capacitor Filter**

Fig.4.19.Capacitors

Fig.4.19. shows the capacitor module, where extra capacitors are connected in parallel to increase the capacitance. The capacitance value is 100 μ F.

viii) Resistance

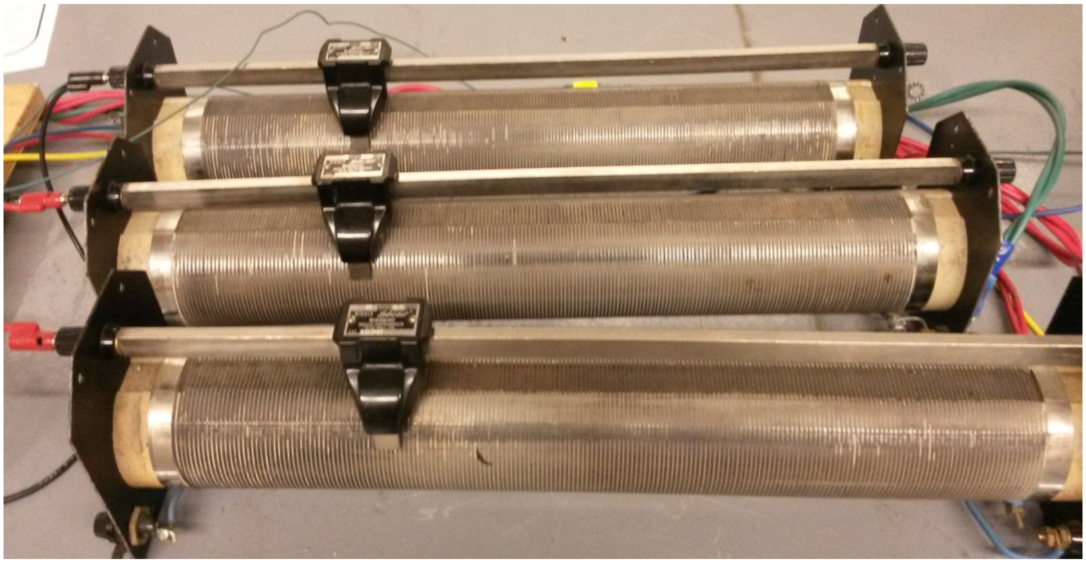

Fig.4.20. Resistors

Each of these resistances has a value of 10 Ω.

ix) Load side

The load side includes resistors as a part of it. Three valves are connected in the load side. Five different steps are done here.

These steps are

a) The load voltage and current at the maximum power point operation

b) The variation of load voltage and current when the electrical load is varying.

c) Output voltage and frequency variation of the PMSG when the hydraulic pressure of the PRO plant is varying

d) Output voltage and frequency variation when the jet velocity is varying

e) Output voltage and frequency variation when the flow rate is varying

The intensity of valves will change according to the changes in the Matlab model.

x) Digital multi-meter

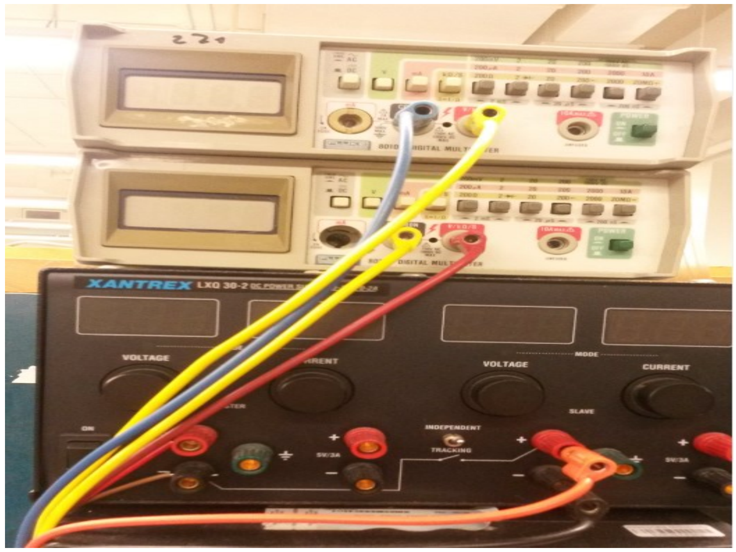

Fig.4.21. Digital multi-meter

The digital multi-meter is connected in the load side. There are two multi-meters shown in the figure. They are used to measure the output or load voltage and current.

xi) Oscilloscope

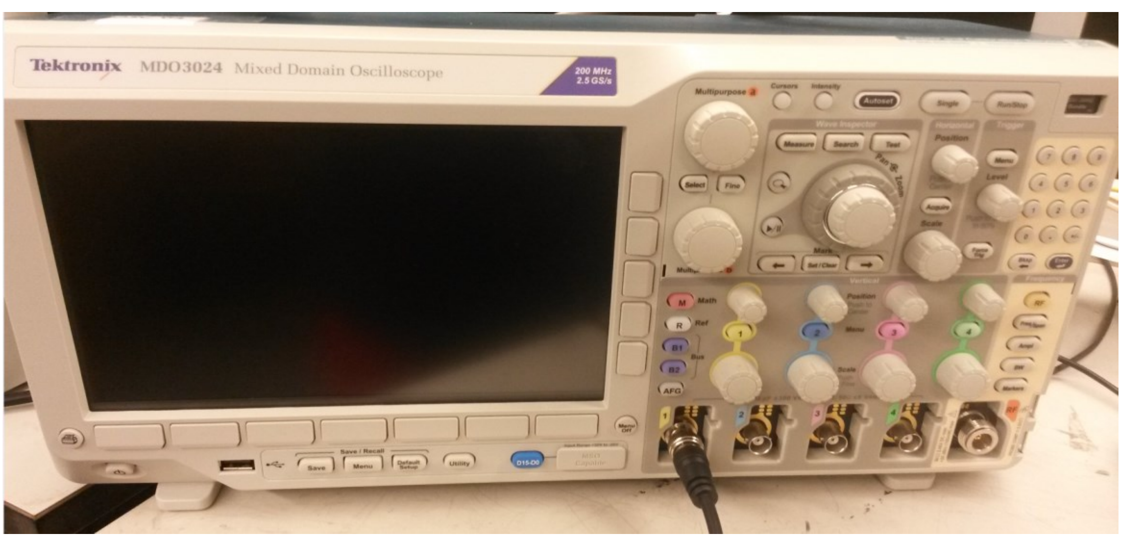

Fig.4.22.Oscilloscope

This oscilloscope here displays and analyzes the output waveforms (voltage and current). It displays the voltage and current outputs from the system.

B) Experimental Results

The proposed system has been emulated with the hardware setup described in the previous section and the results are shown below. Fig. 4.23 (a) shows the load voltage and current at its maximum condition. It happens when hydraulic pressure is half of the osmotic. This figure is similar to the Fig. 4.1 (a) and (b), which is the simulation output of voltage and current at its maximum power point operation. Similarly, Fig.4.23 (b) represents the voltage and current, when the electrical load is varying. This is same as the output of simulation results in the Fig. 4.2 (b) and (c).

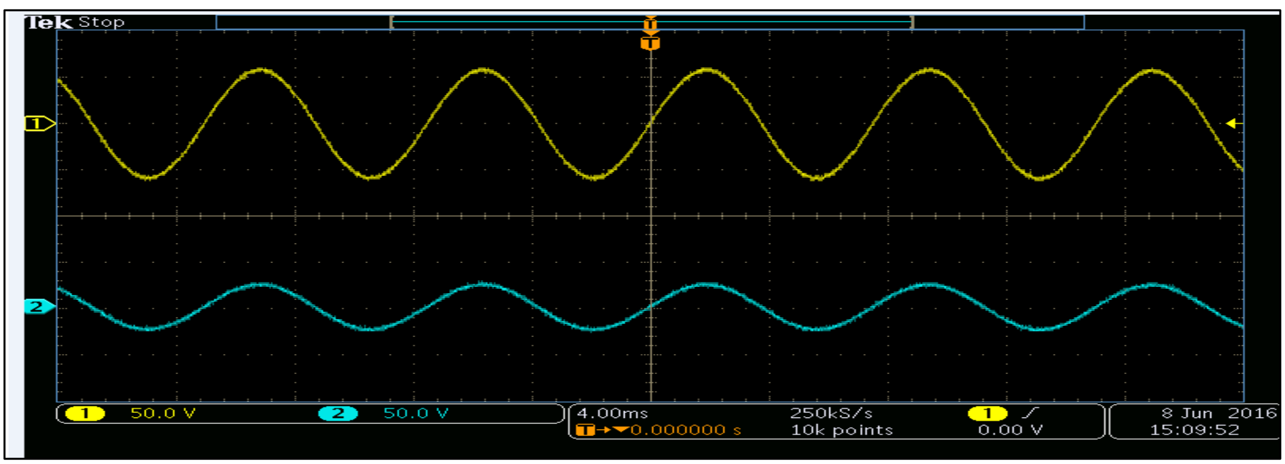

(a)

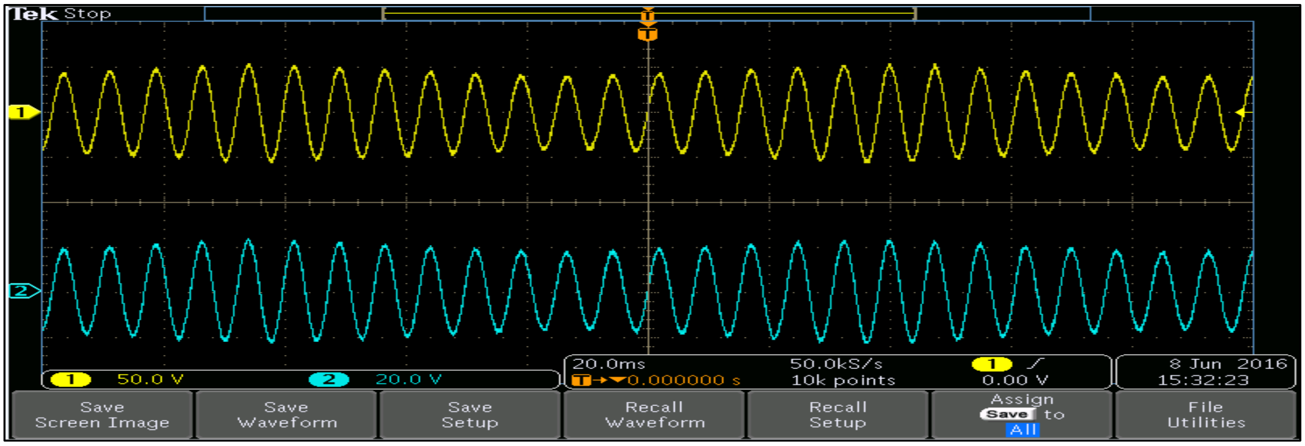

(b)

Fig. 4.23.Experimental results: (a) the load voltage and current at the maximum power point operation; (b) the variation of load voltage and current when the electrical load is varying

As output voltage and frequency will change accordingly with the change in the hydraulic pressure of the PRO, which is shown in the Fig.4.24. (a). And the Fig.4.24 (b) shows the voltage and frequency by changing the jet velocity. As the Fig. 4.3. is the simulation output by changing the hydraulic pressure and the Fig.4.4. is the simulation output by varying the jet velocity.

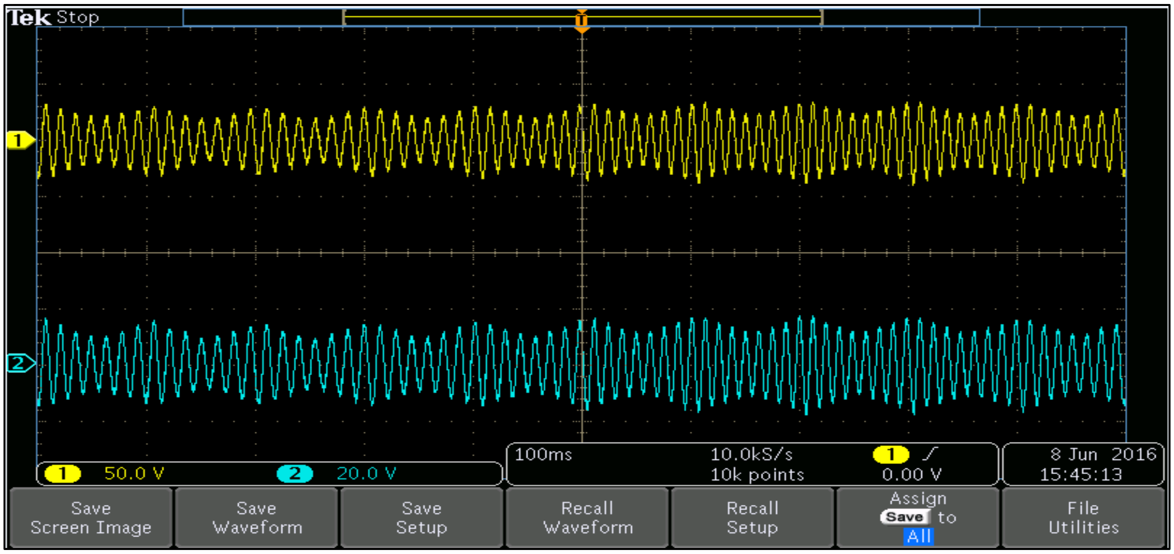

(a)

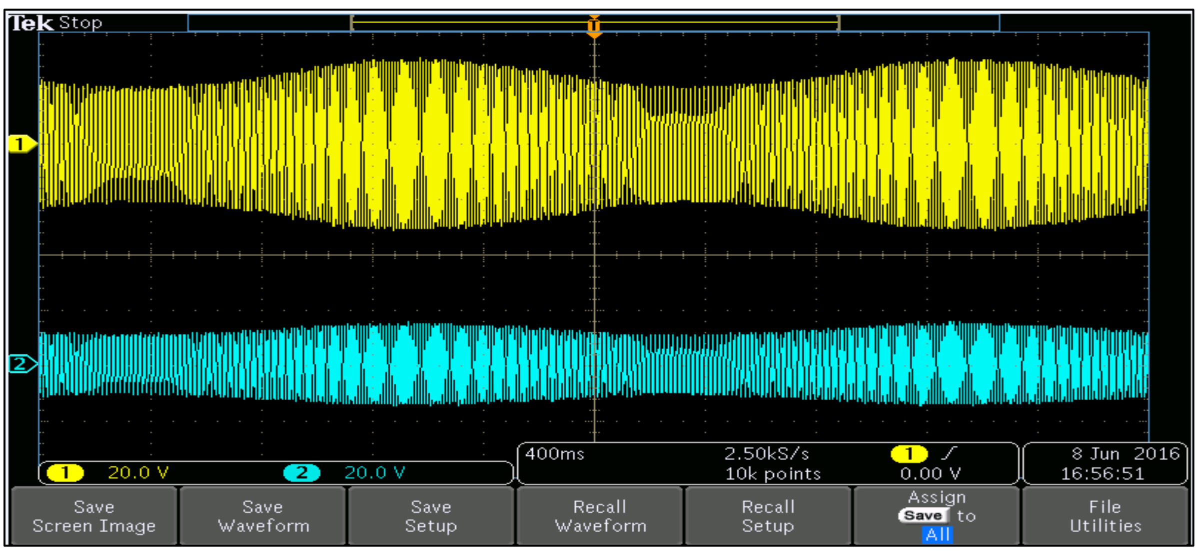

(b)

Fig. 4.24.Experimental results (a) Output voltage and frequency variation of the PMSG, when the hydraulic pressure of the PRO plant is varying; (b) Output voltage and frequency variation within the jet velocity is varying

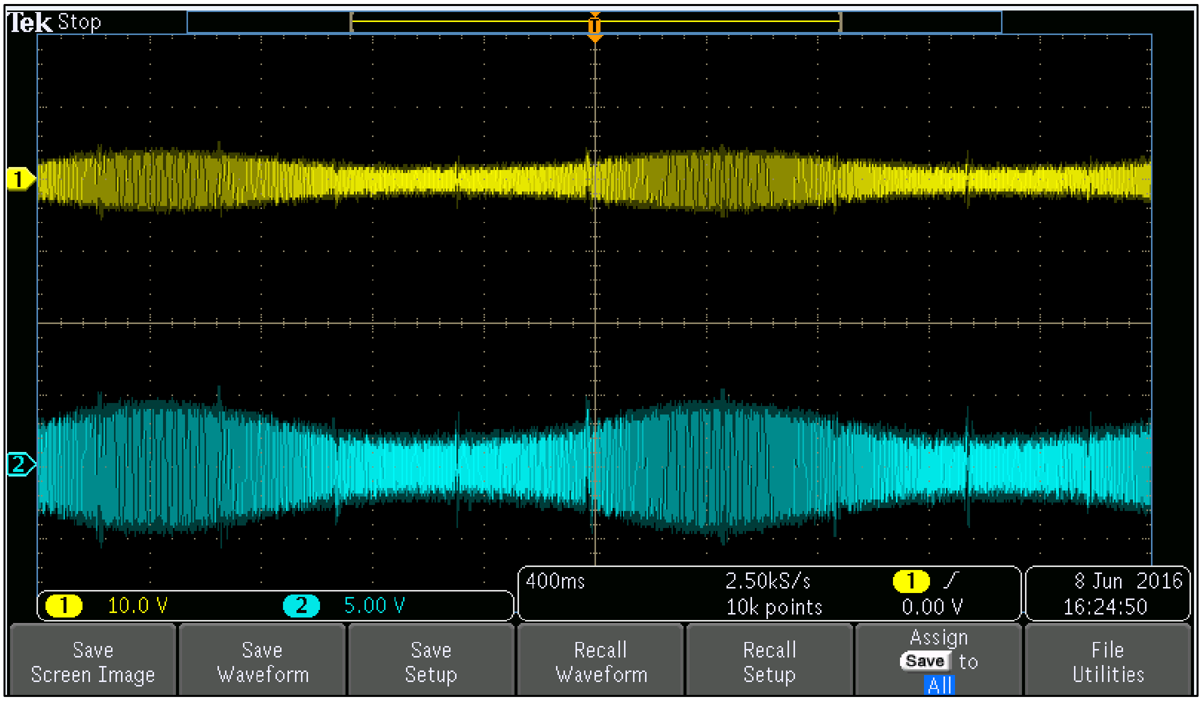

Fig.4.25. Voltage and frequency output by changing the flow rate

As varying flow rate will affect the voltage and current. By implementing the model in hardware and compare the output of the software with the hardware values. Fig.4.25. shows the voltage and current waveforms in the hardware implementation. It is done by varying the flow rate. We apply the same change of the flow rate both in software (Matlab model) and the hardware (experimental setup). Then we compare both the results. As seen that both voltage and current output waveforms are the same in both setups (software and hardware model).The simulation model is presented in the Fig. 4.5, which is the simulation output when the flow rate is varying.

4.5 Simulation Results for Higher Values (For 100 and 250 kW)

A) When the PRO Plant is 0perating at its MPP

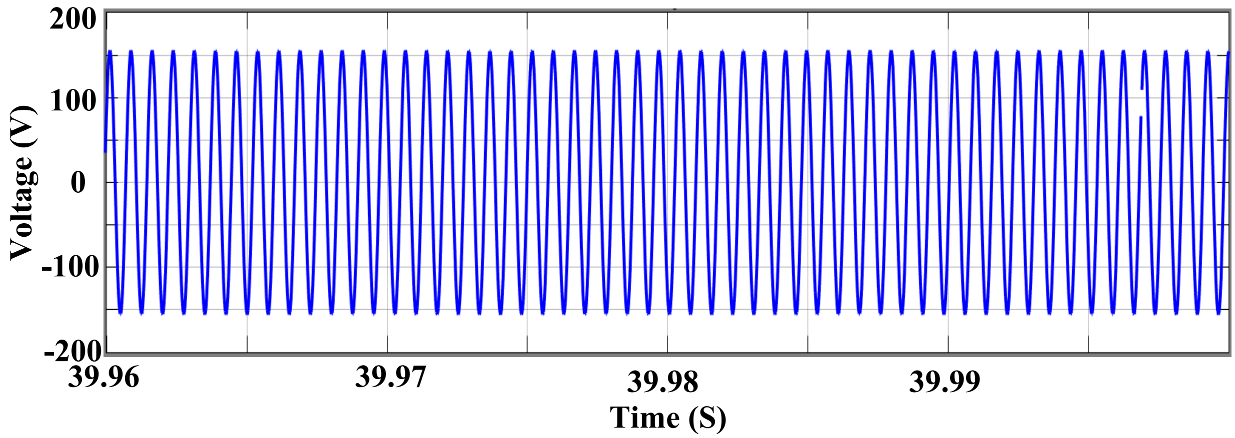

(a)

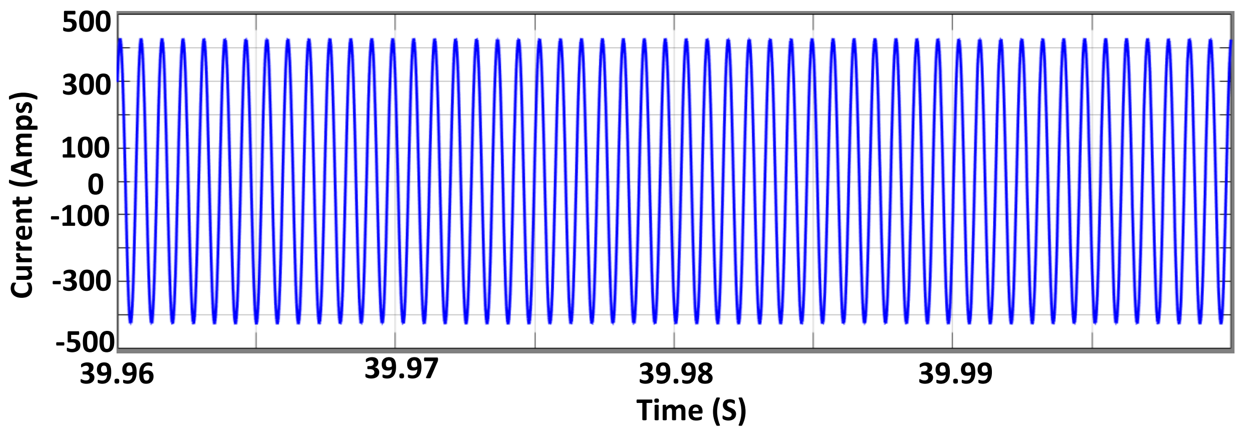

(b)

Fig.4.26. (a) Voltage and (b) Current output of 100 kW model at MPP condition

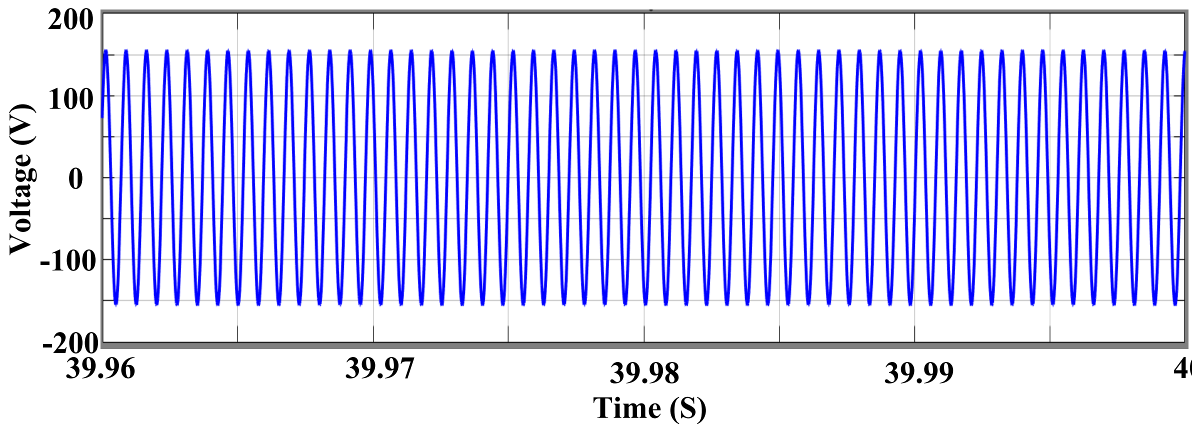

(a)

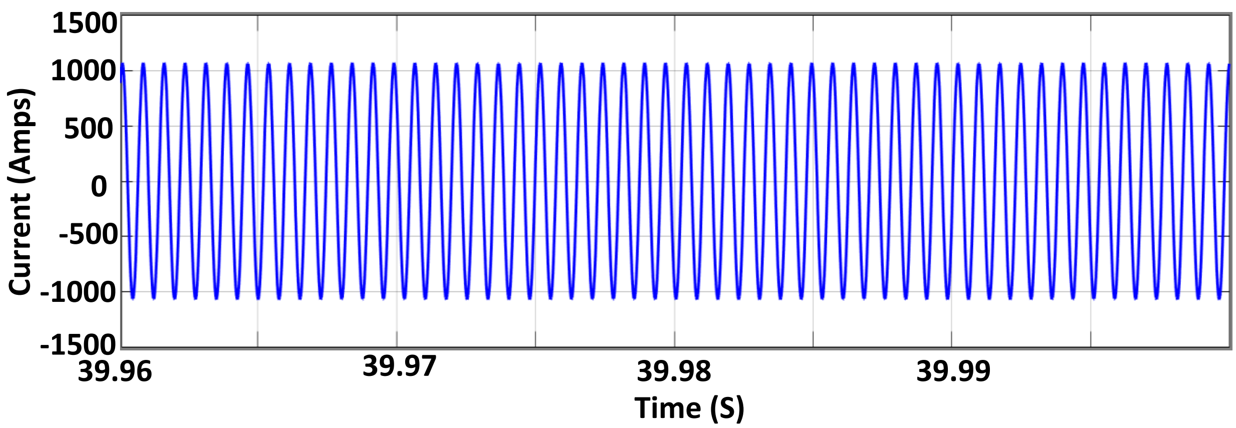

(b)

Fig.4.27. (a) Voltage and (b) Current output of 250 kW model at MPP condition

For 100 kw system the total membrane area (for 12 kW model) is 11120 m, which is multiply by 8.33 to increase the power. And for 250 kW model, the total membrane area is multiply by 20.83. Here it is seen that voltage is remain constant, but current increase when the membrane area increase. In that MPP condition hydraulic pressure is given as half the osmotic pressure to achieve the maximum power.

B) When the Load is Changing

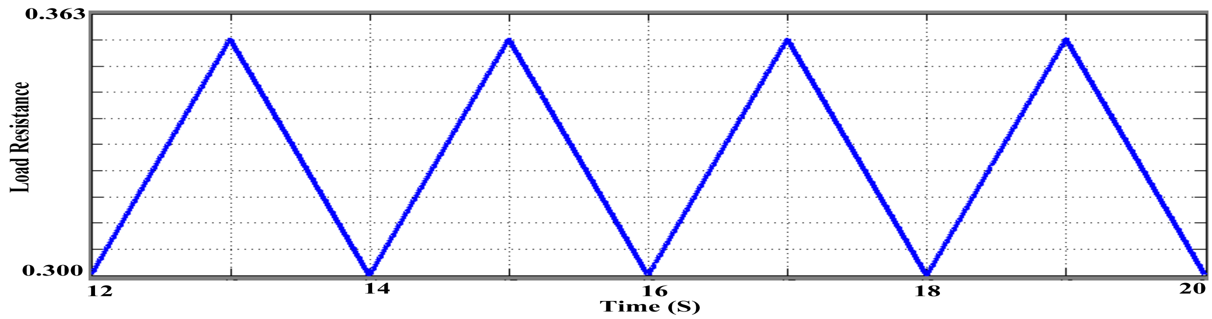

(a)

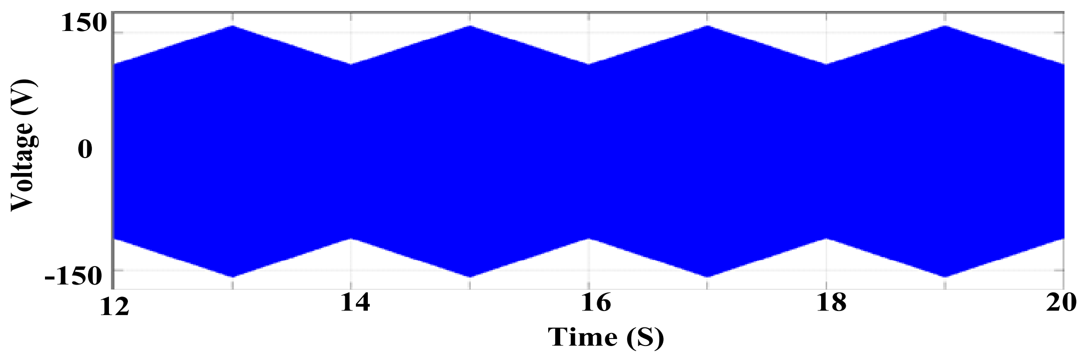

(b)

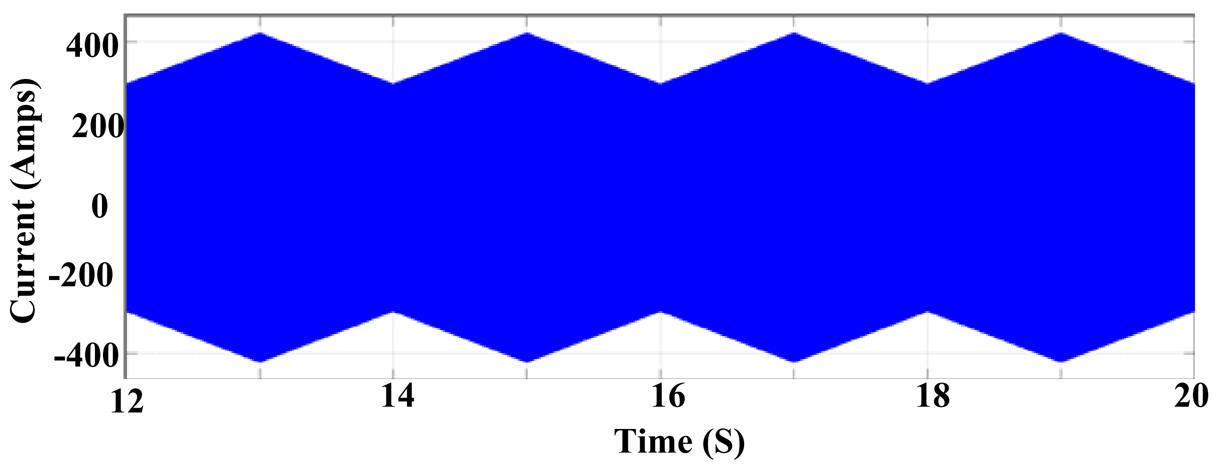

(c)

Fig.4.28.(a) Load resistance change, (b) Output voltage and (c) output current variation when the load is changing for the model of 100 kW

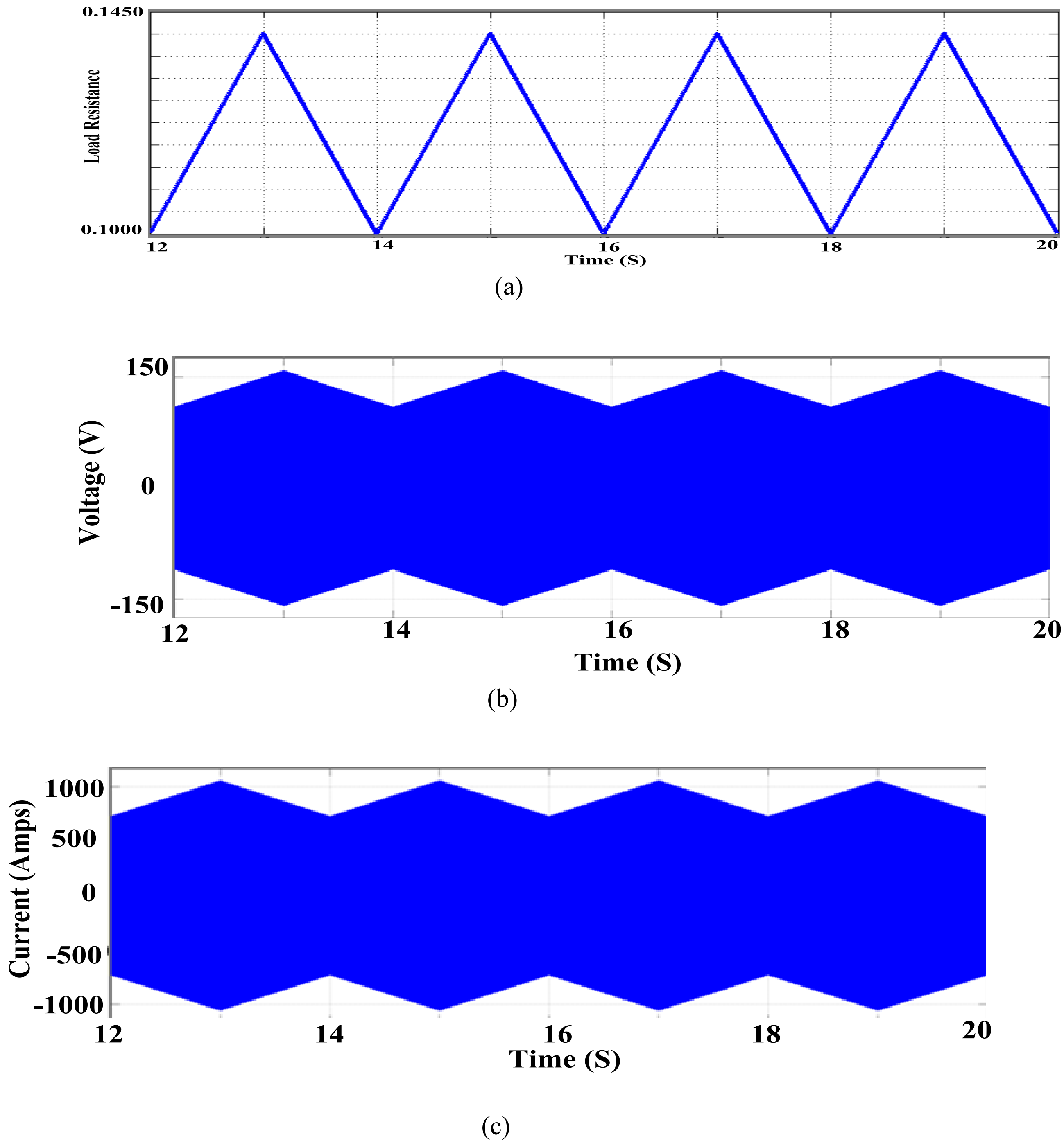

Fig.4.29.(a) Load resistance change, (b) Output voltage and (c) output current variation when the load is changing for the model of 250 kW

C) **Hydraulic Pressure Change**

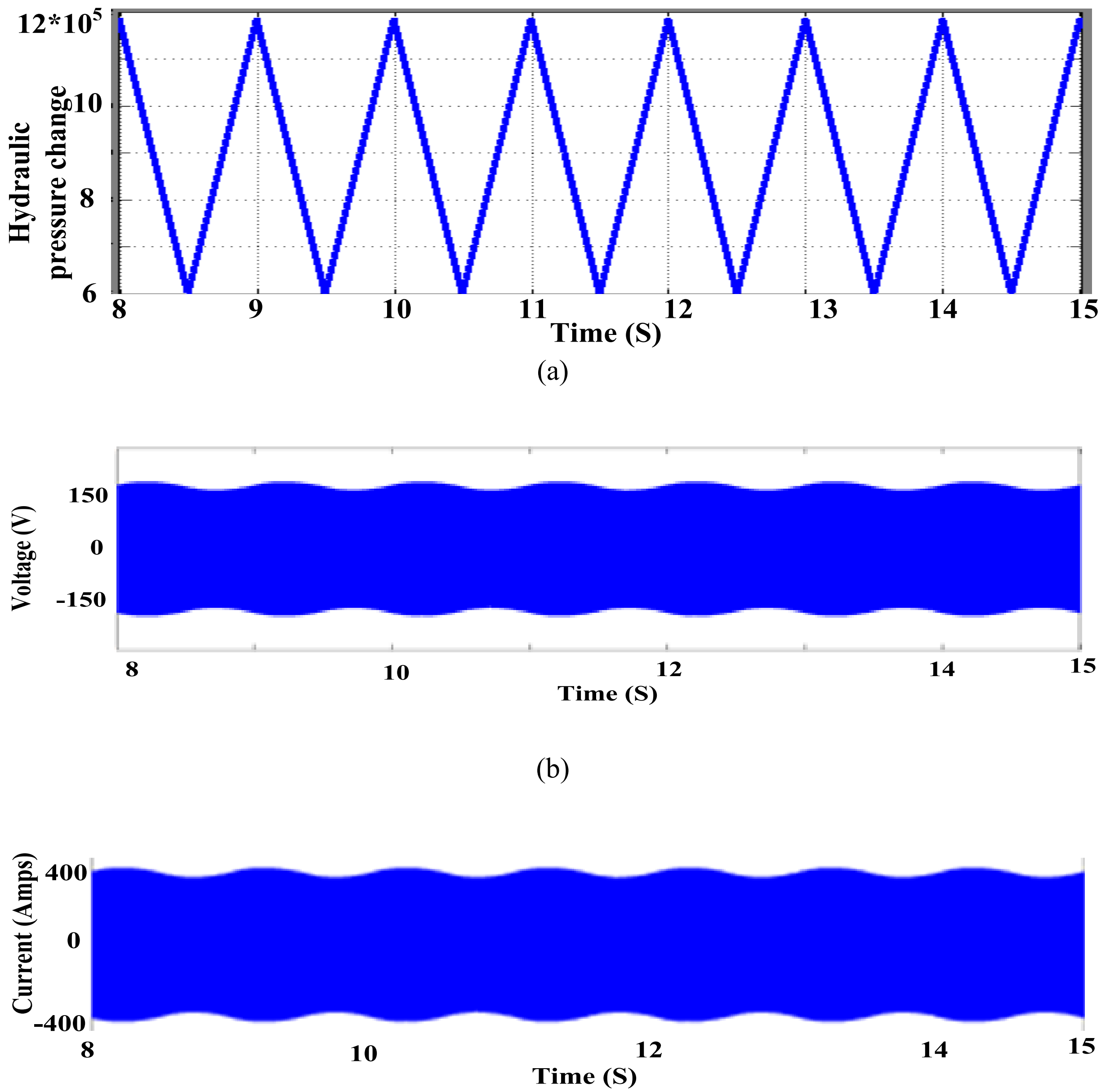

(a)

(b)

(c)

Fig.4.30.(b) Output voltage and (c) output current variation of the PMSG at 100 kW model when the hydraulic pressure of the PRO plant is varying

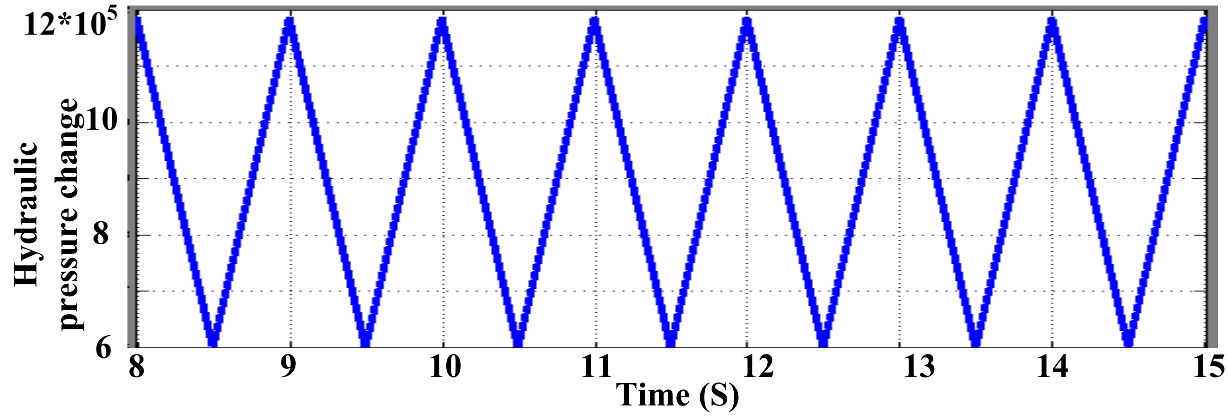

(a)

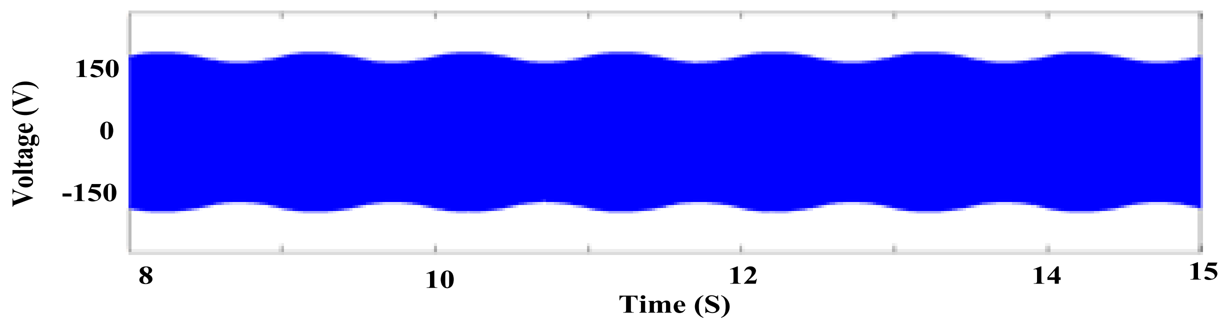

(b)

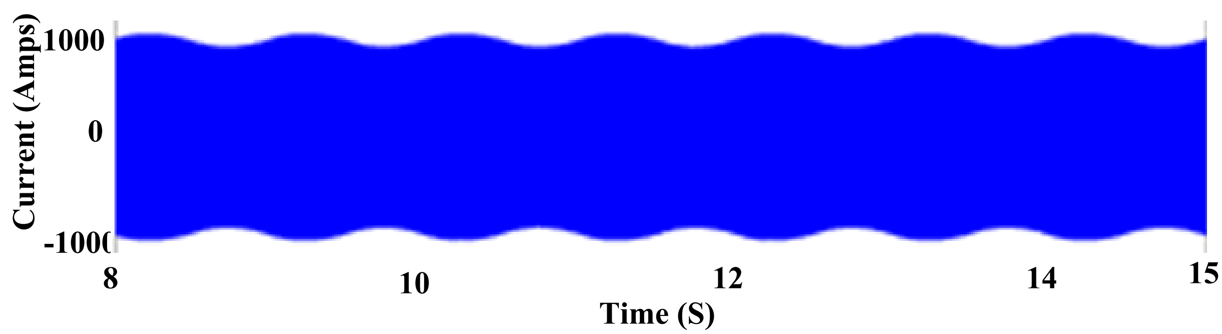

(c)

Fig.4.31.(b) Output voltage and (c) output current variation of the PMSG at 250 kW model when the hydraulic pressure of the PRO plant is varying

Chapter 5 CONCLUSION

Pressure retarded osmotic power plants have the potential for emerging as a renewable alternative power generation system due to the advantages such as stability and predictability of the available energy for remote areas where electric grids are unavailable. This report provides a simplified scheme and design methodology for modeling, design and operation of the PRO power plant. In addition to this, a case study of a pilot power plant of 12 kW capacity has been presented and the system is emulated in hardware using real-time power hardware-in-the-loop. A higher order, 100 and 250 kW power generation have been also calculated in this thesis. The proposed emulator provides an effective and economic method to study and implement control methods to operate the PRO plant efficiently.

Potential Energy of Osmotic Power

- Diesel generators are mainly used to supply electricity in the remote communities in Quebec. As for diesel generators the transportation cost is too high, which increase the total prices. And because of high greenhouse gas emissions and air pollution, this process has a very negative impact. All these reasons making renewable energy more applicable for this overall process [4].
- To meet the peak demand of power only a small portion of river flow rate is required. This helps to mitigate environmental impacts and strong seasonal variations in river water flow rates not going to effect the power production.
- The net electric power capacity is 760 W. But improving the membrane quality, electricity prices can be reduced from 0.13 $/kWh to 0.07 $/kWh [28].

System Modeling

- In the PRO model, one side of semipermeable membrane is fed with draw water (sea water) and the other side is fed with fresh water (river water). Whereas river water is considered as zero concentration.
- A pressure difference occurs, which allows the low concentrated water to flow towards the high concentrated water.
- Water permeate flux can be calculated from the difference between the osmotic pressure and the hydraulic pressure multiplied with the water permeability.
- When the hydraulic pressure is zero, then the water flux is maximum. Maximum power density achieved when hydraulic pressure is half the osmotic pressure.

PRO system circuit model

- The circuit model is the equivalent representation of the PRO model, where both hydraulic and osmotic pressure are represents by voltage sources and inverse of water permeability is represents by the membrane resistance. And water flux is represents by the flow of current.

POWER FLOW MODEL OF THE PRO SYSTEM

- The whole system starts with two reservoir: one is salt water reservoir and another is fresh water reservoir. These two sources mix in the membrane and create a water flux, which pass through the blade to rotate and run it.
- Consideration of turbine selection depends on the flow rate and water head. For high head Pelton turbine is selected. Applied jet velocity is higher than the runner velocity,

as there are some losses occurs in the runner. Whereas the effective jet velocity is 46% of the applied jet velocity.

- Turbine is then connected with the permanent magnet synchronous generator (PMSG). As there is no gear box between the turbine and generator, therefore they will run in the same speed.

Proposed Future Research

- Still now all the osmotic power model including turbine and generator are in experimental stage. There should be lots of things that can be improved in the model. Like mathematical model of the PRO system can be improved by considering membrane distortion and membrane fouling. The selection of turbine is just by calculation s in the paper work. It should be implemented practically and should be seen that the proper turbine is selected. As in the lab experiment, Pelton turbine is represent by some equations.
- Another thing is that in the lab experiments is the ideal condition. In that there is no lose considerations are there. Experiments are taken for 20, 100 and 250 kW. But for practical model losses will be there.
- The turbine blades are generally made by considering only fresh water can pass through it. By using salt water it can make corrosive effect with the turbine blades. Salt can reduce the lifespan of the turbine blade. In that case some improvements can be done on the turbine blades. To get rid from the corrosive effect a coating should be there on the turbine blades. For future work for practical model, should find a way to protect the blades. The overall pipe is narrow and the jet diameter is narrower, where salt can make a layer inside the pipe and even in the jet pipe. It can block the water to

pass through it. As the pipe is very narrow, so cleaning inside the pipe is difficult. So need to find some organic or inorganic method to clean the pipe will be very useful to make the system works properly.

- Some regular cleaning process should be there to clean the overall turbine, as salts can enter in different parts of turbine and can make the whole process difficult to run successfully. Further methods should be install to get rid of these problems.

REFERENCES

[1] S. Nababan, E. Muljadi and F. Blaabjerg, "An Overview of power topologies for micro-hydro turbines," 3rd IEEE *International conference*, *Power Electronics Distributed Generation Systems (PEDG)* 2012.

[2] S. Loeb, "Large-scale power production by pressure-retarded osmosis, using river water and sea water passing through spiral modules," *Desalination*, vol. 143, pp. 115-122, (2002).

[3] B. E. Logan and Menachem, "Membrane-based processes for sustainable power generation using water," *International weekly journal of science*, Nature, vol. 488, pp. 313-319, Aug. 2012.

[4] F. Helfer, C. Lemckert and Y. G. Anissimov, "Osmotic power with Pressure Retarded Osmosis: Theory, performance and trends - A review,"*Journal of Membrane Science* .vol. 453, pp. 337-358, (2014).

[5] M. F. Naguib, J. Maisonneuve, C. B. Laflamme and P. Pillay, "Modeling pressure-retarded osmotic power in commercial length membranes,"*Renewable Energy*, vol. 76, pp. 619-627, 2015.

[6] J Kim, K . jeong, M .Jun park, H .Kyong Shon and J.Ha Kim," Recent advances in osmotic energy generation via pressure-retarded osmosis (PRO): A Review," *Energies* 2015,8,11821-11845.

[7] A. Straub, P. A. Deshmukh and M. Elimelech, "Pressure-retarded osmosis for power generation from salinity gradients: is it viable?," *Energy & Environmental Science*.

[8] Falcao, A.F.D.O., 2010. "Wave energy utilization: A review of the technologies," *Renewable & Sustainable Energy* Reviews 14, 899–918.

[9] A. Achilli, T. Y. Cath and A. E. Childress, “Power generation with pressure retarded osmosis: An experimental and theoretical investigation,” *Journal of Membrane Science*, vol. 343, pp. 42-52, (2009).

[10] N. Y. Yip and M. Elimelech, “Thermodynamic and energy efficiency analysis of power generation from natural salinity gradients by pressure retarded osmosis,” *Environmental Science & Technology*, 46, 5230–5239 (2012).

[11] R.E. Pattle, “Production of electric power by mixing fresh and salt water in the hydroelectric pile,” *Nature* 174, 660 (1954).

[12] J. Maisonneuve, P. Pillay and C. Laflamme, “Pressure retarded osmotic power system model considerations non-ideal effects,” *Renewable energy*, vol. 75, pp. 416-424, (2015).

[13] N.Y. Yip and Elimelech, M, “Thermodynamic and energy efficiency analysis of power generation from natural salinity gradients by pressure retarded osmosis,” *Environmental Science & Technology,* vol. 46, pp. 5230-5239, (2012).

[14] R.E. Pattle, “Production of electric power by mixing fresh and salt water in the hydroelectric pile,” *Nature* 174,660(1954).

[15] J.W. Post, H.V.M Hamelers and C.J.N. Buisman, “Energy recovery from controlled mixing salt and fresh water with a reverse electrodialysis system,” *Environmental Science & Technology*,42,5785-5790, (2008).

[16] J. Veerman, M .Saakes, S.J .Metz and G.J. Harmsen, , “Electrical power from sea and river water by reverse electro dialysis: a first step from the laboratory to a real power plant,” *Environmental Science & Technology*,44, 9207-9212, (2010).

[17] G. Z. Ramon, B.J .Feinberg and E.M.V. Hoek, “Membrane-based production of salinity-gradient power,” *Environmental Science & Technology*, 4, vol. 4423-4434, (2011).

[18] Chillida. and A.E.Childress, “Pressure retarded osmosis: From the vision of Sidney Loeb to the first prototype installation-Review,”*Desalination,* 261, pp. 205-211, (2010).

[19] R. J. Aaberg, “Osmotic power. A new and powerful renewable energy source,” *Refocus*, 4 (2003) 48-50.

[20] The Energy Information Administration, http://www.eia.doe.gov/.

[21] R. E. Pattle,”Production of electric power by mixing fresh and salt water in the hydroelectric pile,” *Nature*, 174 (1954) 660.

[22] S. Loeb, “Production of energy from concentrated brines by pressure-retarded osmosis: I. Preliminary technical and economic correlations,” *Journal of Membrane Science*, vol. 1, pp. 49-63, (1976).

[23] A. Achilli, T. Y. Cath and A. E. Childress, “Power generation with pressure retarded osmosis: An experimental and theoretical investigation,” *Journal of Membrane Science*, vol. 343, pp. 42-52, (2009).

[24] H. H. Jellinek and H. Masuda, “Osmotic-power. Theory and performance of an osmotic-power pilot plant, Ocean Engineering,” Ed. 8 (1981), pp. 103-128.

[25] J. R. McCutcheon and M. Elimelech, “Influence of concentrative and dilutive internal concentration polarization on flux behavior in forward osmosis,” *Journal of Membrane Science*, 284 (2006) 237-247.

[26] K. L. Lee, R.W. Baker and H.K. Lonsdale, “Membrane for power generation by pressure retarded osmosis,” *Journal of Membrane Scienc,* 8 (1981) 141-171.

[27] I. Eziyi and A. Krothapalli,”Effects of salinity and feed temperature on permeate flux of an air gap membrane distillation unit for sea water desalination,” 1st IEEE Conference on Technologies for Sustainability, (2013).

[28] J. Maisonneuve and P. Pillay, “Osmotic power for remote communities in Quebec,” *Power Electronics and Energy (PEER) research group*.

[29] R. Joseph and L. Umanand, "Turbine emulator for development of variable speed microhydro power generation systems," *Sustainable Energy Technologies (ICSET)*, 2012 IEEE Third International Conference on, Kathmandu, pp. 335-340, (2012).

[30] S. Loeb and R. S. Norman,” Osmotic Power Plants,” *Science, American Association for the Advancement of Science*, vol. 189, pp. 654-655, (1975).

[31] B. Singh, S. S. Murthy and S. Gupta, “Analysis and design of electronic load controller for self-excited induction generators,” IEEE Trans. *Energy Converters*., vol. 21, no. 1, Mar. (2006).

[32] J Thake, "The micro-hydro Pelton turbine manual, design, manufacture and installation for small-scale hydro power," ITDG Publishing, UK, (2000).

[33] Bilal, “Design of high efficiency Pelton turbine for micro-hydropower plant,” *International Journal of Engineering and Technology (IJET),* vol. 4, no. 1, pp. 171-183, Jan.-Feb. (2013).

[34] I. U. Atthanayake, “Analytical study on flow through a Pelton turbine bucket using boundary layer theory,” *International Journal of Engineering and Technology (IJET),* vol. 9, no. 9, Oct. (2009).

[35] J. Thake, "The micro-hydro Pelton turbine manual, design, manufacture and installation for small-scale hydro power," ITDG Publishing, UK, (2000).

[36] L. Belhadji, S. Bacha and D. Roye, “Modeling and Control of Variable-speed Micro Hydropower Plant Based on Axial-flow turbine and Permanent Magnet Synchronous

Generator (MHPP-PMSG)," 37th Annual Conferrence. IEEE Ind. *Electron. Society*, pp. 896-901, 7-10 Nov. (2011).

[37] J. L. Màrquez , M.G. Molina and J.M. Pacas, " Dynamic modeling, simulation and control design of an advanced micro-hydro power plant for distributed generation applications," *International journal of hydro-genation energy*, 35, pp. 5772 – 5777, (2010).

[38] N. Mohan, T. M. Undeland and W. P. Robbins, "Power Electronics: Converters, Applications, and Design," *Hoboken*, NJ, Wiley, (2002).

[39] P. A. Dahono and A. Purwadi Qamaruzzaman, "An LC filter design method for single-phase PWM inverters," *International Conference .of Power Electronics and Drive Systems,* 1995, vol. 2, pp. 571–576.

[40] R. Joseph and L. Umanand, "Turbine emulator for development of variable speed microhydro power generation systems," *Sustainable Energy Technologies (ICSET),* 2012 IEEE 3rd International Conference on, Kathmandu, 2012, pp. 335-340.